Design of a Collaborative Gripper for Foam Stickers Handling

by

Francis BILODEAU

THESIS PRESENTED TO ÉCOLE DE TECHNOLOGIE SUPÉRIEURE
IN PARTIAL FULFILLMENT OF A MASTER'S DEGREE
WITH THESIS IN MECHANICAL ENGINEERING
M.A.Sc.

MONTREAL, DECEMBER 20, 2023

ÉCOLE DE TECHNOLOGIE SUPÉRIEURE
UNIVERSITÉ DU QUÉBEC

BOARD OF EXAMINERS

THIS THESIS HAS BEEN EVALUATED

BY THE FOLLOWING BOARD OF EXAMINERS

M. Jean-Philippe Roberge, Thesis supervisor
Systems Engineering Department, École de technologie supérieure

Ms. Julia Guérineau, Chair, Board of Examiners
Systems Engineering Department, École de technologie supérieure

M. Vincent Duchaine, External Examiner
Systems Engineering Department, École de technologie supérieure

THIS THESIS WAS PRESENTED AND DEFENDED

IN THE PRESENCE OF A BOARD OF EXAMINERS AND THE PUBLIC

ON DECEMBER 11, 2023

AT ÉCOLE DE TECHNOLOGIE SUPÉRIEURE

ACKNOWLEDGEMENTS

First and foremost, I would like to express my deepest gratitude to my thesis supervisor, Jean-Philippe Roberge, for his guidance, expertise, and mentorship throughout the course of this research, as well as for giving me the opportunity to work on this project.

Thanks are extended to Exo-S, particularly to the Director of Automation and Robotics, Danny St-Jaques, who instigated the partnership between the University and the industrial partner. A special thanks also to Guillaume Pépin, automation engineer at Exo-S, for his invaluable insights throughout the project.

Acknowledgment goes to the *École de Technologie Supérieure* for the resources and environment that made this research feasible.

Conception d'un préhenseur pneumatique collaboratif pour la manipulation d'autocollants en mousse

Francis BILODEAU

RÉSUMÉ

Les autocollants en mousse sont couramment utilisés sur des pièces automobiles pour réduire les bruits de vibration, mais ils sont pratiquement exclusivement appliqués à la main. L'automatisation de cette tâche présente de nombreux défis qui doivent être abordés pour mettre en place avec succès une station robotique dans les industries. Dans cette thèse, nous attaquons ce problème en concevant un nouveau type de préhenseur qui peut être adapté à une variété de tailles différentes d'autocollants en mousse. Ce préhenseur utilise une combinaison de moyens de préhension mécaniques et pneumatiques pour décoller et placer avec succès les autocollants en mousse. Nous démontrons également comment cinq variations différentes de ce préhenseur peuvent être intégrées dans un effecteur robotique collaboratif et peuvent saisir et placer cinq différents autocollants en moins de 45 secondes. Pour gérer la complexité d'un tel effecteur robotique, nous avons combiné des circuits pneumatiques et des fonctionnalités mécaniques en des pièces uniques imprimées en 3D. De plus, des tests expérimentaux plus approfondis sont menés sur différentes ouvertures à vide pour saisir les autocollants en mousse. Enfin, nous développons une méthode pour appliquer une pression sur les autocollants afin de les faire adhérer fermement. Cette méthode, qui consiste à utiliser une trajectoire générée par admittance à une vitesse plus élevée, a montré des résultats prometteurs.

Mots-clés: mousse, préhenseur, autocollants en mousse, robotique, robotique collaborative, impression 3D, préhenseur pneumatique, préhenseur collaboratif, contrôle en admittance

Design of a Collaborative Gripper for Foam Stickers Handling

Francis BILODEAU

ABSTRACT

Foam pad stickers are commonly used on automobile parts to reduce rattling, but they are practically exclusively applied by hand. Automating this task presents numerous challenges that need to be addressed to successfully implement a robotic station in industries. In this thesis, we attack this problem by designing a novel robotic gripper that can be adapted to a variety of different foam pad sizes. This gripper uses a combination of mechanical and pneumatic grasping means to successfully peel and place foam stickers. We also demonstrate how five different variations of this gripper can be integrated into a collaborative robotic end-effector and can pick and place five different foam pads in under 45 seconds. To manage the complexity of such an end-effector, we combined pneumatic circuits and mechanical functionality into single, 3D-printed parts. Additionally, extensive experimental tests are conducted on different vacuum openings for grasping foam pads. Finally, we developed a method to apply pressure to the foam stickers to firmly stick them. This method, which consists of using an admittance-generated trajectory at a higher speed, showed promising results.

Keywords: robotic gripper, collaborative gripper, foam, foam stickers, foam pads, foam pad stickers, pneumatic, admittance, admittance control, 3D printing, collaborative robotic

TABLE OF CONTENTS

LIST OF TABLES

LIST OF FIGURES

Page

CHAPTER 1

INTRODUCTION

Since their introduction several decades ago, the predominant tasks that industrial robotic manipulators have been utilized for have remained relatively unchanged. For example, they are used to move parts from one fixture to another in a precise manner. They can also operate on the parts themselves, doing operations like drilling, screwing, welding, etc. Most of these tasks have in common that the positions at which the robotic arms operate are constant. The same program runs in repetition and the arm's end effector positions itself again and again, with submillimeter precision, at the same points in space. Additionally, the parts and fixtures of these use cases are made with rigid materials, which is probably why they are so successful with simple point-to-point programming. Yet, many industrial operations involve highly deformable parts, such as tissues or fibers in the textile industry. Sometimes, it is the positions that are variable, like parts or objects randomly disposed on a conveyor that need to be picked up by a robot. Unsurprisingly, the research community has been actively working in the past few years to tackle these challenges. We saw the invention of many different robotic arm end effectors (or grippers) and sensor-driven control strategies. As for the proposed grippers, they are usually designed to be universal, working on a wide range of objects. Contrary to designing a gripper specifically for the task, these more "universal" grippers could reduce the cost of implementing a robotic cell. However, it is the new robotic control strategies that break the most with the classical idea of an industrial robot. These use vision, tactile sensors, force sensors, and complex algorithms. Thus, robotic arms can now correct their movements in real time, enabling the manipulation of highly flexible objects positioned in random ways. With the advancement in AI, this last paradigm is getting closer every year to being adopted in industrial settings. In a sense, these robotic technologies approach slowly the capabilities of what human workers can do. For industrials, the benefits will be undeniable. These will probably come in the form of reduced investment in new robotic cells and a reduced number of workers for a specific project. Furthermore, these new technologies will likely add greater flexibility for the restructuring of production lines or changes in manufactured products.

Nevertheless, there are numerous obstacles for these new technologies to become the norm, which is why the inflexible classical robotic cells are still predominantly used today. One possible obstacle is the robustness of these emerging technologies. In a laboratory setting, a manipulation using sensor-driven robotic control with a 99% success rate could be interpreted as good. Yet, if the same manipulation is applied in an industrial context, that can mean multiple faults every hour[1]. If every one of these faults needs the assistance of a worker, or if the parts are rejected, that can rapidly become costly. Hence, the initial investment in designing and fabricating task-specific grippers and fixtures could be more profitable in the span of several months than betting on newer sensor-driven technology. Another potential obstacle to the adoption of more complex technologies could be the lack of qualified specialists in-house. There is simplicity in the point-to-point programming of a robotic arm; it comes with the predictability of the robot's movements. Also, learning how to program a robot with a teach pendant is quite accessible. On the other hand, troubleshooting a control algorithm relying on a neural network requires more acute knowledge. It seems like the well-established "industrial robotic cell" as known in many industries today is there to stay, at least for the near future.

[1] In the robotic cell developed as part of this thesis, 5 different manipulations need to happen under 45 seconds. This could mean an average of 4 faults per hour if the success rate is 99% for each manipulation.

1.1 Motivation

The work presented in this document focuses on the development of specialized robotic grippers. More precisely, it focuses on a class of grippers used for "foam pad stickers"[2] manipulation, which are deformable objects. The need for such tools comes from the industrial partner Exo-S[3]. Although the project centers around a single robotic station with a handful of different parts, they produce other parts that could benefit from this new class of grippers. This means it could be possible to use this type of gripper on multiple other stations or future projects. These grippers could also serve other manufacturers in need of manipulating similar foam pads or closely related objects. Thus, one of the main focuses of the design of the grippers was to make them viable in an industrial context. Finally, another consideration was the introduction of collaborative robotics at the Exo-S plant.

1.2 Contributions

The principal outcome of our work is the new class of grippers, specifically adapted to the manipulation of small foam pad stickers. There are however other sub-contributions. They are listed in the following bullet points:

- Since the final tool uses five grippers, it shows how it is possible to configure multiple of these grippers on the same end-effector, while also maximizing its collaborative qualities.
- It demonstrates how FDM 3D printing technologies can be used to reduce the cost, complexity, and prototyping time of a robotic gripper. Especially, when the gripper needs to rely on compressed air as an energy source.
- It demonstrates the integration of 3D-printed pneumatic manifolds in functional parts. Furthermore, vacuum generators using the Venturi and Bernoulli effect to generate negative pressure have also been directly integrated into the gripper structure.

---

[2] The "foam pad stickers" are stickers with a foam coating on top. The thicknesses of the foam pads picked up by the grippers are 4 or 5 millimeters. They are rectangles with sides of 14 to 160 millimeters. Images of these foams are presented in the next Chapter.

[3] Exo-S is briefly presented in the Industrial Partner section.

- It explores different geometries of 3D-printed vacuum openings and their performance on grasping the foam pads. These are also compared to a standard vacuum cup.
- It demonstrates how added compliance between the robotic arm and a gripper can increase the effectiveness of a robotic solution. This added compliance reduces the need for precision and facilitates the programming of certain movements.
- It shows a method to calibrate the force of application of sticker-like objects, while the dynamics of the system are partially unknown. This method involves the generation of a trajectory using robotic admittance control and a force plate sensor.

The development of the grippers was subject to many constraints, much of which came from the project's nature as an industrial collaborative robotic cell. Other constraints come from the added specific needs of Exo-S. On top of that, there were also other elements to optimize: such as the simplicity of use, the success rate of manipulations, and the ease of maintenance. More broadly, the whole project is an example of developing an industrial robotic gripper in a highly constrained industrial context. It shows a path from a specific problem to a successful solution. While the solution is somewhat specific to the problem, we hope sections of the path taken could be reused in other contexts or inspire other engineering solutions.

1.3 Industrial Partner

Exo-S is a plastic functional system designer and manufacturer. They produce parts by injection or blow molding. Their target markets are the automotive industry, consumer goods, tools, transportation, and recreational vehicles. The company has three manufacturing plants located in Quebec (Canada), Indiana (United States), and San Juan (Mexico). Quebec's plant is located in the city of Richmond, north of the city of Sherbrooke. As of December 2021, they had a total of 152 unionized employees and 49 executives, but they were still lacking 30 employees. Labor shortages have negatively affected the Richmond plant. Since Richmond is a small city, Exo-S needs to recruit workers principally from Sherbrooke, which is half an hour away by car. Other manufacturers in the city of Sherbrooke compete with them for hiring labor, therefore hiring is especially hard for Exo-S. Additionally, the plant workers work in three shifts. It means

that if a workstation can be robotized, there are three fewer workers to hire. The usual part manufacturing process at Exo-S involves the following operations[4]:

1. The part is molded in a plastic injection press.
2. A ceiling robot takes the part off the mold and then places it on a conveyor.
3. The conveyor carries the part at a workstation with human workers and robotic cells.
4. Workers place foam pads on the part and/or place the part in a robotic cell.
5. In a robotic cell, operations are performed on the part, such as soldering, placing inserts, screwing, etc.
6. The part is taken out of the robotic cell (by a worker or robot) and placed into packaging.

Exo-S has been integrating robots into their production lines since 2007. Most of the tasks easily doable with robots have already been automated. These tasks have the particularity of using classic point-to-point programming and industrial robots in security cages. Operations that are not yet automated include the placement of foam pads and the manipulation of parts between robotic cells. For this last reason and previous ones, the company has sought outside help in the form of collaboration with the university ÉTS (École de technologie supérieure). This collaboration is the reason for the existence of the project detailed in this thesis.

1.4 Thesis Organisation

The chapters of this thesis are organized in the following manner:

- **Chapter 2 - Problematic and Research Objectives.** We describe the challenges and constraints of creating a foam pad gripper and implementing it in a production line. Then, the ensuing research objectives are stated.
- **Chapter 3 - Literature Review.** A review of different gripper technologies is presented. It emphasizes certain technologies that could help in achieving our challenges and research objectives.

[4] Note that operations 4 and 5 are interchangeable and sometimes repeated multiple times per part. There is also inspection of the parts by human workers or vision systems.

- **Chapter 4 - Solution details.** After delving into the challenges and literature, we present our solution. Each component that contributed to the robotic solution is presented in different subsections of this chapter.

Following the description of the solution in Chapter 4, the next three chapters present distinct experiments:

- **Chapter 5 - Pneumatic grasping Tests.** Multiple pneumatic trial prototypes are tested. They are evaluated on their performance in grasping foam pads.
- **Chapter 6 - Grasping Robustness Tests.** Five different gripper variants are evaluated on their success rate for picking up foam pads.
- **Chapter 7 - Admittance Tests.** An admittance control scheme to apply pressure on foam pads is tested. This method serves to firmly stick the foam pad stickers in place.

We conclude the thesis with a comprehensive Discussion (Chapter 8), and a brief Conclusion (Chapter 9).

CHAPTER 2

PROBLEMATIC AND RESEARCH OBJECTIVES

This chapter highlights the challenges of foam pad manipulation without delving into the actual solution. Emphasis is placed on the evaluation of the challenges as they were first assessed and the formulation of research sub-objectives. The principal research objective of the project was to find a way to automate tasks that are done by human workers at Exo-S. This involved the placement of rectangular foam stickers on different plastic parts (Figure 2.1 shows the different foam pads). Furthermore, a specific workstation has been selected in the plant to try and implement the grippers.

Figure 2.1 Five gray foam pads on the plastic parts

In the following sections, we first present the specificities of foam pad manipulation. These are divided into two categories:

- Picking up the foam pad stickers.

- Applying the foam pad stickers on the parts.

Secondly, additional industrial constraints and sub-objectives are discussed. They are essential for the viability of the project in the selected workstation and production line. Lastly, constraints that are associated with the collaborative nature of the robotic station are presented.

2.1 Foam pad manipulation

Foam pad stickers are supplied on cardboard sheets by an Exo-S provider. We focused on the thin rectangular ones. The dimensions of their sizes range from 14 to 160 millimeters, with foam pad thicknesses of 4 or 5 millimeters. On multiple workstations at the Exo-S plant, the foam pads are peeled off from the cardboard sheets by workers and applied to plastic parts.

2.1.1 Picking up foam pads

Human workers use two different techniques to detach the foam pads from the cardboard sheets. The first technique is to peel the very tip of the foam until it sticks to one finger, then peel the rest of it using the adhesion between the finger and the underside of the foam sticker. The second technique involves pinching the side of the foam with two fingers and peeling it. Both techniques share the characteristic that the foam is not detached all at once, but it is peeled from one side at an angle (see Figure 2.2). Attempting to unstick the foam pads from their middle results in tearing the foam before it can be unstuck (as tested in Appendix I).

Therefore, it would be wise to design the gripper solution so it can pick up the foam pads in a peeling motion. Additionally, the force needed to peel a foam sticker is greater than the weight of the cardboard. This implies that the cardboard needs to be fixed somehow, otherwise, the cardboard is lifted with the foam. Another problem to keep in mind is the fact that a foam sticker tends to stick to itself. When that occurs, the foam pad becomes unusable (see Figure 2.3).

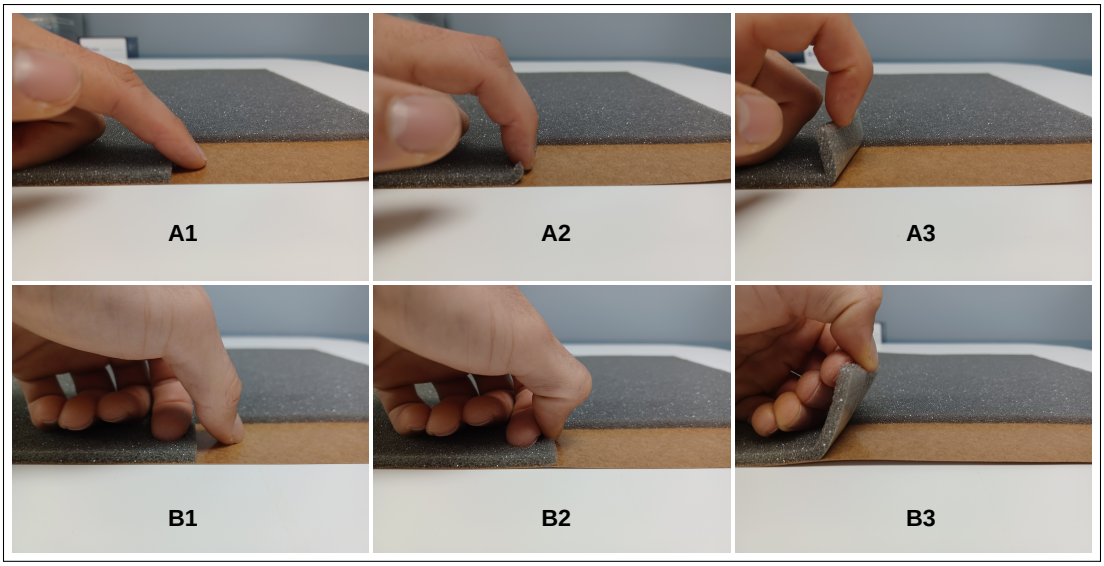

Figure 2.2 Picking foam pads by hand - A1) to A3) Technique 1: sticking a finger to the underneath of the pad. - B1) to B3) Technique 2: pinching the edge of the pad

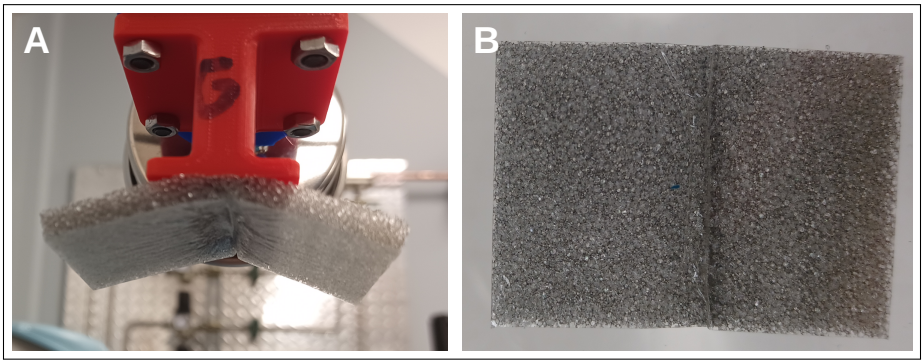

Figure 2.3 A) The foam pad might develop creases or stick to itself if the picking device is inadequate - B) Underneath view of a foam pad after appliance on a glass plate: a fold is visible

On top of that, when the foam has been picked up, it would be useful if the foam is fixed somehow on the gripper so that it doesn't dangle around[1]. Fixing the foam on the tool also has the benefit

[1] For a single foam pad, this issue may not be significant. However, as the complete tool can grasp up to five of them, the foam pads could adhere to other surfaces when others are being applied to their respective plastic parts.

of facilitating the application of the foam sticker (possibly a simpler motion). Below are the research sub-objectives for this section presented as bullet points:

Research sub-objectives for picking up foam pads

- Unsticking the foam in a peeling motion.
- Fixing the cardboard so that peeling of the foam can happen without the cardboard lifting.
- Preventing the foam pad from sticking to itself.
- Fixing the foam on the gripper. To prevent the foam from dangling and to facilitate its application.

2.1.2 Applying foam pads

Foam pads come in various form factors, as do the parts they are applied to. Ideally, the developed gripper should be compatible with all types of foam sizes and could apply them on a variety of different part geometries. Some foams need to be placed inside the parts, close to the plastic edges (see Figure 2.4). The gripper should be able to access these positions without interference with the parts. Also, the applied foam should not have any creases after its application.

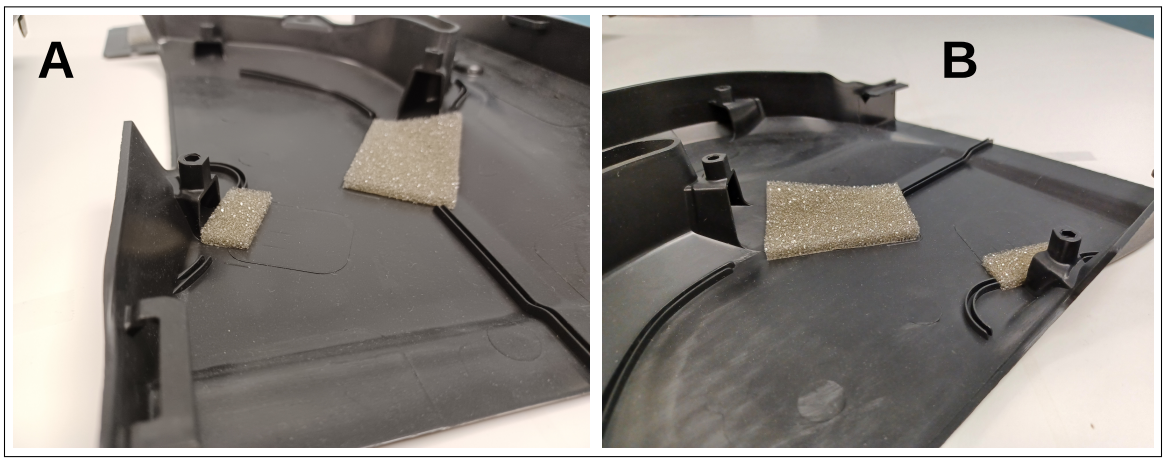

Figure 2.4 Foam pads close to the edges of one of the plastic parts

This might seem trivial, but it did occur quite often during the prototyping phase of the project. Finally, since the pads utilize pressure-sensitive adhesive, a uniform pressure needs to be applied for the foam pads to stick firmly[2]. Listed below are the research sub-objectives for this part of the problematic:

Research sub-objectives for foam pads application

- Permitting different geometry of the gripper for different foams, to adapt to the varying sizes of the foams and prevent interference with the parts.
- Sticking the foam on the part uniformly, without any creases.
- Applying uniform pressure on the foam, so the adhesive can activate.

2.2 Industrial constraints

The developed gripper is designed to be part of a collaborative workstation on a specific production line at Exo-S. For this robotic workstation to be viable, certain performance criteria must be met. Perhaps the most important aspect for the company is to be able to replace enough foam placement tasks on parts. Three workers on the specific production line participate in placing foam pads. There are 5 types of foam pads identified by Exo-S engineers that need to be picked up and placed by the robot. Robotizing the application of these 5 foam pads is the minimum requirement to reduce the number of workers on the line. Furthermore, there is a time limit of 45 seconds for picking and placing these 5 foam pads. This limit comes from the plastic injection press time cycle. Every 45 seconds, new parts come from the press on a conveyor. The subsequent workstations on the line need to have shorter cycle times, so the production of parts can go on continuously. That way, parts do not accumulate before the operations on them are finished and reach the end of the line. Another important requirement of the project is having a high enough success rate for picking up and placing the foam stickers consistently. We do not want the 2 workers on the line to constantly correct errors from the robotic collaborative arm and gripper. Additionally, as a special requirement from Exo-S engineers, the gripper solution

[2] This is a customer requirement

should not rely on complex control algorithms or vision systems. The robotic solution needs to also be utilizable with point-to-point robotic movements. The manufacturer typically works exclusively with "classic" industrial robots and points programming; they do not want something significantly different from their standard methods[3]. Finally, to facilitate operations with the gripper in the long run, the design, maintenance, and reparability of the solution should be taken into consideration. This can be interpreted as having reduced numbers of parts, using standard parts where possible, and ensuring simple assembly of the tool. Below is the list of industrial constraints:

Industrial constraints

- Respecting the cycle time of the production line, which is 45 seconds.
- Picking and placing at least five foam pads during the cycle time so the workstation can go from 3 workers to 2 workers.
- Having a high rate of success and a low rate of part rejection.
- Utilizing point-to-point programming. Ideally, no vision or other sensors to reduce complexity.
- The design should aim for a small number of parts and simple assembly.
- Ensuring easy maintenance and reparability of the gripper.

2.3 Collaborative Constraints

For Exo-S, this project was the first attempt at using a collaborative robotic arm at a Richmond plant. Therefore, it was the first robot to be working outside of a robotic cage and in proximity to workers. Without the need for a robotic cage or other security measures, the initial cost and complexity of the implementation could be reduced. Yet there are different security considerations to be taken when working with a collaborative arm. These considerations are derived from the norms on collaborative robots (ISO/TS 15066:2016) and the safety design

[3] For example, a vision system could be employed to identify the cardboard and foam on the working table. The workers would simply lay the cardboard on the table as they normally do. The robot would then identify the cardboard and then calculate a trajectory to pick up a foam pad from it. This approach requires more advanced control algorithms and introduces added uncertainties.

of end-effectors (ISO/TS 20218-1:2018) by the International Organization for Standardization (ISO). For our project, they are as follows:

Collaborative Constraints

- Reduced speed of movement: While an industrial robot can easily go up to 1000 mm/s, the end-effector of a collaborative robot is usually limited to 250 mm/s.
- The movement speed is further reduced to 100 mm/s if the tool has the potential for clamping human workers between the robot/EOAT and another part of the robotic cell or a fixture.
- The mass of the end-effector should be maintained at a minimum. A low end effector mass can reduce the potential energy transmitted upon impact.
- The geometry of the tool should be taken into consideration. The gripper should not have sharp edges/corners that could injure workers.
- The design should aim for the minimization of gripping forces needed to achieve adequate grasping of an object, instead of the maximum force available.
- Compliance linkages and mechanisms can absorb the energy of contact but should not introduce new risks.
- The grip force, quasi-static, and transient contact should not exceed body part limits as defined in ISO/TS 15066:2016.

A more complete risk assessment has been conducted on the finished end-effector. It is presented in Appendix II.

2.4 Summary

This chapter outlines the challenges, constraints and research sub-objectives related to developing a robotic end effector for foam pad manipulation tasks at Exo-S. The process is divided into picking up foam pads and applying them to plastic parts. Sub-objectives in the pick-up phase include stabilizing the cardboard sheets, the need for a peeling motion for detachment, and ensuring the foam does not stick to itself. In the application phase, the gripper must accommodate various foam sizes and shapes and apply them uniformly to different plastic parts.

Industrial constraints mandate a 45-second cycle time for picking and placing at least five different foam pads, thus enabling the reduction of manual labor by one worker on the production line. Moreover, the end-effector's design must be simple, maintainable, and compatible with Exo-S existing point-to-point programming methods, without requiring complex control algorithms or vision systems.

Collaborative safety constraints, which need to be applied and are guided by ISO standards, focus on worker safety considerations such as limiting the speed and force of the robotic arm. These constraints also ensure that the mass and geometry of the end-effector pose minimal risk.

The next section will delve into the literature review, which could offer inspiration and solutions for addressing these multifaceted constraints and research objectives.

CHAPTER 3

LITERATURE REVIEW

As of February 2023, scientific research that addresses the specific problem of foam pad sticker manipulation is rare. Some commercial products have characteristics close to the desired solution to our problem. For example "RoboTape", is a system that can be used to place several types of tapes on parts with complex geometry using a special robotic end effector (Figure 3.1). This system can also be used to place foam tape and cut it at desired lengths. Unfortunately, only one narrow band of foam can be placed at a time. Adapting this system to our problem would be challenging[2]. While there are no specific research articles for foam sticker picking, a 1999 article detailed a gripper design for picking up polyurethane foams (ZOLLER et al., 1999). Their gripper uses long needles to pierce the foam and lift it (Figure 3.2 a). A pneumatic cylinder extends or retracts the needles for a fast grasping and releasing time. The gripper holds the foam through the friction between the needles and the foam. Again, the literature on grippers that can

[1] Taken from Innovative Automation Inc. (2023). Retrieved from https://robotape.com

[2] Mostly because of the current format of foam pads coming from the supplier (cardboard sheets), but also the variety of sizes of the pads.

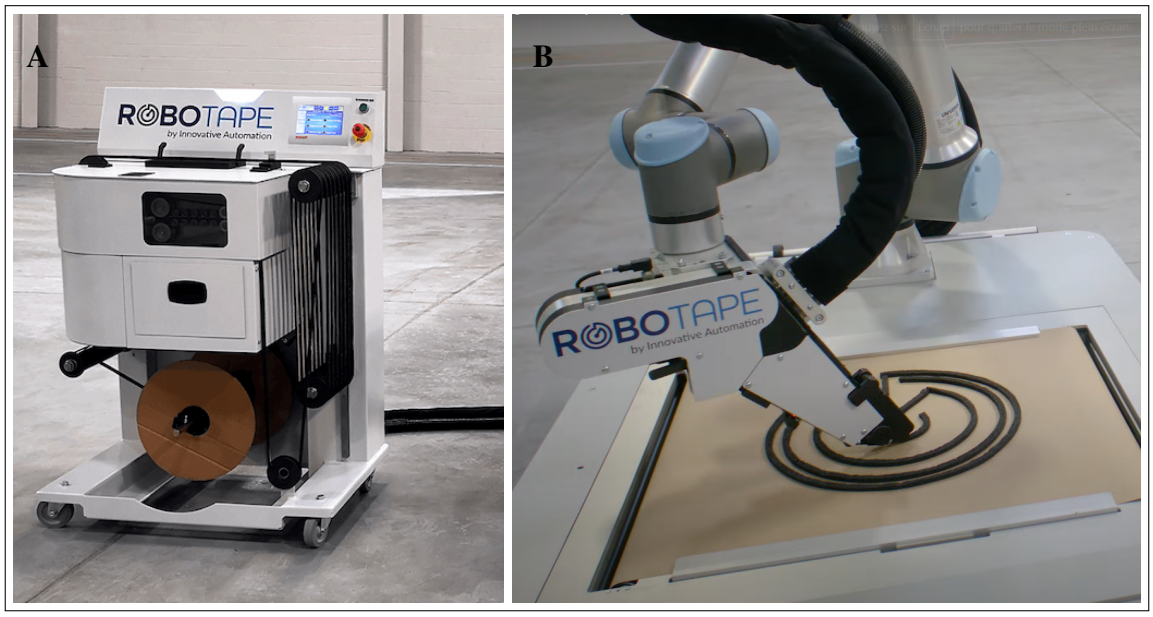

Figure 3.1 RoboTape system - A) Feeder - B) End-effector[1]

pick up foam seems slim. Unhelpfully, researching the term “foam” associated with “gripper” will return almost exclusively “foam grippers” results, which are vacuum grippers made of foam. Like a rubber vacuum cup, these foam grippers can mold themselves to different object shapes, sealing the vacuum in the process (see Figure 3.2 b). Interestingly, despite being the opposite of our proposed gripper solution[3], it indicates that we can use the malleability of the foam to our advantage[4]. Broadening the search, we arrive at the robotic research fields of “deformable objects”, “fabric/textiles” and “food products” manipulation. The first field of research studies the modeling, perception, and control of deformable objects. Research articles in this category primarily aim to find optimal control strategies to manipulate them. Control tasks include grasping clothes, folding clothes, avoiding obstacles, cabling, etc. Most emphasis is placed on control algorithms instead of specific grippers. Recent studies in this field often employ more learning-based methods, reinforcement learning, and neural networks [5]. Unfortunately, these methods are likely not sufficiently effective or robust for our industrial setting.

[3] These types of grippers pick mostly rigid objects using foam, contrary to our solution that picks the deformable foam with a rigid gripper.

[4] Indeed we use the deformability of the foam pads to better seal the vacuum. This is discussed more in detail in Chapter 5 - Pneumatic grasping Tests

[5] One of the observation from a meta-analysis in this field (Yin, Varava, and Kragic, 2021)

[6] Image A) taken from ZOLLER et al. (1999, p. 237). Image B) Taken from FPE Automation Inc. (2023), retrieved from https://www.fpeautomation.com/piabs-kenos-kcs-gripper-for-collaborative-robots

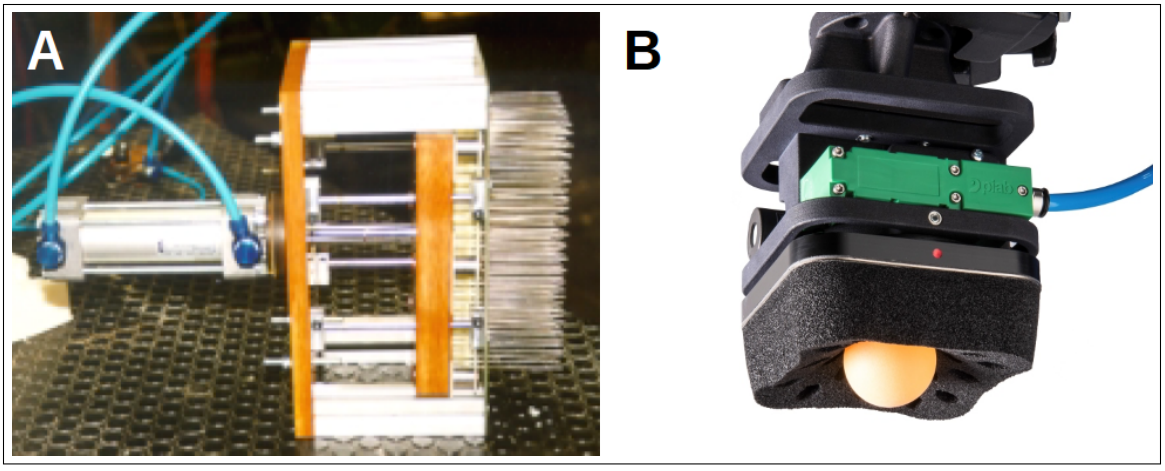

Figure 3.2 A) Gripper made to pick up foam - B) Industrial gripper[6]

Moving on to the research fields of fabric and food handling, we find more examples of specialized grippers. In terms of similarities to foam pads, textiles share more characteristics than food products do. Fabrics can be thin and porous, just like foam pads. Thus, technologies used for fabrics could potentially be adapted to address our grasping problem. Subsequent sections present different gripper technologies potentially suitable for handling foam pad stickers. As expected, these types of grippers often originate from the fabric handling research field.

3.1 Gripper Technologies

Koustoumpardis and Aspragathos (2004) offer a comprehensive classification of various gripper technologies for fabric handling, including mechanical, pneumatic, electrostatic, adhesive, and velcro. These categories encompass various interesting gripper technologies that could potentially handle foam pads. The subsequent sections focus on the gripper types falling under the first three categories, as they are the most promising options.

3.1.1 Mechanical Grippers

Grippers that use solely solid parts to pick up objects are part of this category. Perhaps the most classic example is the two-fingers pinching gripper. It can lift a wide range of objects, given that the objects fit in the gap of the fingers. Mechanical grippers also include needle grippers that pierce the object to be handled.

3.1.1.1 Pinch Grippers

Multiple companies offer pinch grippers, including Robotiq, Schunk, PHP Inc, Festo, and IRP worldwide (examples in Figure 3.3). Birglen and Schlicht (2018) conducted a statistical review detailing the common specifications of these industrial grippers. Here are some of the key characteristics:

- Stroke length from 1mm to 50mm.

[7] Image A) taken from Robotiq (2023), retrieved from https://robotiq.com/products. Image B) taken from Festo Ltd. (2023), retrieved from https://www.festo.com/ie/en/p/parallel-gripper-id_DHPS

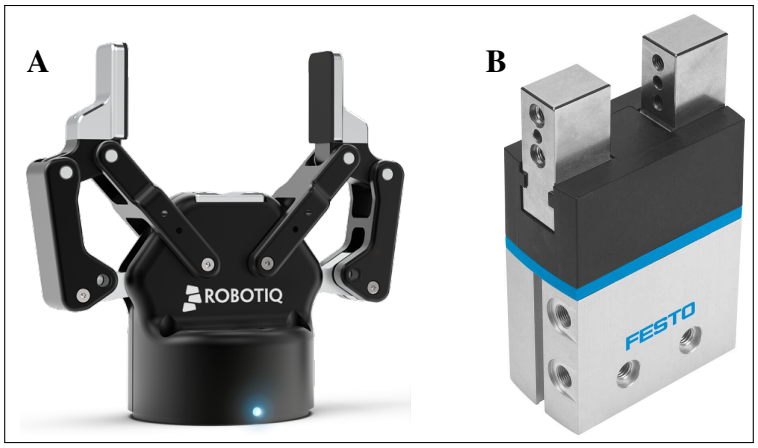

Figure 3.3 A) Robotiq gripper - B) Festo parallel gripper[7]

- Clamp force from 100 N up to 4000 N.
- Weight from 0.1 kg to 10 kg.

This is to say that there is a wide range of sizes for pinch grippers already available from robotic equipment manufacturers. This type of gripper can also be used to pinch fabric from the top (Taylor et al., 1996) (figure 3.4 a). Besides commercially available mechanical grippers, there is also a variety of other designs studied by academics. These range from designs featuring multiple articulated fingers (Koustoumpardis et al, 2014) to soft robotic grippers (Teeple et al, 2022) (Wang, 2020) (Figure 3.4 B, C, and D). All have in common that their way of securing the grasp is by pinching/clamping the object. When handling fabric, a main disadvantage of pinching is that it creates folds, which can stay in place after the grasp (Koustoumpardis and Aspragathos, 2004, p. 231). If we consider the foam alone, this might not be a problem since it will takes back its original shape. Nevertheless, with its adhesive backing, the folds/wrinkles could make the foam pad stick to itself. As explained in the challenges section, this is undesirable because the foam pad would be unusable afterward. Fortunately, in contrast to fabric, the foam's thickness and deformability make it possible to secure a grasp without necessarily introducing folds in the foam pads (as discussed in Section 4.2.3). Pinch grippers can furthermore qualify as non-intrusive mechanical grippers, contrary to the next type, which are needle grippers.

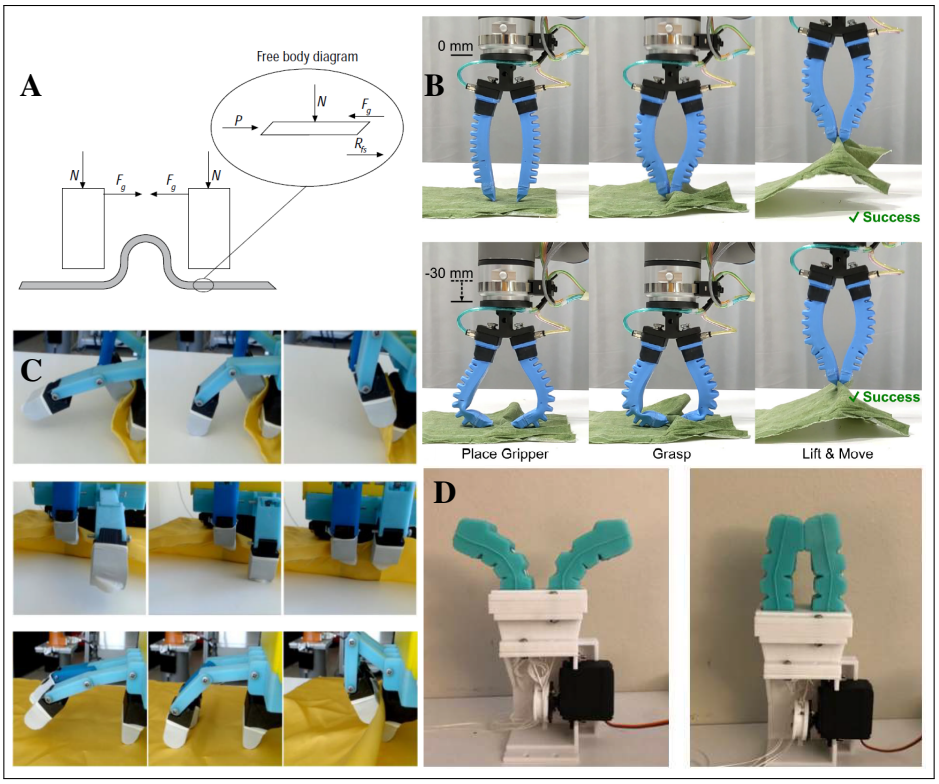

Figure 3.4 Grasping of fabric with mechanical grippers - A) Forces diagram of two fingers pinching a piece of fabric, note that the friction with the table is an important parameter - B) Soft finger gripper - C) 3 fingers gripper for fabric - D) Soft finger gripper[8]

3.1.1.2 Needle Grippers

Needle grippers are commonly used for handling textiles or other materials that are soft enough to be pierced by needles (Figure 3.5 a). The most common configuration has the needles pointing in opposite directions at an angle. This way, the force exerted by the extending needles is equivalent on each side and they can penetrate the material without moving it. EMI, a needle gripper manufacturer, describes these grippers as suitable for the textile and food industry and specially adapted for handling highly porous materials that are hard to grab with vacuum cups[9]. Unsurprisingly, the main disadvantage of this type of gripper is that it can cause damage to the

[8] Image A) taken from Taylor et al. (1996, p. 18), image B) taken from Teeple et al. (2022, p. 731), image C) taken from Koustoumpardis et al. (2014, p. 8), and image D) taken from Wang (2020, p. 97).

[9] From EMI Corporation. (2023), a needle grippers manufacturer (https://www.emicorp.com/products/214/Needle-Grippers/).

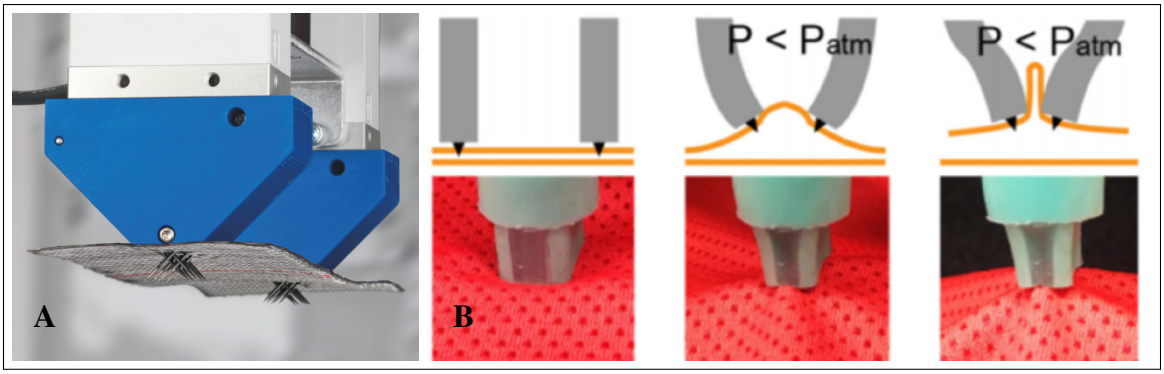

Figure 3.5 a) Industrial needle gripper - b) Experimental Micro needle gripper[10]

object being handled, especially if it is being grasped repeatedly. Our foam picking application only requires a single pick and place, if the foam doesn't tear while being unstuck the damage might be negligible. Microneedles can also be used to mitigate this damage. An example is the gripper created by Ku et al. (2020) that uses a combination of a vacuum and small 0.5 mm long needles to lift fabric (figure 3.5 b). Another evident disadvantage of needle grippers is that they can't be used for collaborative robotics because of the risk of injury. Although direct contact between the gripper and a human worker is not intended in a collaborative workstation, sharp or cutting edges or needles should not be present in the potential area of contact between the operator and the robot system (ISO 15066:2016 Robots and robotic devices — Collaborative robots, p.16).

3.1.2 Pneumatic Grippers

Pneumatic grippers rely on negative pressure (vacuum) to lift objects. Usually, the vacuum created is not perfect and can be quantified by a percentage[11]. There is also a theoretical limit to these grippers: for a perfect vacuum, the maximum lifting force per unit area equals the atmospheric pressure (101 kPa). Technologies that create a vacuum have a trade-off between

[10] Image A) taken from Schmalz India Pvt. Ltd. (2023), retrieved from https://schmalzindia.tradeindia.com/sng-needle-grippers-6979683.html. Image B) taken from Ku et al. (2020, p. 4853).

[11] A 100% vacuum is equivalent to a perfect vacuum, which represents a negative pressure of -1 atm relative to atmospheric pressure.

the percentage of vacuum and air flow rate. As shown in Figure 3.6, in general, a high vacuum percentage means a lower flow rate and vice-versa (Fleischer et al, 2016). There are multiple ways of creating a vacuum and various forms that can take the gripping device. One of the most recent and detailed reviews has been done by Mykhailyshyn et al., (2022). Here we will focus on technologies that can still create a vacuum while the material handled is somewhat permeable to air. Since the foam on the pads is open cell[12], it is permeable to air and a constant flow can go through it. Thus, technologies that do not rely on a central compressed air supply or vacuum pumps are not well suited for our problem (such as the one studied by Schaffrath et al., 2021). Examples of these unsuited grippers are shown in Figure 3.7. This leaves us with two categories of pneumatic gripper principles: vacuum and air jet. Koustoumpardis and Aspragathos, (2004) have also chosen only these two categories in their systematic review of fabric grippers.

[12] In foam materials, "cells" refer to the tiny pockets of gas, usually air, that give the foam its structure and cushioning properties. Closed-cell foam has sealed cells, making it less permeable to air. Whereas Open-Cell foam has broken cell walls, making it more permeable to air.

[13] Taken from Fleischer et al. (2016, p. 575)

[14] Taken from Schaffrath et al. (2021, p. 78)

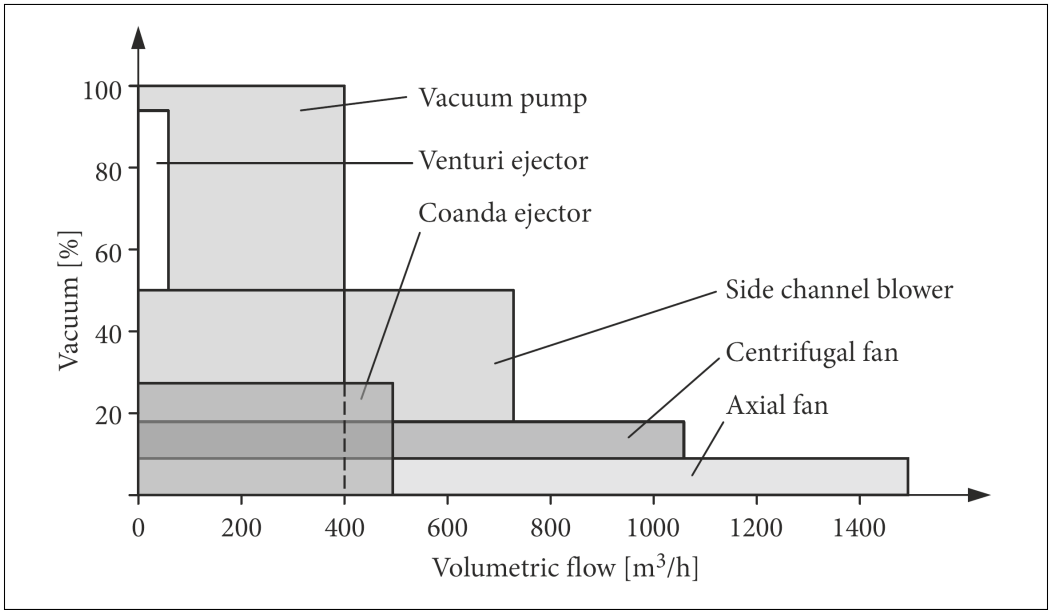

Figure 3.6 Flow rate and vacuum levels of different negative pressure sources[13]

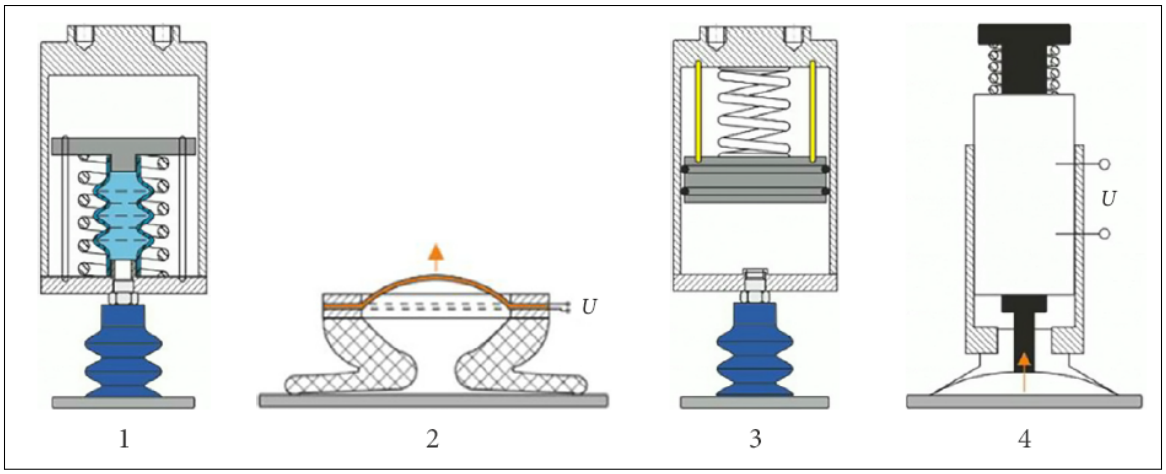

Figure 3.7 Example of unsuited pneumatic grippers for our application (Pneumatic gripper without "continuous" negative pressure supply) - 1) SMA wire - 2) Dielectric elastomer actuator - 3) Twisted nylon fibers - 4) Electric hoisting, lifting magnet[14]

3.1.2.1 Vacuum Grippers

This category of grippers uses vacuum generators or vacuum pumps as a source of negative pressure. Usually, the grippers have a chamber with contours that make direct contact with the

[15] Images A) to F) taken from Fujita et al. (2018, p. 284), and image G) taken from Gabriel et al. (2020, p. 549)

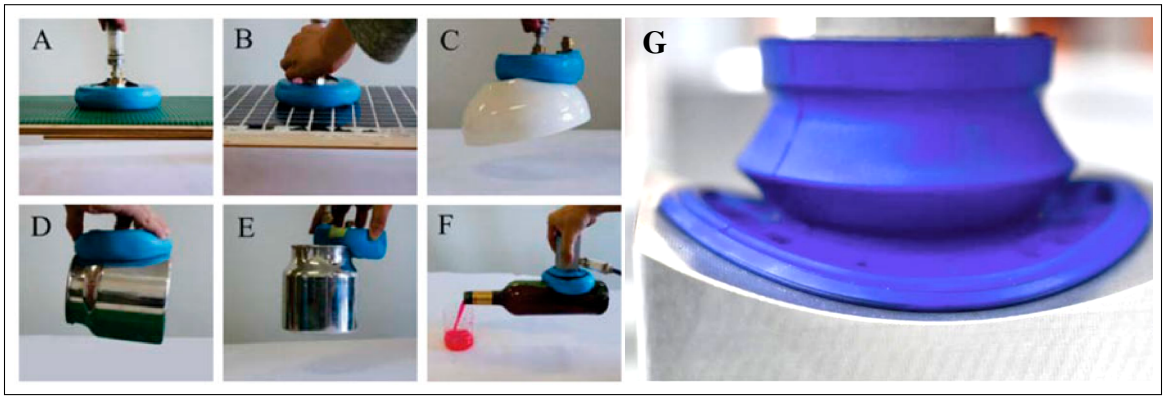

Figure 3.8 Deformable vacuum chambers - A) to F) "Universal Vacuum Gripper" which uses the jamming transition of coffee powder inside a contour balloon to seal an uneven surface - g) Experimental setup to study a rubber vacuum cup on different shape configurations[15]

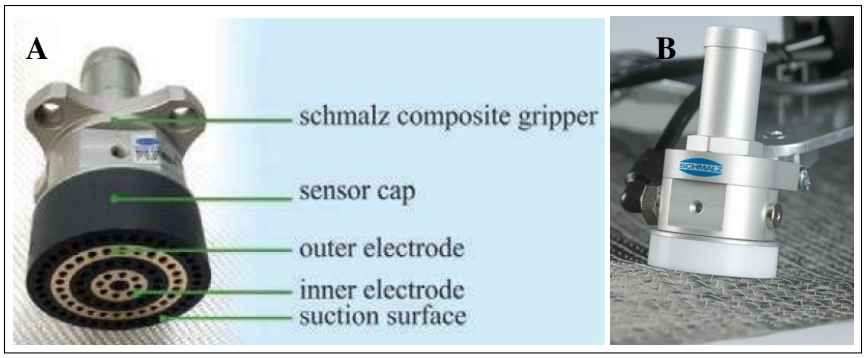

Figure 3.9 Conda vacuum grippers with small openings. - A) Vacuum gripper with pressure sensors optimized for compressed air consumption - B) Schmalz "flow gripper"[16]

grasped object. To maximize the vacuum force, it is sometimes important that the contour creates a seal between the chamber and the object grasped. This is why many grippers use flexible material as illustrated in Figure 3.8. Even so, many materials are too permeable and will prevent the creation of a high vacuum because of the air going through them. Furthermore, flexible materials can be sucked into the gripper if the vacuum opening is too big. This is why it can be more effective to grasp highly flexible materials with a multitude of smaller openings rather than one large one. Fleischer et al. (2016) optimized a gripper of this type for fabric handling (Figure 3.9). While the shape and material of the gripper are important, the choice of the right vacuum source is also crucial. Vacuum technologies cover different ranges of vacuum percentage and airflow level, as illustrated in Figure 3.6. Commonly in robotics, vacuum generators such as the Venturi ejector are often preferred (Figure 3.10). This is probably due to the simplicity of the design; they do not have moving parts like vacuum pumps, are low-maintenance, and can be rapidly activated. Additionally, they use the energy of compressed air to create a vacuum that can reach 80%. If the application needs a high flow rate more than a high vacuum percentage, a Coanda gripper may be preferable. Like the Venturi effect, the Coanda effect can be used to generate negative pressure simply from a compressed air source. Coanda grippers, also called flow grippers, usually consume more compressed air for the same lift force as Venturi-based grippers.

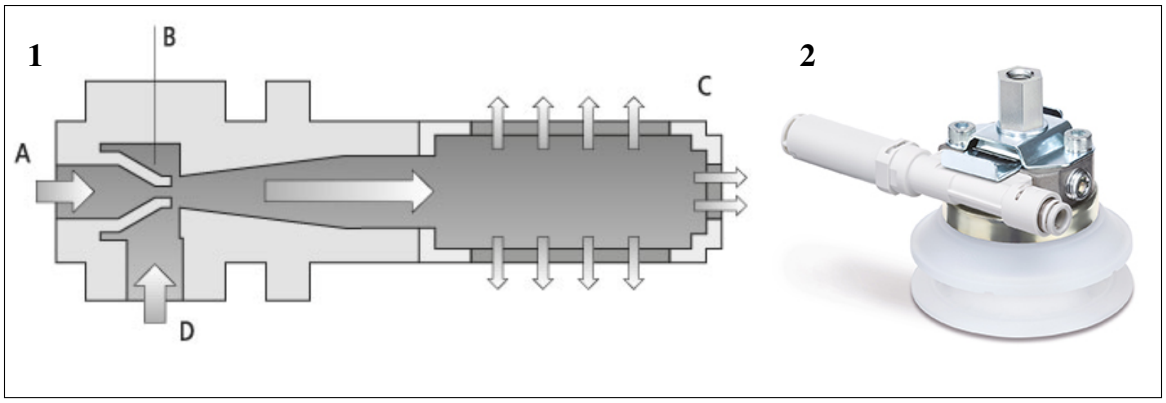

Figure 3.10 Venturi vacuum generator or "Venturi ejector" - 1) Pneumatic diagram of a Venturi vacuum generator: A is the compressed air source, B the low-pressure chamber, C is the atmospheric pressure air output and D is the negative pressure flow - 2) Vacuum cup robotic end effector with a Venturi ejector directly on it[17]

3.1.2.2 Air Jet Grippers

Jet grippers use the Bernoulli effect to generate negative pressure. This effect occurs when airflow is accelerated: the energy transported by air shifts from potential energy (pressure) to kinetic energy (speed of the airflow), resulting in a decrease in local pressure. Bernoulli grippers use this effect to lift objects, sometimes without any direct contact with them (Liu et al., 2020). When compared to other suction technologies, they demand more energy for the same lift force but can lift porous, more brittle, and more easily deformable materials than other pneumatic grippers (Mykhailyshyn et al., 2022). Figure 3.11 illustrates objects which can be grasped by this type of gripper. There are three different configurations of jet grippers for grasping flat objects:

- Downward ejection
- Side ejection

[16] Image A) taken from Fleischer and al. (2016, p. 576). Image B) taken from Schmalz (2023), retrieved from https://www.schmalz.com/en/vacuum-technology-for-automation/vacuum-components/special-grippers/flow-grippers/flow-grippers-scg-306274

[17] Image 1) taken from Schmalz (2023), retrieved from https://www.schmalz.com/en/vacuum-knowledge/the-vacuum-system-and-its-components/vacuum-generators/vacuum-ejectors. Image 2) taken from SMC Corporation of America (2022), retrieved from https://www.smcusa.com/products/zhp-vacuum-pad-with-generator~133355/

- Vortex

The downward ejection configuration is the simplest design (see Figure 3.12 A). It consists of a hole surrounded by a flat surface. At a distance, the gripper pushes, rather than pulls, the object to be grasped. Lifting only occurs when the gripper is close enough so that the air is accelerated radially. Dini and al. (2009) found that this simple configuration generates the highest lifting force when grasping a smooth object. For rough and porous objects, the side ejection configuration is more suited for the task. Given that the foam pads aren't smooth, we can hypothesize that a side ejection configuration is also preferable for our gripper application. The side ejection configuration is a little more complex to manufacture owing to the internal deflector's presence and the small gap required between the parts (as shown in Figure 3.12 A). Lastly, it is also possible to create a vortex by accelerating air to generate negative pressure. To create the vortex, a jet of air shoots out sideways inside a cylindrical chamber, thus moving the air inside in a circular motion (Figure 3.12 C). At the level of the grasped object, the air still escapes radially like the other design. An experimental comparison between a Bernoulli gripper (direct ejection types) and a vortex gripper was conducted by Li et al. (2015). While the Bernoulli gripper consumed more compressed air, the vortex gripper required a higher pressure for the same lifting forces. As seen in Figure 3.13, the pressure distributions under both grippers are comparable. From a geometrical standpoint, due to its cylindrical cavity, the vortex gripper is not suited for applying uniform pressure on the grasped object. Therefore, foam pad stickers are unlikely to be applied using this type of gripper.

3.1.3 Electroadhesion Grippers

Electroadhesion (EA) grippers use high voltage to generate electrostatic forces. Typically, these grippers consist of alternating negative and positive electrodes, separated by a thin dielectric substrate layer. When an object is close enough to the EA gripper, electrical charges move

[18] Image A) taken from Vuototecnica (2023), retrieved from https://www.vuototecnica.biz/cup.php. Image B) taken from Liu et al. (2020, p. 742).

[19] Taken from Li et al. (2015, p. 2086).

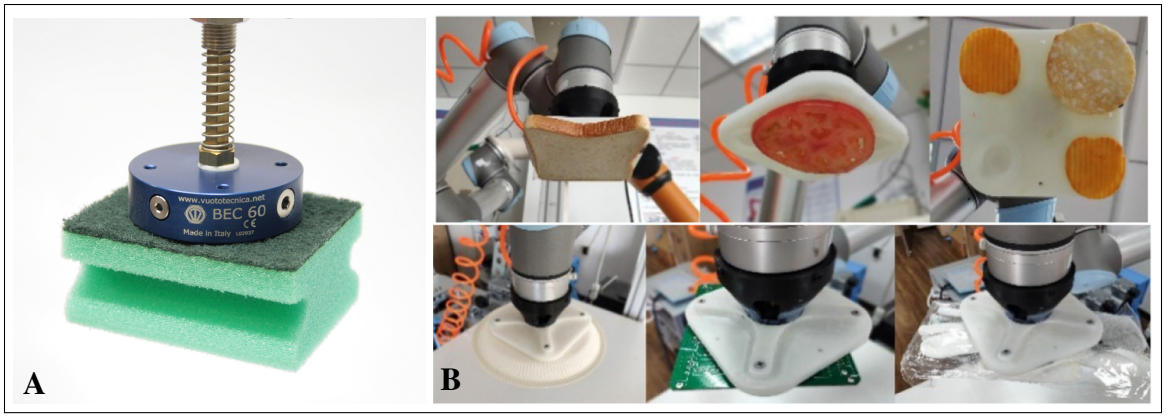

Figure 3.11 a) Bernoulli gripper lifting a sponge - b) Experimental quadruple Bernoulli gripper lifting various objects[18]

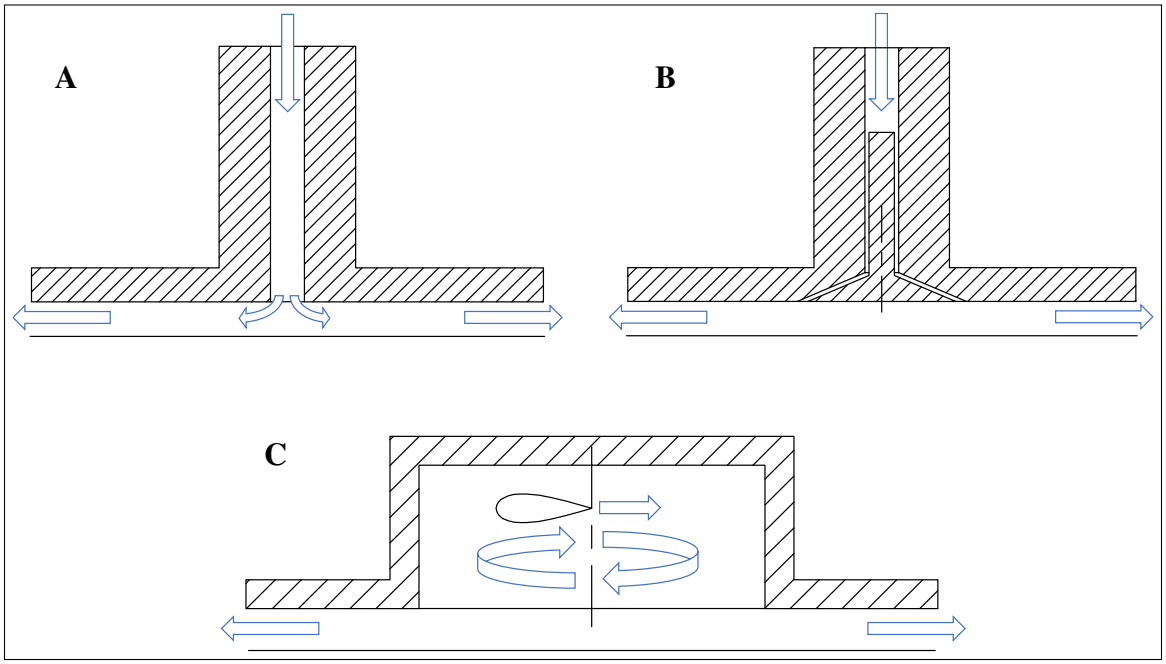

Figure 3.12 Air jet gripper types: A) Downward ejection, B) Side ejection, and C) Vortex

toward the electrodes from within the object's material, which in turn creates a lifting force (see Figure 3.14). EA has many advantages compared to other lifting technologies:

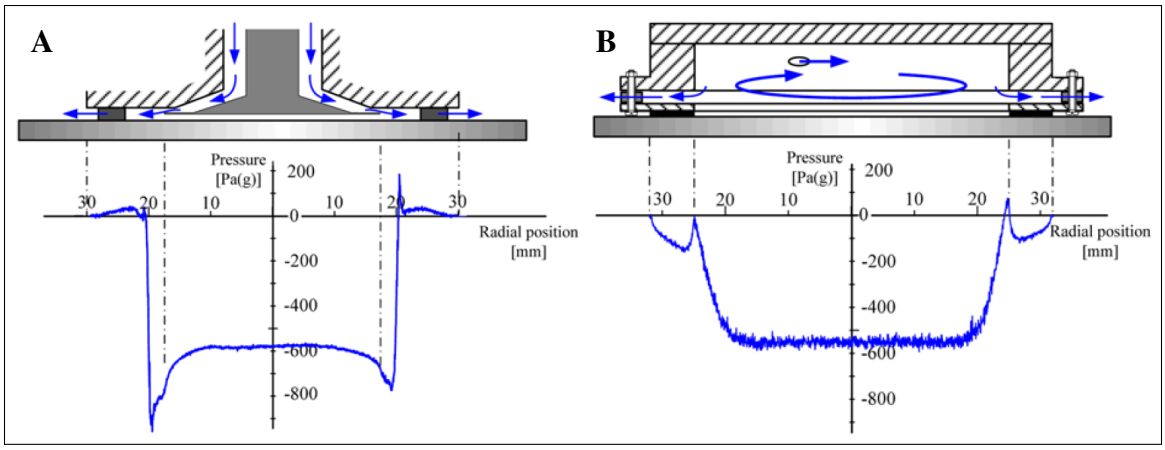

Figure 3.13 Pressure distribution under a Bernoulli gripper (A) and a vortex gripper (B)[19]

- It uses mechanically lightweight and simple materials and structures, unlike some alternative gripping devices that commonly use energy-intensive pumps or compressors (Guo et al., 2016).
- It can adhere to or lift almost any material, both insulator and conductor. EA enables systems with low energy consumption, as only a minimal electrical current usually flows through the EA pad despite the application of a high voltage (Guo et al., 2020).
- EA can also lift delicate and high-value objects through noncontact suspension or soft EA pads. For example, semiconductor silicon wafers for electronics can be handled by using that method (Asano et al., 2002)

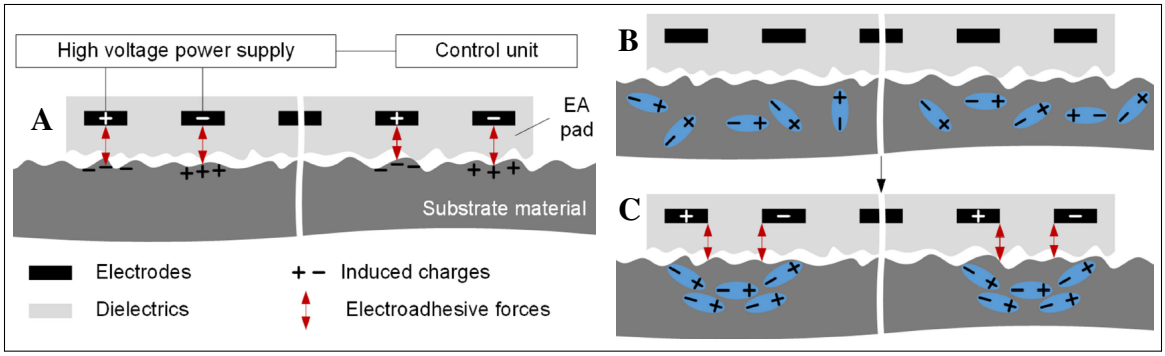

Figure 3.14 Cross-sectional perspective diagram of an EA system. - A) Electroadhesion involving conductive substances. - B) & C) Electroadhesion involving insulating materials. The symbol "+" indicates positive charges, while "–" represents negative charges[20]

The main disadvantage of EA technologies is the very limited force per unit area that they can generate (Rajagopalan et al., 2022). West and al. in 2020 focused on optimizing a square EA gripper design; the optimal EA design they tested produced a mere 0.22 kPa of lifting force. Often to counter the low normal force, EA pads are used in a shear configuration, which greatly enhances the lifting capability of these devices (see Figure 3.15 A, B, and C). Unfortunately, this shear configuration has not been employed for highly deformable objects like fabric. EA grippers made for handling fabric must rely solely on the weak normal force they can generate (He et al., 2022) (see Figure 3.15 D). Due to its deformable nature, this limitation probably applies to foam pads as well. Furthermore, EA is certainly not suitable for unsticking the foam pads from the cardboard, due again to the low lifting force. Still, it would probably be strong enough to secure the foam pads while the gripper is in motion, thus preventing any dangling. Compared to pneumatic grippers, EA grippers might offer significantly better energy efficiency and cost savings for this part of our solution. Additionally, although these grippers typically use high voltages ranging from 600V to 6000V, the charged electrodes are insulated with a thin layer of dielectric substrate. Moreover, the devices that supply the high-voltage DC power to these grippers typically draw only minimal currents in the order of a few mA (Rajagopalan et al., 2022). Thus, even in the event of a short circuit, direct contact with the electrodes would feel like a static electricity shock.

3.2 Sticker Grippers

In the previous sections, we reviewed lifting technologies that could be suitable for manipulating foam pads. As noted earlier in this review, there are no specific scientific articles describing a solution for our specific problem, nor are there any specific existing products meeting all the project's constraints and requirements. This section delves into the "sticker part"; the backing underneath the foam pad stickers. Therefore, robotic systems capable of picking up or applying "sticker-like objects" are reviewed.

[20] Taken from From Guo et al. (2020, p. 313).

[21] Images A) and B) taken from Shintake and al. (2016, p. 232), image C) taken from Prahlad and al. (2008, p. 3032), and image D) taken from He and al. (2022, p. 2411).

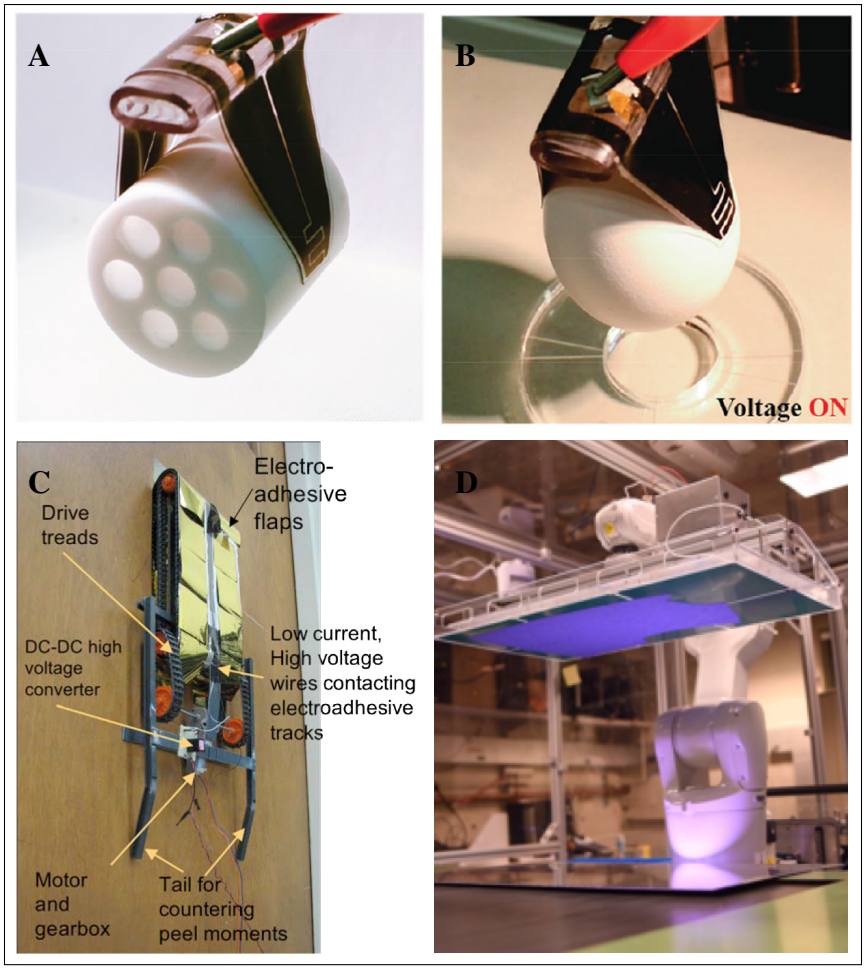

Figure 3.15 Electroadhesion application examples - A) and B) EA soft gripper - C) EA wall climbing robot - D) EA gripper for fabric[21]

3.2.1 Sticker Pickup

A related problem studied in the context of robotic unsticking is the removal of the prepreg's backing paper, which is a protective layer on composite fiber sheets (see Figure 3.16 A and B). Björnsson et al. (2013) explored potential methods of automating the removal of this backing layer. They determined that merely using a vacuum cup was inadequate. A preliminary separation of the backing from the composite was necessary before the vacuum cup could detach the backing using a peeling motion. Despite the differences between the backing and foam pads, a similar challenge was evident in both situations: the vacuum strength is insufficient to separate

the “sticker part” at the edge; a different approach is needed to initiate the separation. After the initial separation, the vacuum was sufficient when used in a peeling motion to lift the backing paper. For the initial detachment, Björnsson suggested combining mechanical and vacuum methods, a strategy we also adopted. Björnsson et al. explored two separate methods to initiate the detachment of the prepreg from its backing paper. The initial method utilized compressed air to facilitate separation at the interface. A needle is employed to puncture the backing paper, after which compressed air is blown underneath it to promote the separation (see Figure 3.16 D).

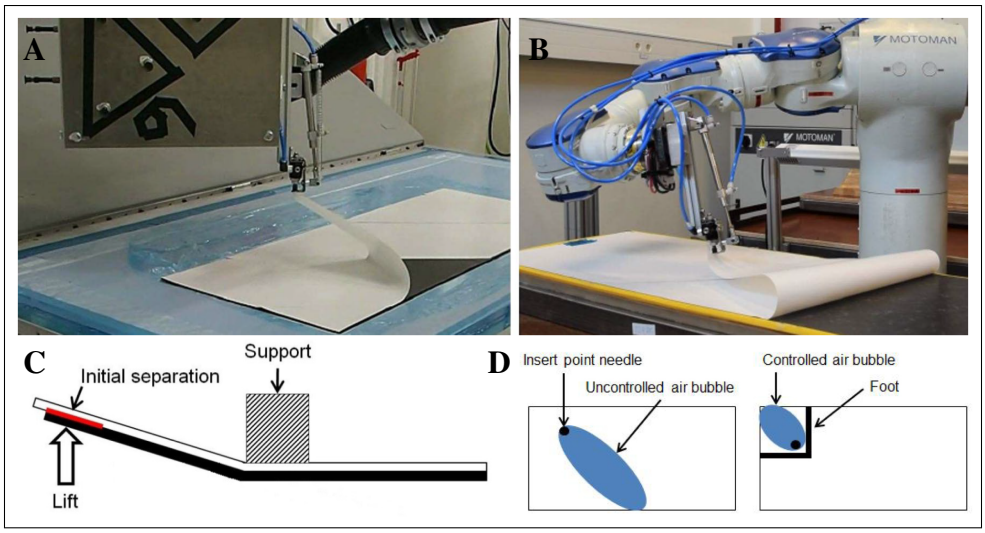

Figure 3.16 A) and B) Examples of prepreg backing paper removal by a robotic end effector - C) and D) Proposed ways of creating an initial separation of the backing paper[22]

The second method involves controlled mechanical bending of the layers, replicating the manual separation procedure typically executed by operators (see Figure 3.16 C). Beyond prepreg backing paper removal, robotic tools for unsticking are also prevalent in the labeling industry. Unlike the previous prepreg application, in the labeling industry, labels are often unstuck using a specialized tool first and then picked up by a robotic gripper that applies them to an object afterward. The specialized tool, often referred to as a “label dispenser,” which automatically dispenses labels one by one, is a well-established technology (see Figure 3.17 A for an example). Such a dispenser mechanism can even be integrated into the end-effector, like the one developed

[22] Images A) and B) taken from Björnsson and al. (2017, p. 447). Images C) and D) taken from from Björnsson and al. (2013, p. 8).

by Lin and al. (2016, Figure 3.17 B). Typically, a roll of labels is loaded into the label dispenser. The loading process involves placing the roll onto a spindle or holder and threading the labels through the dispenser mechanism. After loading, the dispenser mechanism facilitates the separation of the labels from their backing. This separation is often achieved by maneuvering the material over a sharp angle (for example in Figure 3.17 A).

3.2.2 Sticker Application

The application of stickers can also be considered a part of the labeling industry. When using a robotic arm, labels are retrieved from a dispenser using a specialized gripper before being applied to a box or other item. CAB, a robotic equipment manufacturer, provides two gripper models capable of this operation. Both utilize negative pressure and feature compliance: one is constructed from a flexible material (see Figure 3.18 A and B), while the other incorporates a roller, also constructed from a flexible material (see Figure 3.18 C). Added compliance seems to be frequently used in research for applying adhesives on solid surfaces. For example, a robotic tape applier end effector was developed by Yuan and al. in 2018 and 2020 (see Figure 3.18 D). According to the author: "the spring mechanism of the taping tool provides passive compliance for the robot to avoid hard contacts and thereby protect the taping tool and the workpieces." They further increased this compliance by having a High-density polyethylene (HDPE) roller at the tool's tip, enabling the tool's tip to conform to the shape of the part being taped. Indeed, industrial and collaborative robotic arms are practically perfect "position source" because of the high gear ratio inside the joints. This makes them difficult to use for applying force on rigid objects without "crashing" them or triggering a torque limitation violation error. In contrast, robots designed as a more optimal "force source"[23] would likely not necessitate such additional compliance.

---

[23] For example, a robotic joint actuated by an electrical motor with a small gear ratio, or a hydraulic/pneumatic actuated joint.

[24] Image A) taken from CAB (2023), retrieved from https://www.cab.de/en/marking/label-dispenser/hsvs/. Image B) taken from Lin and al. (2016, p. 5).

[25] Images A) to C) taken from CAB (2023), retrieved from https://www.cab.de/en/news/news/robotic. Image D) taken from Yuan et al. (2018, p. 4107).

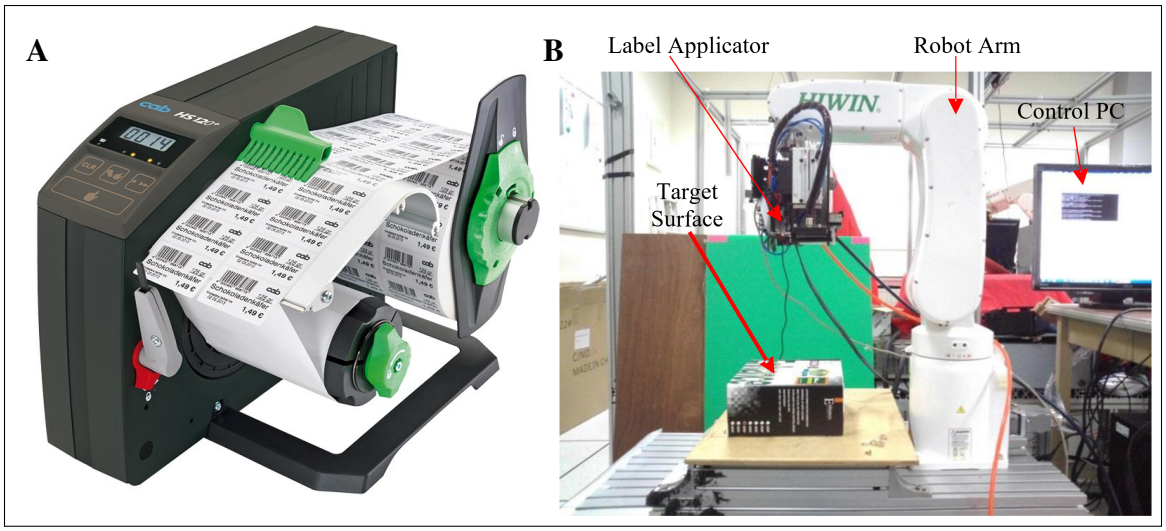

Figure 3.17 Examples of label dispensers - A) CAB electric label dispenser - B) Robotic end effector label dispenser and applicator[24]

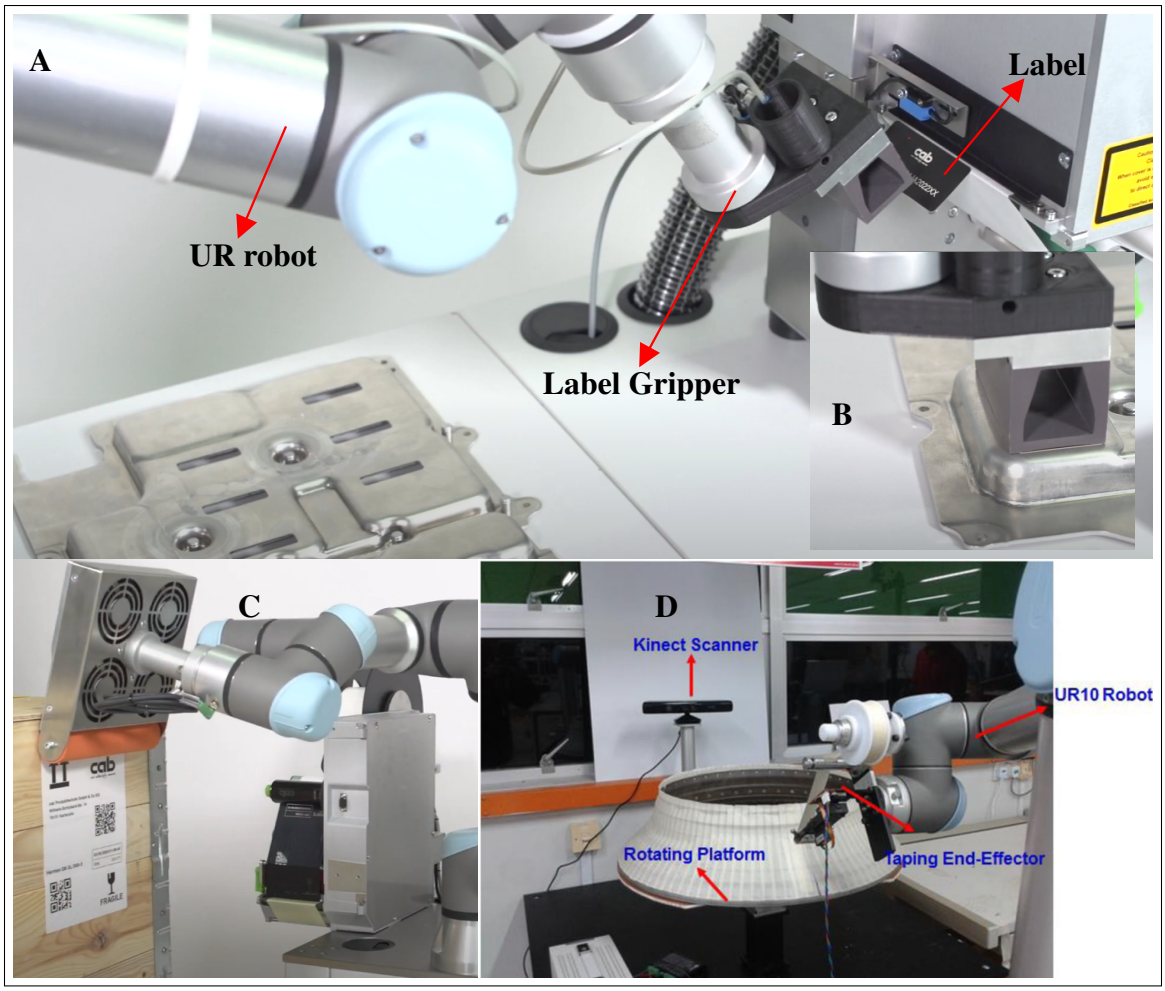

Figure 3.18 Examples of grippers for sticker-like object application - A) Robotic setup for a compliant CAB label gripper - B) Application of the label on a part - C) Another type of CAB label gripper with a compliant roller for application (orange part) - D) Experimental setup of the "Automatic robotic taping system with compliant force control"[25]

CHAPTER 4

SOLUTION DETAILS

4.1 Overview

Drawing upon industrial constraints and existing gripper literature, we have made design choices to develop an end-effector. The components of it are described in detail in section 4.2 (Design choices). We have chosen to tackle our challenge with an end-effector that has 5 different grippers, one to pick and place each of the foam pad stickers. Additional features of the solution are enumerated in the subsequent bullet points:

- Every gripper has a clamp to firmly secure the foam during the unsticking.
- Every gripper has a negative pressure mechanism to fix the foam pad into place on the gripper while moving.
- For the medium and large foam pads, a curvature in the gripper helps with the pickup and application operations.
- Every gripper has added compliance that also facilitates the pickup and application.
- The gripper's main parts acts as pneumatic manifold to reduce the complexity of the end-effector.
- Fixing of the foam pad cardboards is achieved with specially designed vacuum plates.
- Admittance control can be used to apply the foam pads with a predetermined force if necessary.

Figure 4.1 shows the 3D model of the end-effector on a UR10, the different grippers (in red), and a close view of the end-effector with and without the top parts. Figure 4.2 shows images of the gripper installed on a CRX-20A in "real life" to evaluate the system in production.

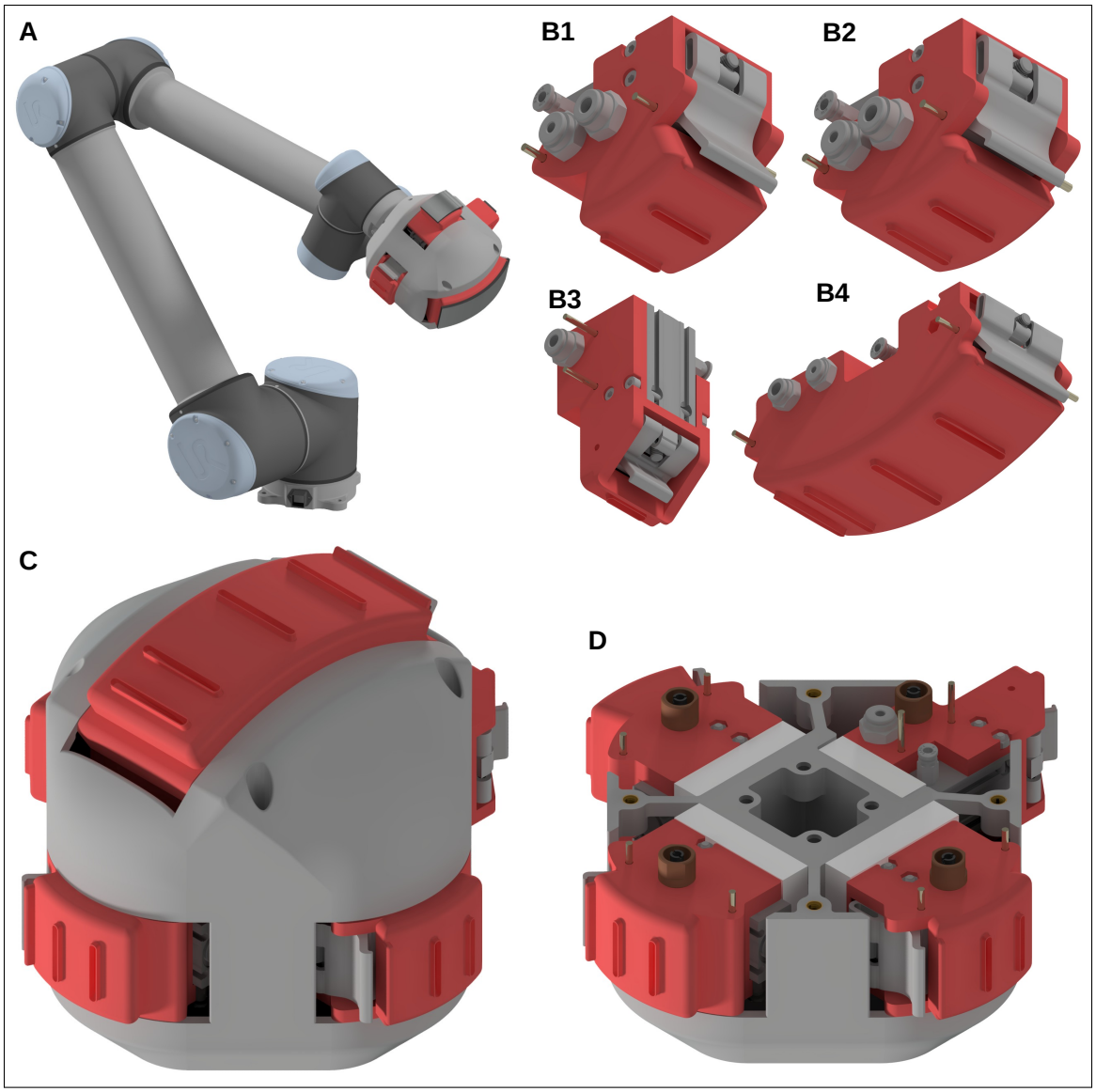

Figure 4.1 CAD model views: - A) End-effector mounted on a UR10 - B) The four variants of the gripper: B1 & B2 are for the medium foam pads but different parts, B3 is for the small foam pad, and B4 is for the large foam pad (not to scale) - C) Close-up view of the end-effector - D) View of the end-effector without the top parts

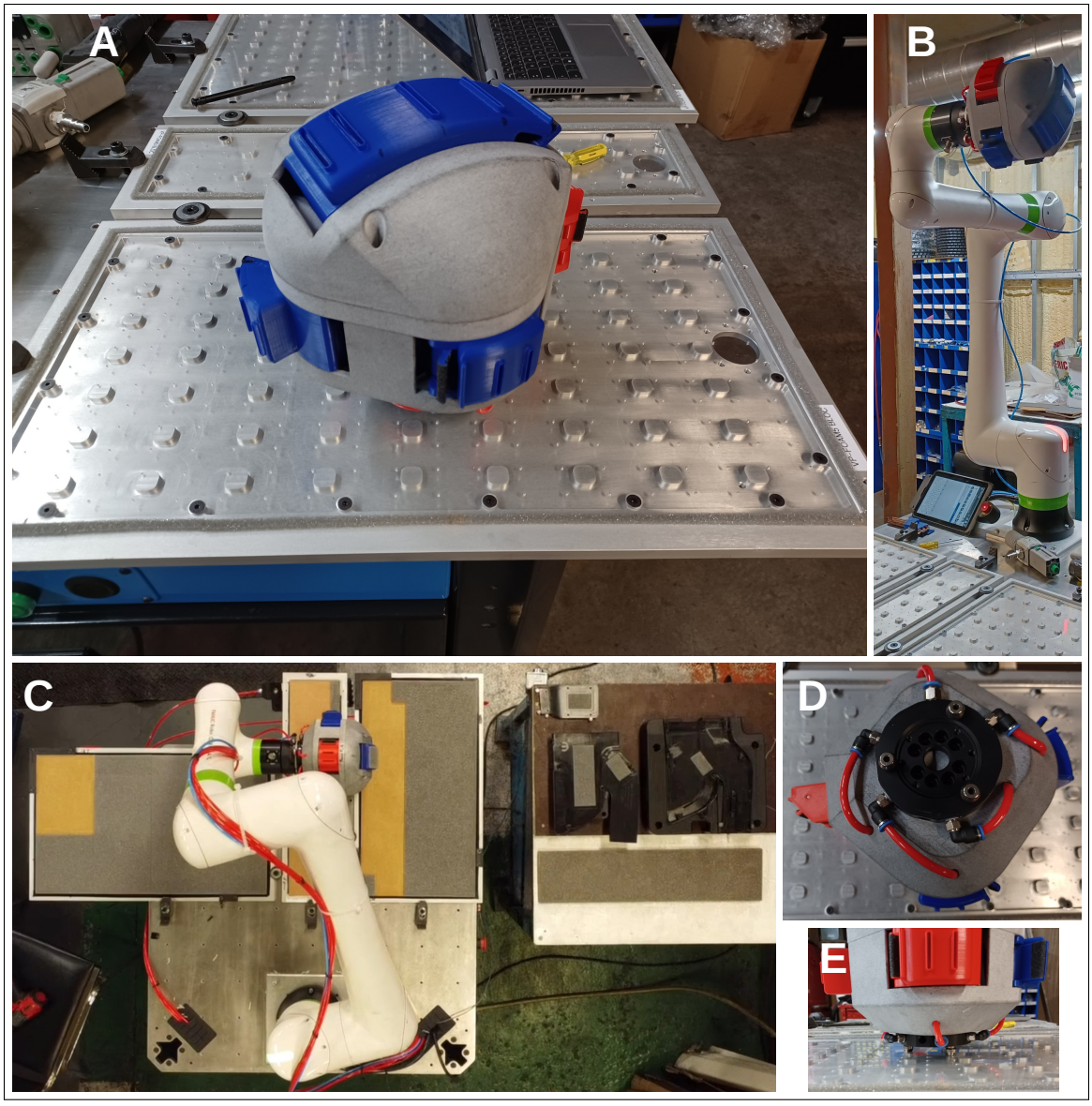

Figure 4.2 Real setup views: - A) Close-up view of the end-effector on one of the vacuum plates - B) End-effector installed on a Fanuc CRX collaborative robot - C) Top view of the setup for testing the system in production. The robot is picking up the small foam on one of the cardboard pieces held by its vacuum plate (on the left). The parts with the foam pads on them are about to be changed with new ones (on the right). - D) and E) Views of the pneumatic coupling system installed underneath the end-effector (pneumatic lines are the red tubes). This system serves for quickly connecting and disconnecting the tool

4.2 Design choices

With the constraints detailed in the *Problem Overview* and the gripper technologies described in the *literature review*, we are poised to discuss the design choices. In this section, we explain in detail each component of our solution and the rationale behind each choice.

4.2.1 Type of the solution

The main industrial objective of the project was to make a robotic end effector that can unstick five foam pads and place them on different parts. Given the range of sizes of the foam pads[1] and where they need to be placed on the parts, it would have been hard to make a gripper that can adapt to every task. Furthermore, the time limit of 45 seconds means that the five foam stickers need to be picked up at the same time, and then placed on the parts[2]. Thus, the end-effector needs to have five grippers for each of the foam pads, if the collaborative speed limits are to be respected[3]. These five grippers could have been the same, adaptable to every foam pad. There are two problems with this approach. First, the minimum size of the grippers would have been constrained by the bigger foam pad, which means more weight and a bigger final end-effector. Secondly, given the geometry of certain parts, the gripper would probably need additional mechanisms to adapt to every situation. This augments the complexity of the grippers and probably the risk of failure. Hence, the constraint of permitting different geometry of the gripper for different foam and part geometries opposes the constraints of the time cycle and simplicity of design (for repairability and maintenance). The compromise to resolve this issue is to have grippers that are specific to the foam pad sizes. Instead of relying on a highly adaptable

[1] The thicknesses of the foam pads picked up by the grippers are 4 or 5 millimeters, but their side sizes vary greatly: 27x14mm for the small one, 60x40mm for the medium one, and 160x55mm for the large one. All three foam pads are identical.

[2] See Figure 4.2 C for the workplace configuration. All the parts are close together on jigs, enabling the operator to change them rapidly. Likewise, the cardboards, each with foam pads on them, are also located closely. Three of the five foam pads are identical, enabling them to be picked up rapidly in succession (medium foam pads). Furthermore, this configuration allows time for the operator to change all the parts while the robot is picking up the next foam pads, a necessary measure to meet the cycle time.

[3] More details on collaborative requirements are discussed in Appendix II

and complex gripper, they are made for one foam pad size but share the same operating mode. The adaptability came from the design, which is adaptable to other foam sizes at the CAD level (for example in Figure 4.1 B, the B2 design was adapted to create the B1 and B4 grippers). With a minimum of effort, the base geometry can be changed to another foam dimension. These grippers are also designed to be 3D printable in a minimum of components. All other parts that go on them are standard and do not need modification (see Figure 4.3 for an exploded view of one of the grippers).

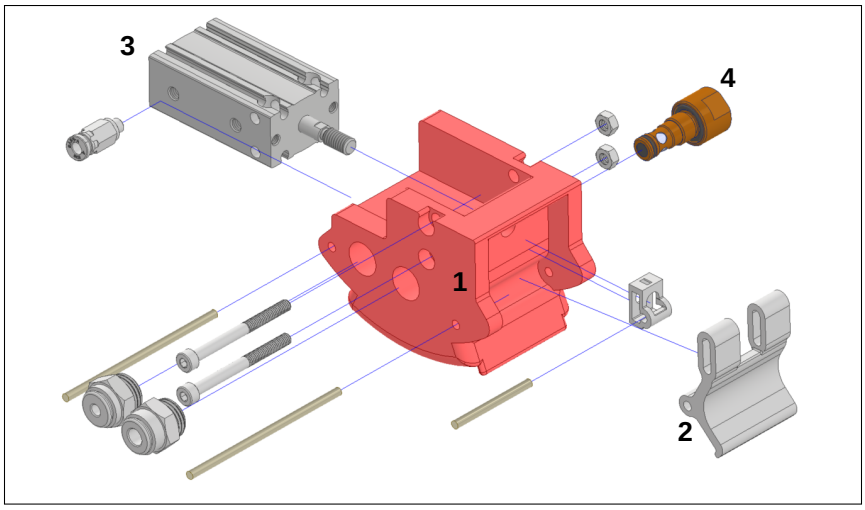

Figure 4.3 Exploded view of a gripper; the principal components are the base part (1), the clamp (2), the pneumatic cylinder (3), and the Venturi cartridge (4). Other components are screws, nuts, pneumatic fittings, and pins

Ultimately, other grippers could be designed rapidly for other projects using these base gripper designs. The end-effector configuration also allows rapid change of one of the grippers by a spare one (in Figure 4.1 D, the red grippers can easily be changed by unscrewing the top shell first).

4.2.2 Energy source and pneumatic circuit

Compressed air has been selected as the energy source for the grippers. The primary reason for this selection is the existing compressed air network at the Exo-S facility. Compressed air can easily be transformed into mechanical work using a pneumatic cylinder, which actuates the

clamps on the grippers. Either Venturi ejectors or the Bernoulli effect can be used to create negative pressure using compressed air. Venturi vacuum generators are inexpensive and have the potential to be 3D printed directly into the gripper. In the actual design, each gripper is connected to a single pneumatic line; the pneumatic cylinder and Venturi ejector share the same compressed air supply. Figure 4.4 shows a schematic of the pneumatic system. Alternatively, the Bernoulli effect can be used instead of the Venturi effect. Likewise, it can be 3D-printed directly in the gripper structure. In Chapter 6, for comparative purposes, tests are conducted with a Venturi gripper and a Bernoulli gripper for the medium foam pads.

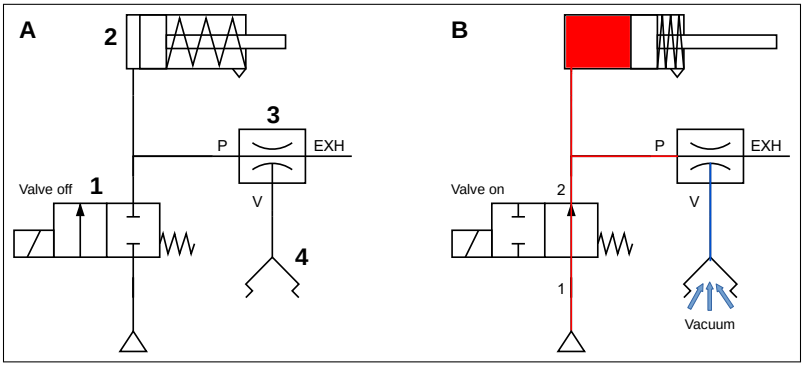

Figure 4.4 Pneumatic diagram of the gripper (Venturi version) - A) The pneumatic components are the solenoid valve (1), the pneumatic cylinder (2), the Venturi vacuum generator (3) and the vacuum opening (4) - B) Red lines represent the pressure when the valve is open; the cylinder extends and a vacuum is formed in the vacuum opening. EXH stands for the exhaust of the Venturi

Double-acting pneumatic cylinders could have facilitated rapid clamp opening and closing. Moreover, the Venturi ejector could have been detached from the cylinder, allowing for independent actuation of all actions. However, this arrangement would increase the total number of pneumatic lines to 15. Once again, for simplicity and to reduce the number of parts, the selected option was to use a spring-return cylinder that shares the pneumatic line with the Venturi generator. An additional advantage of combining compressed air with 3D printing is the possibility of integrating pneumatic circuits directly inside printed parts. This further reduces part count by transforming the grippers into pneumatic manifolds, as shown in Figure 4.5.

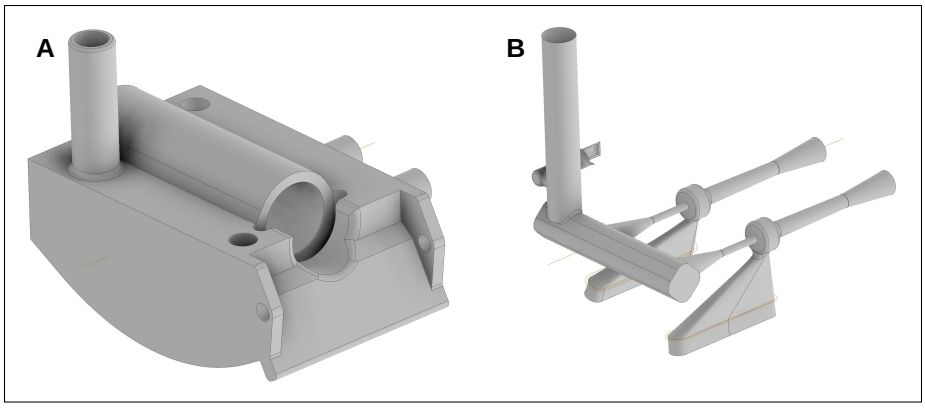

Figure 4.5 A) External view of a 3D-printed gripper prototype - B) Internal view of the pneumatic circuit within the gripper. This version incorporates two Venturi ejectors directly into the 3D-printed component. The performance of two 3D printed Venturi vacuum generator is evaluated in Appendix III

4.2.3 Clamp

Unlike fabric, foam pads possess additional thickness and excellent elasticity. This makes it possible to directly pinch the material without creating any folds. In fact, experiments conducted during this research found that the most reliable way to detach foam pads was to utilize a clamp mechanism. No other tested grasping technologies proved robust enough for the unsticking operation. Additionally, the clamp should grasp the foam pads at their edges to detach the foam stickers with minimal force. Grasping a foam pad in the middle causes it to tear before it can be detached[4]. Ensuring safety or 'collaborativeness' was another important aspect of the clamp design. Therefore, we have intentionally limited the size of the pneumatic cylinder that actuates the clamp. Applying additional grip to the clamp, such as anti-slip tape, can also aid in securing the foam by preventing slippage, while maintaining a lower closing force.

[4] Appendix I contains the results of these trials; when grasped from its center, the foam pad tears before being unstuck, and the force exerted by the gripper is more than five times greater than when the pad is unstuck from its side.

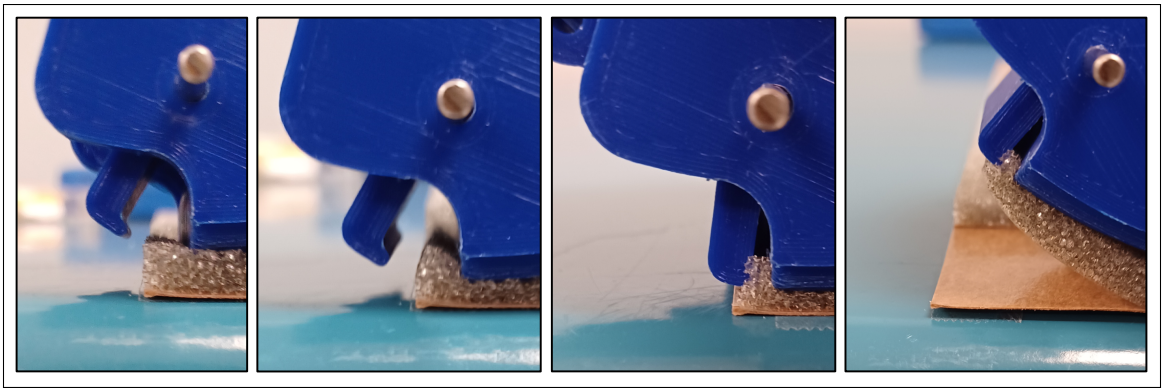

Figure 4.6 Clamp close-up views - From left to Right, the action of the clamp closing on a foam pad and peeling it off the cardboard

4.2.4 Pneumatic grasping

An additional mechanism was needed to secure the foam pads to the grippers. Otherwise, they would dangle and could stick to themselves. Given the effectiveness of the existing clamp in securing one side of the foam pad, employing a similar clamp at the opposite end could have been a viable strategy. However, a negative pressure grasping mechanism was chosen as the preferred solution. There are multiple reasons for this choice:

- An additional clamp would introduce more moving parts and potential failure points, thereby increasing the complexity of the tool's assembly and maintenance.
- The pneumatic cylinder that actuates the clamp is relatively large compared to the gripper (as indicated by the rectangular part (3) in Figure 4.3). Incorporating another one into each gripper would increase the size and weight of the final end-effector.
- Given the curvature of the grippers, it would be necessary to sequentially activate the clamps. The two clamps at the front and back would need to be independently actuated, which means doubling the pneumatic lines to a total of 10.

Since the initial clamp accomplishes most of the work in unsticking the foam pad, adding another clamp could be considered somewhat 'excessive'. A vacuum cup proves sufficient for simply holding the foam in place on the gripper. Potentially, the primary advantage of using a second clamp instead of negative pressure could be a reduction in compressed air consumption. Indeed,

Venturi ejectors and Bernoulli grippers utilize a significant amount of compressed air while active. Conversely, a pneumatic cylinder consumes a minimal amount of compressed air when activated and requires no additional air to maintain its position. Nonetheless, implementing a Venturi ejector or leveraging the Bernoulli effect leads to fewer moving parts, a simplified assembly, and more compact grippers. These considerations underpin their incorporation into the proposed solution. Alternatively, as discussed in the literature review, electroadhesion presents a potentially viable alternative to pneumatic grasping [5]. While this approach could markedly reduce operating costs, it would necessitate the integration of an entirely new electrical system into the gripper, thereby further increasing its complexity. In Chapter 5, we experimentally tested different vacuum openings trial prototypes, a vacuum cup trial prototype, and a Bernoulli trial prototype. Later in Section 6.2.1, we compare three of these prototypes, each incorporated on a different gripper. Figure 4.7 illustrates the three distinct types of pneumatic grasping designs tested on the grippers.

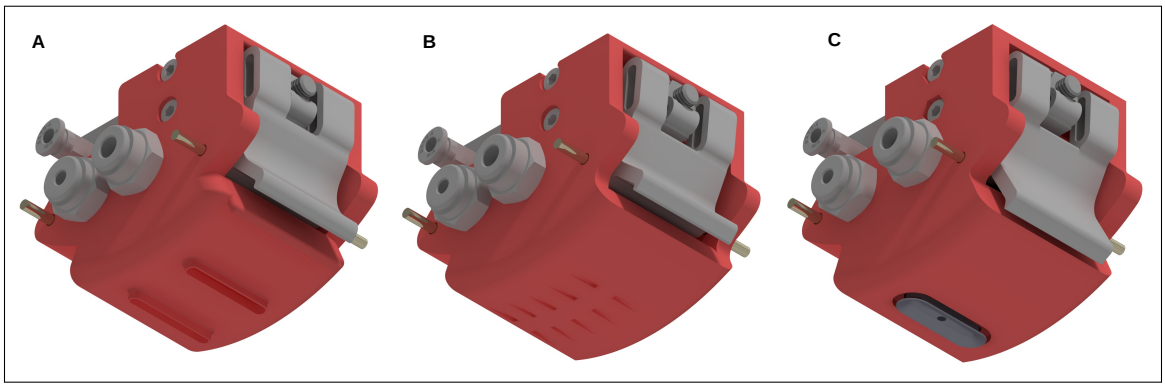

Figure 4.7 The 3 different pneumatic grasping gripper types tested - A) Ridge vacuum openings gripper - B) Bernoulli effect gripper - C) Vacuum cup gripper

[5] EA pads would probably be strong enough to secure the foam pads while the gripper is in motion. For example, the medium foam pad weighs approximately 0.5 grams with an area of 60mm*40mm=2400mm^2. West and others 2020 optimize an EA pad up to 0.22 kPa of lifting force per area. If that EA pad covers all the medium foam pad area, it could lift 100 times the foam pad weight.

4.2.5 Curvature of the grippers

Another important design consideration was deciding whether or not to include a curvature in the grippers. For the medium and large foam pads, an added curvature in the tool was incorporated for two main reasons. First, it enables the gripper to maintain constant contact with the foam while peeling the foam pad, ensuring proper vacuum buildup and secure attachment of the foam pad to the gripper (see Figure 4.8). Secondly, the curvature in the grippers reduces the force required during the application phase. Indeed, if the gripper was flat, the force needed for the application would be proportional to the area of the foam pads. With a curved gripper, the pressure is concentrated to practically a line. This results in a higher force per unit area applied to the pads, and a lower maximum force is needed from the collaborative robot arm. This configuration might prolong the lifetime of both the grippers and the robotic arm. In contrast, the smaller foam pad, which can be picked up and applied with a flat tool due to its small area, does not necessitate any curvature.

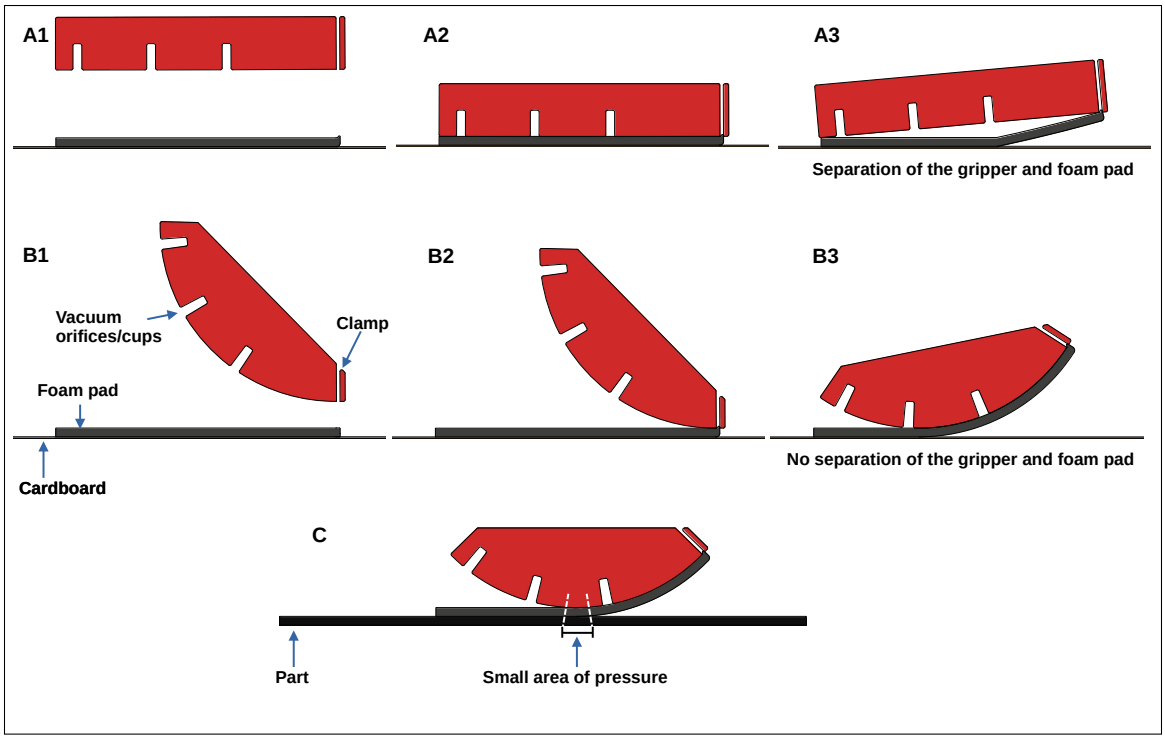

Figure 4.8 Gripper with curvature versus flat: The grippers are depicted in red, the foam pads in gray. Vacuum orifices are represented as grooves on the underside of the grippers. The clamp is shown as a detached piece. - A1) to A3) display the steps to pick up a foam pad with a flat gripper; the gripper surface separates from the foam pad during the peeling process. - B1) to B3) show a curved gripper not experiencing the same issue when picking up the pad. - C) Gripper applying a foam pad; there is a limited contact area between the gripper and the pad

4.2.6 Compliance

The gripper's compliance adds mechanical complexity but has some advantages. First, it allows the application of pressure on the foam pads without overloading the robotic joints. Indeed, because robotic arms are rigid, it is difficult to limit the joint forces when working close to or in contact with solid surfaces[6]. For example, when picking up the foam pads, the gripper needs ideally to press on the foam before the clamp closes. Without compliance, a small distance needs to be kept between the gripper and the table surface, ideally less than 1mm. A small imprecision in the robot movement can make the gripper press on the table and drastically increase the torque forces in the robotic joints. For a collaborative robot, this means triggering joint limitations and stopping the robotic arm. In theory, the repeatability of the collaborative robot is on the order of a submillimeter, but while performing a curved trajectory (peeling motion), the interpolations between the different points are imperfect. These factors make it challenging to program the movements of the grippers for the application and grasping of the foam pads. Furthermore, in the application phase, a minimal force needs to be applied to stick the foam pads. Controlling the application force without compliance could be troublesome, as any minor imprecision in the robot's movements could create a rapid spike of force[7]. Thus, compliance primarily cushions these minor imprecisions, making the gripper more robust. This is also consistent with the literature for applying "sticker-like objects" (Yuan and others, 2018 and 2020). Furthermore, it allows programming the robot arm with simple point-to-point movements[8]. A block of polyurethane foam is used to provide compliance between the grippers and the end-effector main part. The positioning of the grippers is facilitated by a V-shaped ridge on each side of the grippers (see Figure 4.9 B to C). This V shape also allows for some lateral movement of the gripper, which helps with the imprecisions of the picking operation. Without compression, the

[6] A robot controlled by a force-based strategy, such as hybrid force-position or impedance control, would not suffer from this problem.

[7] This is discussed in greater details in Section 4.2.8

[8] As opposed to perfectly defined curvilinear trajectories, the gripper can easily be programmed with a teach pendant by a worker.

gripper positions itself at the bottom of the V, which ensures optimal positioning of the clamp for the picking-up phase. The compliance is highlighted in blue in Figure 4.9 B to C.

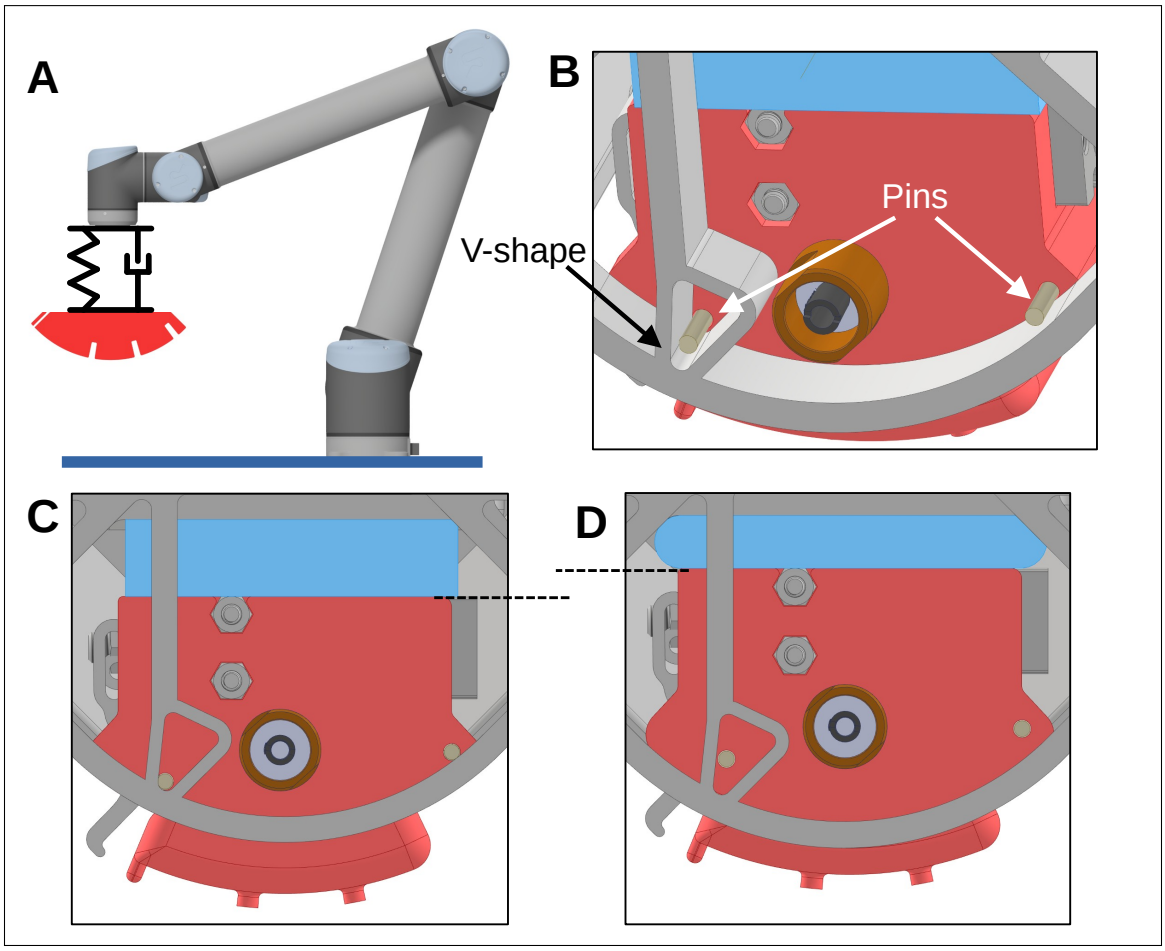

Figure 4.9 Gripper Compliance - A) The compliance is equivalent to a spring-damper system between the robot and the gripper. - B) Close-up view of the pins and V-shaped guide - C) and D) Side views of the compliant part, highlighted in blue, at rest and compressed, respectively. Note the change in the position of the pins

4.2.7 Vacuum Plates

At the outset of the project, one pivotal decision was whether or not to employ a specialized feeder device for the foam pads. Similar to label dispensers presented in section 3 of the literature review, we could have designed a foam pad dispenser. However, this option was dismissed due to the complexity of altering the format of the foam pad cardboard sheets already in use with the

current supplier. Also, most of the other foam pads in the Exo-S plant came in rectangular sheets, not in a roll. Finding a solution that works with all the existing formats of foam pad cardboard sheets was considered more beneficial. As a result, we proceeded with the development of the foam pad gripper, but a mechanism to hold the sheets in position was still required. To this end, we used vacuum plates. These are plates filled with a large number of small holes, connected to a multistage Venturi ejector. When a sheet of foam pads is put on it, a vacuum is created under the cardboard, securing it in place. To further enhance the vacuum force, a border made from a flexible material can be included to seal the cardboard's edges. The CAD design is depicted in Figure 4.10; they can also be seen in Figure 4.2 A, and 4.2 C with the cardboard sheets on.

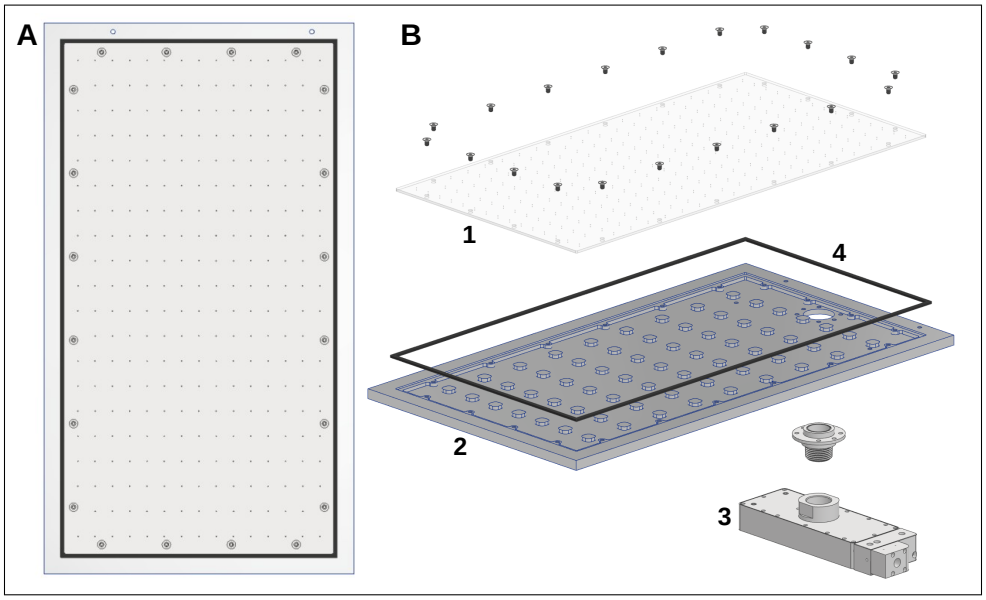

Figure 4.10 Vacuum Plate for Medium Foam Pads: - A) Top View - B) Exploded View, including 1) Plexiglass plate with small holes, 2) Aluminum base, 3) Multistage Venturi ejector, 4) Flexible and airtight contour

4.2.8 Force control for the appliance

Since the foam pads have a pressure-sensitive adhesive backing, application pressure is needed to firmly stick them[9].In the context of the Exo-S collaborative station, applying pressure wasn't

[9] The application of a predetermined minimal pressure by a robotic system is also a requirement stipulated by Exo-S's customers.

a hard constraint for the prototype gripper. Indeed, the subsequent robotic cell that solders the plastic parts together also applies pressure to the foam pads, using a roller. This subsequent cell already adheres to the 45-second cycle time, which means that moving the appliance of pressure operations to the collaborative station wouldn't yield time savings[10]. The collaborative robot can simply position the foam pads on the parts without exerting pressure, just as the worker previously did. However, the option of directly applying pressure via the foam gripper enhances the tool's functionality. For other potential projects, the ability to have the robot apply pressure directly while positioning the foam pads on the parts could be advantageous. In this context, an admittance control was used. This enables the application of a predetermined force for the foam pad application motion, regardless of the compliance part's characteristics of the gripper[11]. The control loop was developed in Python using the Real-Time Data Exchange API (RTDE) to control a Universal Robot (UR5e). While it makes it easy to predetermine an appliance force, the admittance control becomes unstable at speeds relevant to our application. To resolve this issue, a base trajectory is generated at low speed, which can then be utilized at higher speeds. A speed-up of 16 times has been tested this way, but there is a tradeoff between speed and force accuracy. The performance of this solution is presented in Chapter 7. Figure 4.11 illustrates the appliance motion.

---

[10] The injection press produces a set of plastic parts every 45 seconds. Subsequent stations that do operations on the set of parts need to complete their operations in less than 45 seconds, otherwise, there would be an accumulation of parts before that station. Saving time in a subsequent robotic station would result in more idle time for that station, but no real production gains (parts per minute). A hypothetical gain in time could make it possible to add operations in the robotic station, that are usually done by another station (human or robotic). Then, in that case, it may be possible to save one station on the production line. However in our case, all easily robotized operations are already automatized, and the gain in speed is not enough to reduce the number of robotic stations either.

[11] For example, the compliance of the grippers could be replaced in the future by springs. Furthermore, as it stands now, the compliance is achieved by a block of polyurethane foam, which has dynamic behavior that is hard to model. For both these reasons, an admittance control was preferred, as it bypasses the need for accurately modeling the dynamics of the robotic system (it bypasses the need to implement a control based on predetermined characteristics of the system).

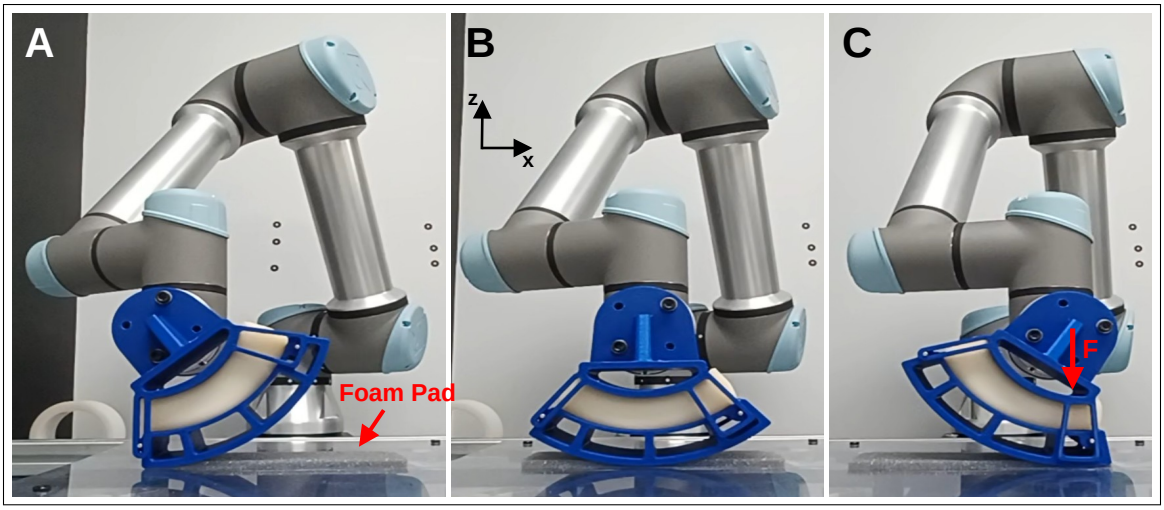

Figure 4.11 Appliance force control. The test tool for the admittance control (in blue) is described in Chapter 7 - A) Starting position - B) Middle position - C) End position - The end-effector rotates at a constant rate while also translating the center of rotation of the tool. The height is controlled in admittance to apply the downward force F

CHAPTER 5

PNEUMATIC GRASPING TESTS

In this chapter, we conduct a comparative analysis of the grasping efficiency across diverse trial prototypes. These have been empirically evaluated for their maximum exertion of grasping force on foam pads and assessed for the potential creation of creases or folds. In the first section (5.1), we describe the different trial prototypes tested, and the reason for testing them. In the second section (5.2), the testing methodology and result of the force test are presented. Section 5.3 presents the methodology and results of the fold test. Finally, in the last section (5.4) we give an interpretation of the result for both tests.

5.1 Trial Prototypes

There are a total of six different trial prototypes tested, four of these prototypes are 3D-printed vacuum openings. The fifth prototype is a standard polyurethane vacuum cup. Each of the vacuum openings and the vacuum cup utilizes negative pressure derived from a Venturi vacuum generator. The sixth prototype uses the Bernoulli effect to generate a lifting force. A comprehensive description of the testing setup is provided in Section 5.3. Figure 5.1 displays an image of the first five 3D-printed trial prototypes. The Bernoulli trial is displayed later (in Figure 5.5). Each of the trial prototypes is described in the next sections (5.1.1 to 5.1.6), and motivation for their testing are given.

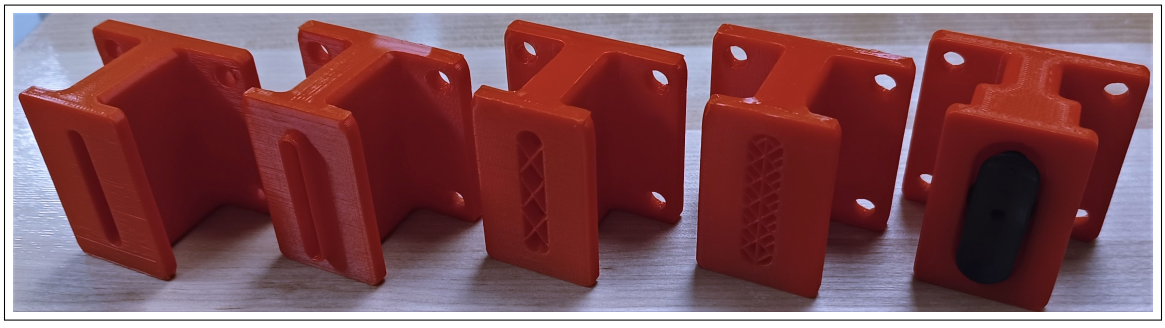

Figure 5.1 Vacuum openings and vacuum cup trial prototypes

5.1.1 Standard Oblong Opening

A primary objective of the project was to develop simplified gripper designs to minimize the complexity of the total end-effector assembly and its subsequent maintenance. Consequently, the direct integration of a vacuum opening into the 3D-printed principal component of the gripper is desired. An oblong design provides the simplest solution for accomplishing this task. The longitudinal axis of the oblong opening is perpendicular to the direction of peeling, enabling a rapid seal formation as the gripper rotates. Figure 5.2 A depicts the design of the trial prototype for this opening.

5.1.2 Ridge Oblong Opening

This opening is characterized by a three-millimeter ridge that is located on the perimeter of the oblong shape. Early testing has shown that this specific geometry prevented the folding of the foam pads and the formation of creases (see Figure 5.2 B). The reasoning behind the ridge is that it could apply acute pressure around the opening, potentially sealing it faster.

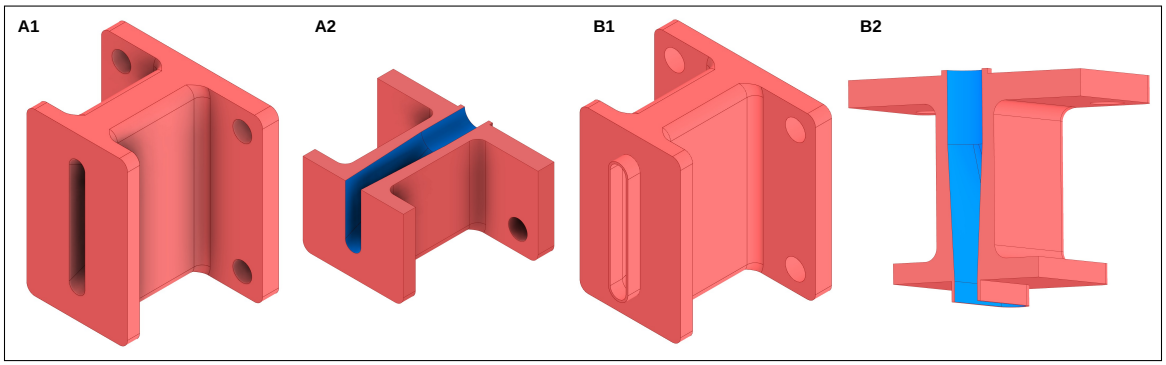

Figure 5.2 Standard and ridge oblong openings - A1) Standard oblong opening design - A2) Cutaway view of the Standard oblong opening, where the vacuum cavity is highlighted in blue - B1) Ridge oblong opening design - B2) Cutaway view of the ridge oblong opening, where the vacuum cavity is highlighted in blue

5.1.3 Large Grid Oblong Opening

For this trial prototype, a grid has been incorporated into the opening to prevent the foam from being drawn into it. It is an attempt to create an opening that doesn't fold the foam pad while having a preferable geometry for the appliance. By preventing the foam from being sucked into the opening, it acts similarly to a gripper with multiple small openings, like the one optimized by Fleischer et al. (2016). It is illustrated in Figure 5.3 A.

5.1.4 Small Grid Oblong Opening

As the previous one, this opening has a grid pattern that prevents the foam from being sucked in. The only difference is that the grid pattern is smaller. This opening serves as a direct comparison for the larger grid pattern (see Figure 5.3 B). The grid pattern is approximately three times denser for this one.

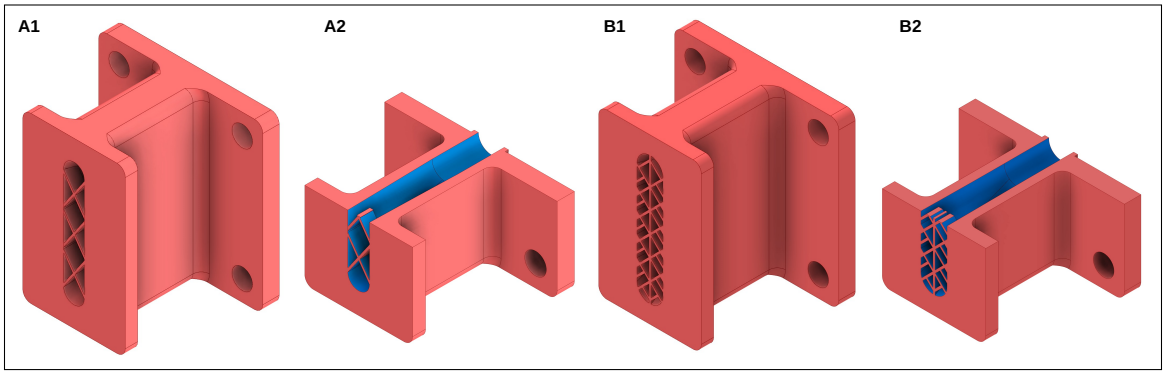

Figure 5.3 Large and Small grid oblong openings - A1) Large grid opening - A2) Cutaway view of the Large grid opening, where the vacuum cavity is highlighted in blue - B1) Small grid opening - B2) Cutaway view of the small grid opening, where the vacuum cavity is highlighted in blue

5.1.5 Polyurethane Vacuum Cup

This trial prototype used a standard polyurethane vacuum cup (see Figure 5.4 A). These types of vacuum cups are used to pick a multitude of objects but are probably more suitable for air-impermeable materials. With these types of materials, the vacuum cup can create a perfect

seal and maximize the grasp force. It's unknown if this sealing effect will apply to the foam pads, which is why a vacuum cup is also being tested. To fix it to the gripper, it is possible to 3D-print the "nipple" shape to which it usually connects. Hence, only the polyurethane cup is added as an additional part (see Figure 5.4 B).

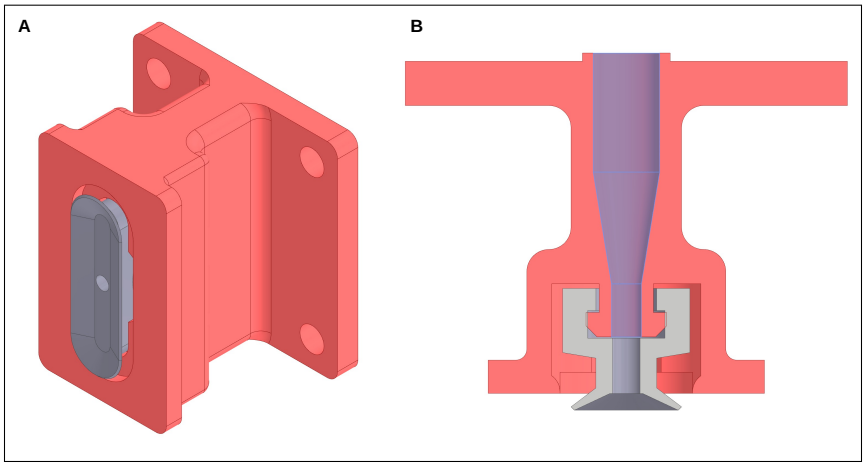

Figure 5.4 A) Vacuum cup trial prototype - B) Cross-section view of the vacuum cup trial, where the vacuum cavity is highlighted in blue

5.1.6 Bernoulli

This last trial prototype used the Bernoulli effect to generate a grasping force. It serves as a comparison to the Venturi effect. Additionally, Bernoulli grippers are widely studied and used to grasp permeable material, as presented in the literature review section. Hence, it is justifiable to subject it to empirical testing. Using the Bernoulli effect can also reduce the number of parts on the gripper; it does not require a vacuum generator and can be directly printed in the gripper itself. Thus, it is the technology that reduces at a minimum the number of parts on the grippers, reducing the price of buying these parts (the Venturi vacuum generators). Furthermore, it has a flatter surface compared to the vacuum openings. This could mean more uniform pressure application during the application phase. To create the Bernoulli effect, small openings on the surface of the gripper redirect the compressed air on both sides (see Figure 5.5 A and B).

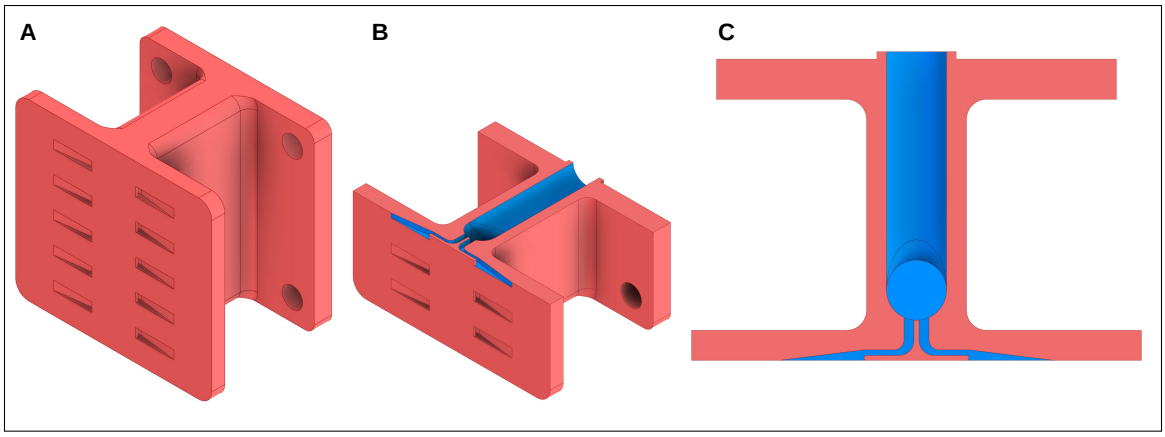

Figure 5.5 A) Bernoulli trial prototype - B) Cutaway view of the Bernoulli trial, where the pressurized cavity is highlighted in blue. - C) Cross-section view

5.2 Force Tests

5.2.1 Methodology

The force test compares the capacities of different trial prototypes to generate a lifting force on the foam pads. For the first five opening prototypes, a Coval vacuum cartridge (CVP90x12) is used. While the vacuum cartridge is set to operate at a specific pressure, its airflow consumption remains constant regardless of what happens at the vacuum opening end[1]. For this reason, it is simple to compare the different vacuum openings based on their ability to transform an equal quantity of constant power (compressed airflow) into an actual force on the foam. The sixth trial Bernoulli prototype serves to compare two different technologies: the Venturi effect versus the Bernoulli effect. The experimental setup consists of a robotic end effector on which a trial

[1] Whether the opening is completely obstructed, partially obstructed, or clear, the pressure and airflow consumption of the Venturi device is constant. Appendix III presents the results of the different Venturis tested (the Coval cartridge and two 3D printed versions). The only relationship that exists for air consumption is dependent on the operating pressure of compressed air.

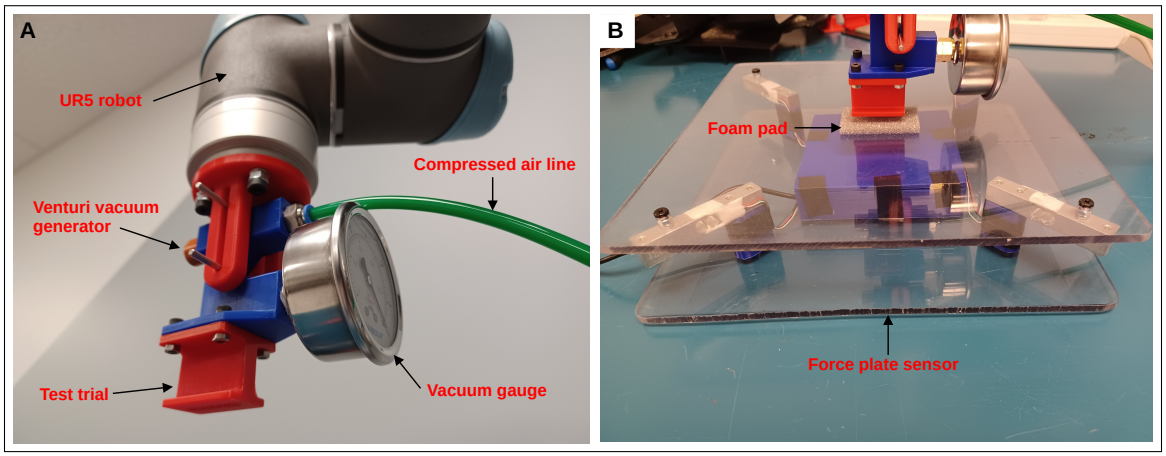

Figure 5.6 Experimental setup for force Test - A) The force test end effector is displayed with all the components visible - B) The trial prototype is positioned over the foam pad, which is stuck to the force plate sensor. This force plate sensor is made of four load cells positioned on each corner. They support the top plate, so the force acting on the plate is equal to the sum of the load cell readings (Appendix IV gives more details on the components and presents the results of calibration for each load cell)

prototype is installed, a force plate sensor[2] with a foam pad attached, and a vacuum gauge (see Figure 5.6). The end-effector used for the five vacuum openings is the same. The vacuum trial prototype can be swapped out underneath, and the connection is sealed by a Toric joint to prevent any vacuum loss between the Venturi generator and the test trial. The vacuum gauge is also connected to the same conduit. For the Bernoulli trial prototype, there is no Venturi or vacuum gauge installed on the end-effector since the vacuum is created directly on the surface of the test trial. To measure the force, the robot approaches the trial from above until there is complete contact with the foam pad, then it slowly raises until separation (at a rate of 0.1 mm/s). The force from the plate sensor is recorded every 0.01 seconds for the entire duration of the test.

The procedure of the force tests consists of the following operations:

1. Install a trial prototype on the robotic test setup.
2. Select the operating pressure on the pressure regulator to 30 psi.
3. Place a new foam pad on the force plate sensor.
4. Start the recording of forces.
5. Start the video recording of the vacuum gauge.
6. Start the robotic program that is going to approach the trial prototype until it presses on the foam pad, then slowly lift the trial until there is no longer contact between the trial and foam pad. The robotic program repeats the previous step for 30 total cycles.
7. Turn off all the recordings when the robotic program is completed.
8. Repeat starting from step 2 with an operating pressure of 50 psi, and then 80 psi.
9. Repeat, starting from step 1 with another trial prototype, until all have been tested.

5.2.2 Results

The test results corresponding to pressure levels of 30 psi, 50 psi, and 80 psi are delineated in Figures 5.7, 5.8, and 5.9, respectively. In these graphics, the blue bars denote the average peak

[2] See Appendix IV for details and evaluation of the force plate sensor precision.

force calculated over each test of 30 cycles. The black bars symbolize the recorded minimum and maximum values of the peak forces for a given test.

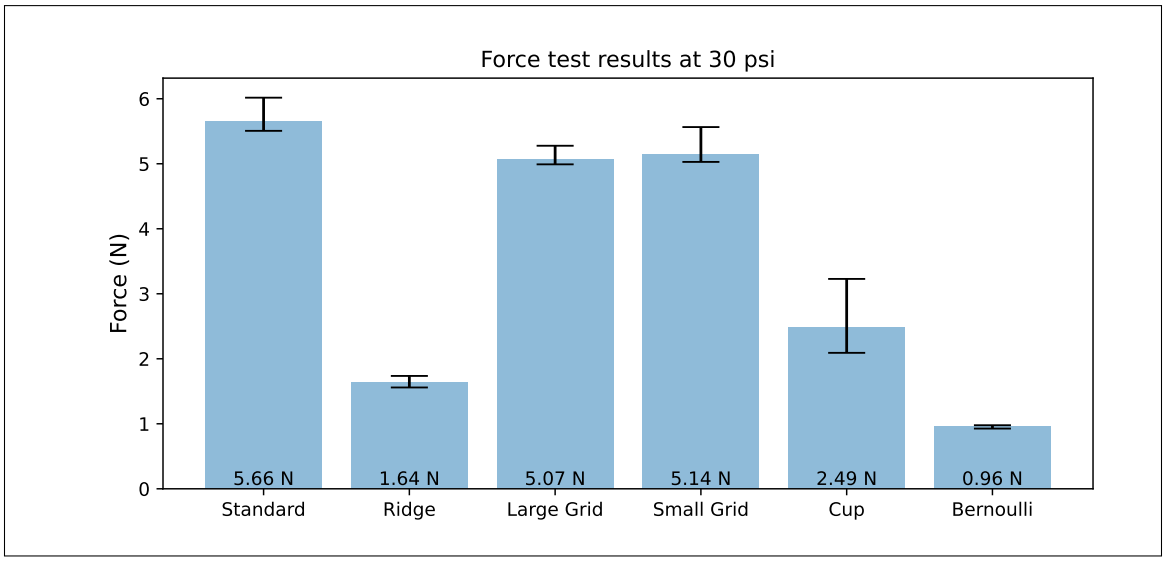

Figure 5.7 Force result at 30 psi for tested trial prototypes

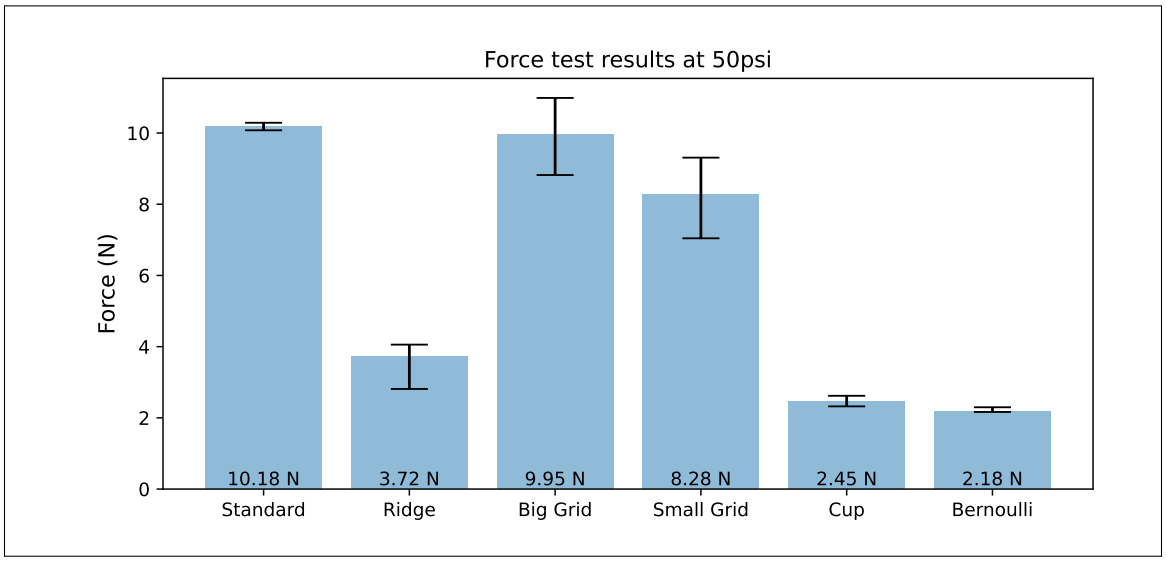

Figure 5.8 Force result at 50 psi for tested trial prototypes

The Venturi vacuum generator, used for the first five trial prototypes, consumed air at rates of approximately 18 L/min at 30 psi, 23 L/min at 50 psi, and 28 L/min at 80 psi. The Bernoulli trial consumed approximately 69 L/min at 30 psi and 90 L/min at 50 psi. At 80 psi, the Bernoulli

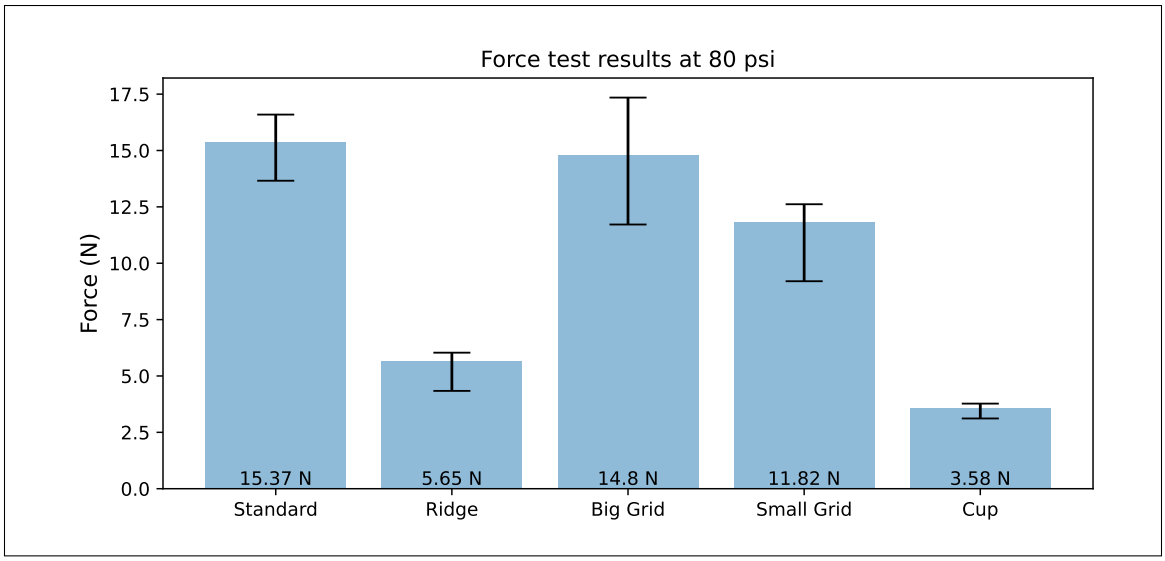

Figure 5.9 Force result at 80 psi for tested trial prototypes

trial's air consumption exceeded the 100 L/min limit of the utilized flowmeter. Due to the uncertainty in energy consumption, a comparison with other trials under the same conditions is not possible. Consequently, the Bernoulli hasn't been tested at this pressure. At 30 and 50 psi, the Bernoulli trial was found to be 18 times less efficient at converting energy into a lifting force when compared to the standard oblong opening. On a separate note, to improve the comparison between the five vacuum opening types, their exerted force can be normalized by their opening area (see Table 5.1). Upon normalization by area, the results shift slightly. In the case of the vacuum cup, there is both an interior and a complete area. The interior area ($67mm^2$) corresponds to the rigid interior, while the complete area ($257mm^2$) includes the flexible contour. Finally, the maximum vacuum levels reached for the five vacuum prototypes (using the Venturi effect) are detailed in Table 5.2 (averaged over the 30 cycles for each set). These values do not coincide temporally with the peak forces.

Table 5.1 Average force results corrected per area of opening (OP = Operating pressure)

Vacuum Opening	Area of vacuum opening (mm^2)		Force per area (N/mm^2)					
			OP 30 psi		OP 50 psi		OP 80 psi	
Standard	140		0.04		0.073		0.11	
Ridge	140		0.012		0.027		0.04	
Large Grid	119		0.043		0.084		0.124	
Small Grid	117		0.044		0.071		0.101	
Vacuum Cup	67	257	0.037	0.01	0.037	0.01	0.053	0.014

Table 5.2 Averaged maximum vacuum results at different operating pressure

	Vacuum Opening	Standard	Ridge	Large Grid	Small Grid	Vacuum Cup	No opening
Vacuum level (-kPa)	OP 30 psi	27.22	27.39	27.25	24.0	28	28
	OP 50 psi	45.96	44.35	45.34	42.77	46.45	49.33
	OP 80 psi	74.07	65.88	69.01	66.35	78.89	90

5.3 Qualitative Grasp Tests

5.3.1 Methodology

The qualitative grasp test aims to verify that the tested openings do not induce excessive folding or creasing in the foam pads when they grasp them. Given the challenge of quantitatively assessing the degree of "creasing", this test has a significant qualitative aspect. It involves the trial prototypes freely grasping the foam pads. Figure 5.10 illustrates the pick-up procedure. Firstly, a foam pad is placed on four spikes, which reduces the contact area with the adhesive to a minimum. Afterward, the trial prototype is robotically lowered to grasp the foam pad and then lifted for inspection. Finally, the foam pad is then lowered and affixed to a transparent surface for further inspection. When the foam is suspended in the air, inspection criteria include the angle at which the foam pad bends and the presence of noticeable folds. After being stuck, the

inspection focuses on apparent folds, bumps, or creases on the top or underneath of the foam pads. Based on these criteria, a performance evaluation scale was developed to compare the trial prototypes (see Table 5.3). If the folds were evaluated as unacceptable, subsequent tests for that specific trial prototype were not conducted at elevated operating pressures. Images of these tests can be found in Appendix VI.

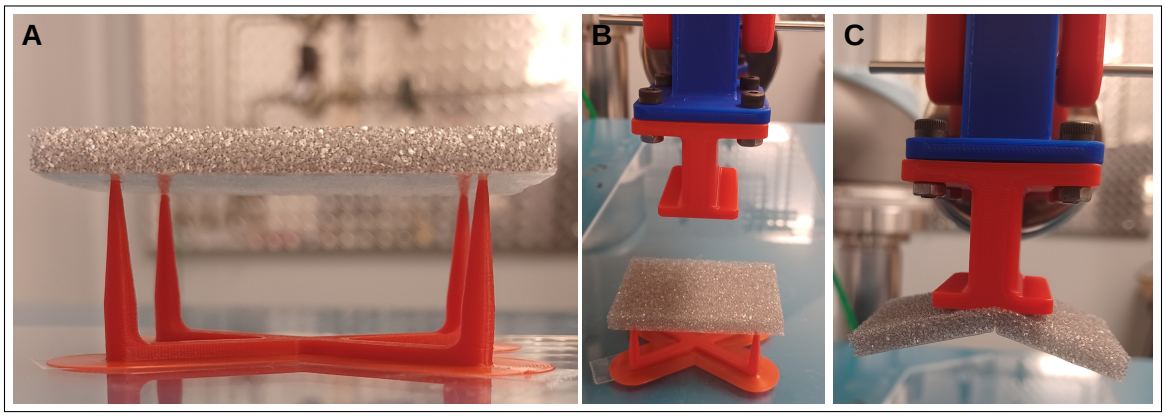

Figure 5.10 Experimental setup for the fold test - A) Foam pad placed on the four-spike setup - B) The trial device approaching the foam pad - C) The trial device lifting the foam pad into the air

Below are the procedure steps for the grasp tests:

1. Install the first trial prototype on the test setup.
2. Set the operating pressure to 30 psi.
3. Place a foam pad on the four spikes.
4. Lower the robotic arm until contact is established between the trial opening and the foam pad.
5. Raise the robotic arm until the foam pad is completely supported by the trial prototype alone.
6. Capture images of the side and underneath of the foam pad.
7. Lower the foam pad onto a transparent plate to stick it. Lower until the trial setup fully weighs on the foam pad, then turn off the compressed air and raise the trial prototype.
8. Capture images of the underside and top of the attached foam pad.

9. If the result of the test is acceptable (score lower than 10), repeat the test at increased pressure settings of 50 psi and 80 psi, starting from step 2.
10. Continue the test until all trial prototypes have undergone testing.

Figure 5.11 shows examples of inspection images of a grasped and applied foam pad. Table 5.3 displays the criteria used to evaluate the performance of the test. The different levels can be added together to obtain a performance score. For example, a 10-degree bend angle, with creases visible when grasped, combined with a small bump on top and a visible fold underneath when stuck, will give a score of 0 + 2 + 1 + 2 = 5 (the smaller the score, the better).

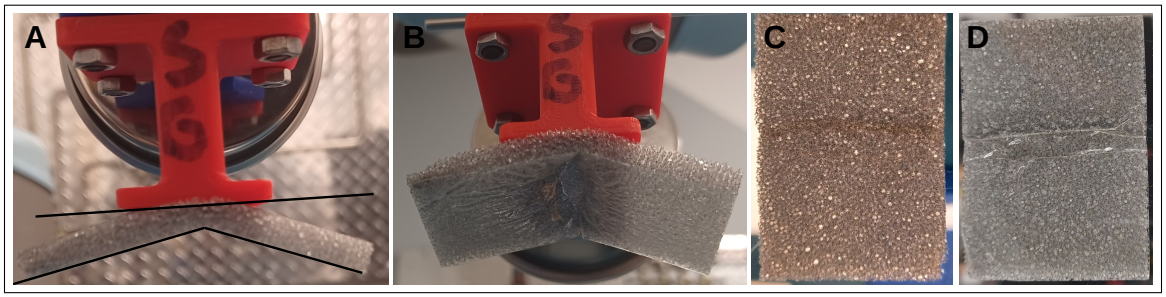

Figure 5.11 Qualitative folds test example - A) Side view of the grasped foam pad. The black lines are used to determine the bend angle (average of the two angles between the trial prototype and the bent foam pad). B) View of the underside of the foam pad in the air. C) Top view of the adhered foam pad. D) Underside view of the adhered foam pad

Table 5.3 Qualitative folds test criteria. For each criterion, there is a level of acceptability from 0 (best) to 3 (worst)

	Suspended in the air		Stuck on a transparent surface	
Criteria	Bend angle	Underside	Top	Underside
Level 0	< 5°	flat surface	flat surface	flat surface
Level 1	> 15°	deformation	small bump(s)	small fold(s)
Level 2	> 20°	creases	bump(s)	Fold(s)
Level 3	> 25°	fold	big bump(s)	big Fold(s)

5.3.2 Results

The results for the qualitative grasp tests are shown in the next table:

Table 5.4 Qualitative folds test results. The score is the sum of all the levels for each criterion (lower is better). A score equal to or greater than 10 was deemed as unacceptable. In general, the results worsen as the pressure increases

Trial prototype	Operating pressure	Bend angle	Underside (air)	Top	Underside (stuck)	Scoring
Standard	30 psi	36°	fold	big bump	big Fold	**12**
Ridge	30 psi	-3.2°	deformation	flat surface	flat surface	**1**
	50 psi	23°	fold	big bump	big Fold	**11**
Large Grid	30 psi	16°	fold	small bump	fold	**7**
	50 psi	23°	creases	big bump	big Fold	**10**
Small Grid	30 psi	17°	fold	small bump	small Fold	**6**
	50 psi	15°	fold	small bump	small Fold	**5**
	80 psi	17°	creases	bump	fold	**7**
Vacuum Cup	30 psi	1°	deformation	flat surface	flat surface	**1**
	50 psi	1°	creases	flat surface	small Fold	**3**
	80 psi	10°	creases	small bump	small Fold	**4**

5.4 Results Interpretation

The force test demonstrated the ability of the trial prototypes to grasp a foam pad that was adhered to a rigid surface. The standard and the two grid oblong openings showed greater maximal forces than those of the ridge and vacuum cup openings. When corrected for area, the results remained unchanged. Surprisingly, there is no correlation between the maximal vacuum achieved by the Venturi trials and their maximal exertion force. Maximal vacuum pressures were obtained when the trial prototypes were not under force loading. These variations in maximal forces, not correlated with the area or maximal vacuum, suggest that more complex phenomena occur between the vacuum openings and the foam pad. For example, we can consider the differences between the Standard and Ridge trials, as shown in Figure 5.12. When there is no pulling force, both trial prototypes exert pressure on the foam pad and create a seal separating the vacuum opening from the exterior. The downward force exerted is equivalent to the vacuum-generated force. For the ridge opening, this downward force is concentrated on the smallest possible area. In contrast, for the standard opening, pressure is exerted on a greater surface area. Despite this difference, both trials, at an operating pressure of 30 psi, reach a vacuum level close to the optimal level (see Table 5.2). However, this changes when the operating pressure increases to 50 psi and subsequently to 80 psi. At 50 psi, the standard opening is 3.4 kPa short of the optimal possible vacuum, and the ridge opening is 5.0 kPa short of it. At 80 psi, there is a 15.9 kPa difference in pressure loss for the standard trial and 24.1 kPa for the ridge trial. In other words, the pressure loss disparity between the two trial prototypes escalates as the operating pressure rises. These variations between the two trials could be explained by the larger volume of foam that air needs to permeate through in the standard trial, resulting in a lower leakage flow rate at elevated operating pressure. Alternatively, this difference could be explained by a non-linear relationship between the permeability of the foam as a function of the compressive pressure exerted on it. The mystery deepens as there is almost a threefold difference in maximal force between the two trials when pulling up. In short, interactions between the foam pad and vacuum openings are complex: the permeability of the foam varies as it is compressed, the vacuum level depends on the permeability of the foam, and the compression force exerted on the foam

depends on the vacuum level. Considering that foam pads are highly deformable, modeling these phenomena would be a challenging and time-consuming task. This goes beyond the scope of this thesis which focuses on finding a robust solution to a robotic automation problem. Instead, what we can conclude from this force test are the following points:

- The standard opening, the small grid opening, and the large grid opening trials create a better seal than the ridge opening trial. This is likely due to the larger surface area which presses and thus seals the foam pads more effectively.
- The vacuum cup trial reaches a higher maximum vacuum than the other trials, but this does not translate into a greater force. At 50 and 80 psi, the lifting force of the vacuum cup is even lower than the ridge trial.
- The Bernoulli trial generated a force equal to or lower than that of all the other trials. At 30 and 50 psi, the Bernoulli trial was found to be 18 times less efficient at converting compressed air into lifting force compared to the other five Venturi-based trials.
- These results only hold validity when the foam pad is placed on a rigid backing.

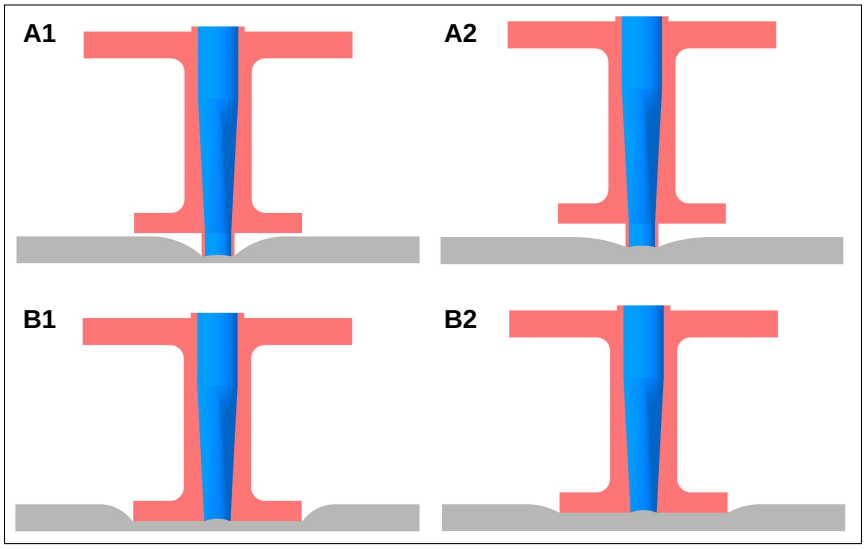

Figure 5.12 Force test : standard vs. ridge trial - A) Cross-section view of the ridge trial grasping a foam pad. - B) Cross-section view of the standard oblong trial grasping a foam pad

Measuring the maximal force exerted by the trial prototype on the foam pads is useful to determine how effectively they convert energy into grasping force, although, the significance

of this test does not lie in ensuring the pneumatic grasping ability to lift the foam pads. All prototypes can easily lift the weight of the foam pads; for instance, even at 30 psi, the Bernoulli trial generates a force 200 times the necessary amount to lift a medium foam pad[3]. Instead, the pneumatic grasping mechanism is there to ensure that the foam pads remain on the surface of the gripper when an external force interacts with it. This could be caused by an imperfect peeling motion, which could necessitate a greater force to keep the foam in place. Moreover, the foam pads are sometimes harder to separate, which subsequently requires a greater force to keep the foam pad secured on the gripper. Pneumatic grasping thus contributes to the robustness of the overall solution. Yet, what the first force test doesn't take into account is that when gripped freely, the geometry of the orifice might lead to folds in the foam pads. As explained previously, this may result in permanent creases or folds as the underside of the foam pad adheres to itself. Subsequent application on a surface can then create bumps on the surface of the foam pads. The fold tests are designed to verify that the trial openings can grasp foam pads without leading to these issues. Although qualitative in nature, it resembles how Exo-S employees visually inspect them to ensure proper application. This qualitative test showed that:

- The standard oblong opening performed poorly when freely grasping the foam pads, creating an instant fold in the pad.
- The large and small grid openings were better than the standard one but still created bumps and folds on the applied foam pads. Which got worse as the pressure increased.
- The ridge opening performed well at the lowest operating pressure of 30 psi. Unfortunately, at 50 psi, this positive result was not maintained as it performed comparably to the standard opening.
- The vacuum cup performed as well as the ridge opening at 30 psi. Even at higher operating pressures, its performance remained good compared to the others.
- The Bernoulli trial does not suffer from the same problems as the Venturi ones, and its performance can be considered excellent for this test.

[3] The weight of the medium foam pad is approximately 0.5 grams, while the large foam pad weighs about 2 grams.

The two tests performed in this section can inform us in making comprehensive design decisions. Firstly, if the goal is to lift a cardboard sheet of foam stickers from the top, a simple oblong opening could suffice. Since the cardboard provides a rigid backing, this scenario is similar to the force test setup. Furthermore, the standard oblong is on par in terms of force with the grid openings, while having the simplest geometry. A robotic setup that positions cardboard sheets of foam pads could effectively use this opening to maximize the grasping force while minimizing the compressed air consumption. This is not the case with our current solution, in which workers manually position the foam pads, but it could be useful information if this operation gets automated. For our current problem of peeling off foam pads, the only viable options are probably using a flexible vacuum cup or the Bernoulli effect. Primarily because they do not create excessive creases or folds in the foam pads. As for which of the two is better, it depends on what is more important to the manufacturer. If uniform pressing on the foam during application is most important, then the Bernoulli effect could provide the most uniform surface. However, if energy consumption is deemed important, then the vacuum cup would consume significantly less energy to operate.

In conclusion, the force test evaluated the grasp strength of various trial prototypes on foam pads. Although maximal force is useful for assessing energy conversion into grasping force, the key objective of the pneumatic mechanism is to ensure the foam pads adhere to the gripper. Additional fold tests determined the ability of the trial openings to handle foam pads without creating creases, indicating that the Bernoulli trial and the vacuum cup had better performance. These tests inform design decisions, suggesting a simple oblong opening for robotic setups lifting the cardboard sheets of foam, and a flexible vacuum cup or the Bernoulli effect for peeling off foam pads.

CHAPTER 6

GRASPING ROBUSTNESS TESTS

After the foam pads have been grasped by the grippers, there are no inherent challenges in placing the foam pads on the plastic parts properly. In fact, the central challenge of the project lies in picking up (unsticking) foam pads. Multiple factors complicate the process of picking up foam pads, as listed below:

- Achieving good positioning for the clamp on the edge of all the foam pads on a cardboard sheet.
- Certain foam pads tend to stick to each other or the side of the cardboard sheet. Sometimes, this might result in the unintended detachment of an adjacent foam pad, or worse, lifting the entire cardboard sheet (if the grasped foam pad sticks too firmly to the edge of the cardboard sheet).
- Ensuring a smooth rotation of the tool for the peeling motion. This depends on the type of robot used, the precise programming of the movements, and the execution speed.

Despite these challenges, when the robotic movements are diligently programmed, the solution has proven surprisingly robust. The next sections will discuss the methodology, results, and interpretation of the different tests conducted throughout the course of this thesis.

6.1 Methodology

The grippers tested were the following: the medium foam pad gripper in three different versions, the small foam pad gripper (ridge oblong opening version), and the large foam pad gripper (ridge oblong opening version). The three different gripper variations for the medium foam pad were : the ridge oblong opening, the vacuum cup, and the Bernoulli[1]. Figure 6.1 shows images of all of these.

[1] The ridge grippers were tested before the completion of the tests in the previous chapter. The Bernoulli and Vacuum Cup gripper were added afterward.

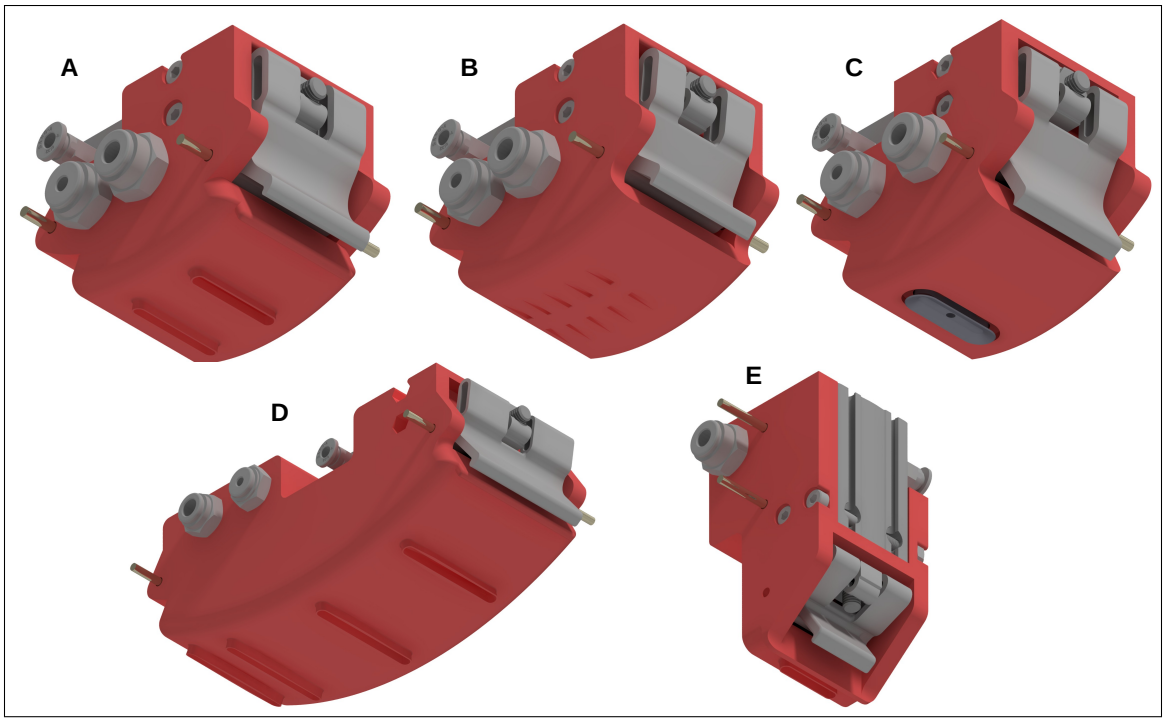

Figure 6.1 Grippers tested for robustness. - A) Medium foam pad gripper with ridge oblong vacuum openings. - B) Bernoulli effect medium foam pad gripper - C) Vacuum cup medium foam pad gripper - D) Large foam pad gripper with ridge oblong vacuum openings - E) Small foam pad gripper with ridge oblong vacuum opening

The procedure for these tests was straightforward. Firstly, a cardboard sheet with foam pads was positioned on the vacuum table or stuck to a table. With the pneumatic line deactivated, the robotic arm was programmed to move the gripper correctly in a peeling motion. Once the programming was set for one foam pad, the test was conducted with the pneumatic line activated. If an obvious problem with the movement scheme arose, the movement was reprogrammed[2]. Subsequently, tests were conducted on a significant number of foam pads, often half a cardboard sheet or a complete cardboard sheet. After each pick-up, the grasped foam pad was applied to a flat surface, freeing the gripper for the next attempt. The robotic pick-up program was set to operate until all foam pads were targeted for pickup by the gripper. The overall performance of each gripper was then assessed based on the success rate of successful foam pad grasps.

[2] The specifics of the movements for each tested gripper are described in their respective results sections 6.2.1 to 6.2.3

6.2 Results

6.2.1 Medium Foam Pad Grippers

Three different medium foam pad grippers have been tested (see Figure 6.3 A, B, and C). All three grippers performed similarly. During the testing of the vacuum cup version, only one issue arose: the foam pad adjacent to the one being grasped was inadvertently detached. It appeared that both foam pads were not completely separated; it happened only once for this foam pad size during all tests. Programming these grippers was straightforward. It consisted of determining the optimal clamp position and peeling motion. We present the results in Table 6.1.

Table 6.1 Medium foam pad robustness tests for the three gripper variants.

Medium foam gripper version	Ridge openings	Vacuum Cup	Bernoulli
Number of successful grasps	40/40	39/40	40/40

6.2.2 Small Foam Pad Gripper

Optimizing the motion of the small foam pad gripper proved to be more challenging. The foam pads often adhered to each other along their long side. This resulted more than often in the simultaneous peeling off of the adjacent foam pad(s). To resolve this issue, we introduced an additional side movement to ensure their separation (see Figure 6.2). Once this side motion was integrated, the grasping became notably reliable. This gripper achieved a success rate of **78/78** grasps.

6.2.3 Large Foam Pad Gripper

The large foam pad tended to adhere more firmly to the very side of the cardboard[3]. This often caused the cardboard to be lifted off the vacuum table during the peeling motion. Under these circumstances, we halted the test (which is what happened on Tests 1 and 2 of Table 6.2). To

[3] We assume this is due to the cutting process of the cardboard sheets. This is discussed in more detail in the Result Interpretation (Section 6.3 and in the Discussion (Chapter 8)

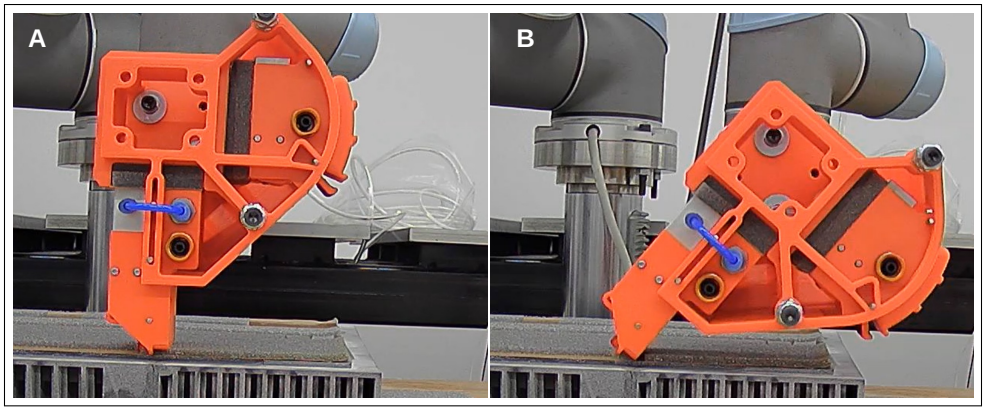

Figure 6.2 Small foam pad unsticking motion. - A) The clamp closes on the small foam pad. - B) The gripper first rotates (the center of rotation is in the middle of the foam pad), then a small side motion separates the foam pad from the others (the side motion to the left is barely visible on the image)

mitigate the lifting of the cardboard, we had to place the clamp at such a distance from the side, that when closing, it would unstick the very side of the foam pad (first one or two millimeters). After closing the clamp, with the side of the large foam pad already partially unstuck, the peeling could proceed without lifting the cardboard. Test 3 of Table 6.2 was done by positioning the clamp that way to pre-starts the peeling.

Table 6.2 Large foam pad gripper robustness tests - Tests 1 and 2 failed due to the cardboard lifting off the vacuum plate. After adjusting the clamp position relative to the side of the foam pads, in Test 3 the system became more reliable

	Test 1	Test 2	Test 3
Number of successful grasps	0/1	4/5	28/28

6.3 Results Interpretation

We tested a total of 5 different grippers for picking up foam, all of which employed a clamp in combination with a pneumatic grasping mechanism. The first three grippers were tested on the medium foam pad. These first robustness tests also served to compare different pneumatic mechanisms: the ridge vacuum opening, the vacuum cup, and the Bernoulli effect. Each of

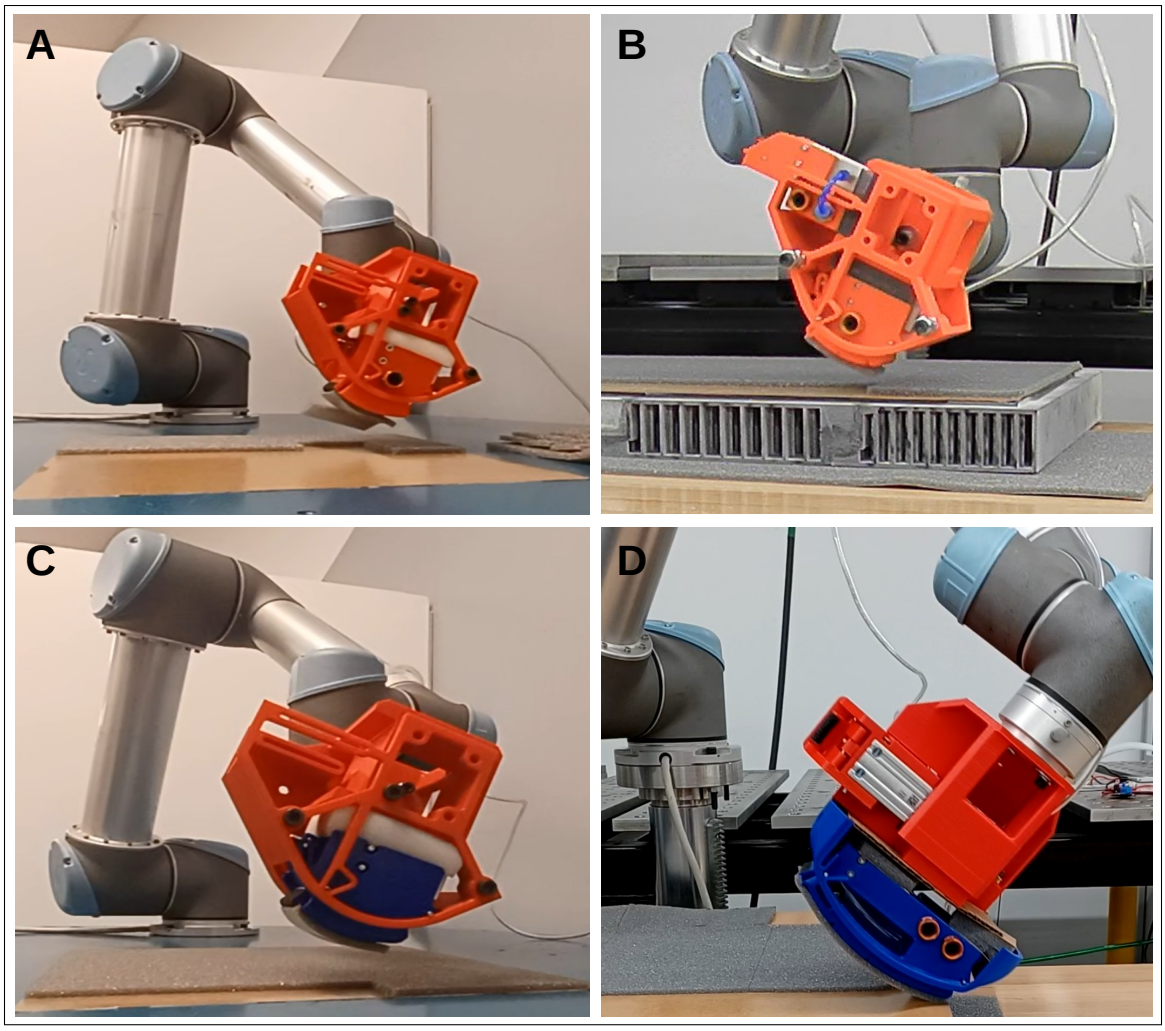

Figure 6.3 Robustness test images - A) Medium foam pad vacuum cup gripper. The only inadvertently detached medium foam pad is visible. -B) Medium foam pad ridge openings gripper. - C) Medium foam pad Bernoulli gripper. - D) Large Foam pad gripper

these three technologies performed equally well, collectively grasping 119 foam pads out of 120. All the other difficulties encountered with the foam pads of different dimensions were due to them being partially stuck to each other or stuck to the side of the cardboard sheets. This is most certainly a result of their manufacturing process, and it might be possible to improve

the situation with a conversation with the foam pads supplier[4]. In the case of the smaller foam pads, an additional movement was required to ensure the separation of the foam pad. For the larger foam pads, extra care was needed to find the right position for the clamp at the cardboard edge. After these specificities were addressed, the picking of the foam pads became reliable. As for the programming process, all movements were implemented via the teach pendant, using simple point-to-point programming. The easiest way to proceed was to define the position of the tool (in the teach pendant) as the center of rotation of the gripper curvature. Then the peeling or application motion could be constructed by points close together, with a small rotation and translation of the tool between each of them. Additionally, it is imperative to mention that while these tests showed that when correctly programmed, the grippers were as robust as they could be, the assumption is that the cardboard sheet is precisely positioned on the vacuum plate. If workers are careless when positioning the cardboard, then the results could get worse. In practice, we find that this positioning imprecision needs to remain ideally under 3mm[5], so the grippers can stay reliable. Exo-s is currently working to implement a positioning jig on the vacuum plates to ensure a faster and more precise positioning of the cardboard. In conclusion, the five tested grippers performed promisingly in foam pad peeling, with the main challenges linked to the foam pads sticking to each other and the cardboard, likely due to their manufacturing process. These aspects, including the vacuum plate setup, could be further improved in the future.

---

[4] The cardboard with foam pads is manufactured in the following way. First, a large cardboard roll with an adhesive layer is unrolled; this thin adhesive layer will become the adhesive backing of the foam pads. Next, the polyurethane foam mixture is applied onto this adhesive side and then cured. At this point, the cardboard is covered with a uniform foam layer (this can be seen as one single foam pad that covers the entirety of the cardboard). Finally, blades cut this foam layer into multiple smaller ones, then other cutters separately cut the cardboard roll into multiple sheets. The first blades need to cut at exactly the right height/pressure to separate the foam pads (foam and adhesive layer), without cutting the cardboard backing. This process does not seem to be perfect, as sometimes some foam pads are not completely separated. Additionally, when cutting the edge of the cardboard, it seems that blade pressure activates the pressure-sensitive adhesive at the cut, which makes it harder to peel the foam pads that are on the cardboard edges.

[5] Defined as the maximum allowable error in the positioning of the perimeter of the cardboard sheets.

CHAPTER 7

ADMITTANCE TESTS

In this chapter, we study the use of an admittance force control for the application of foam pads. Since the foam pads have pressure-sensitive adhesive, the grippers must apply pressure for the pads to adhere securely. Ideally, the gripper would maintain an adequate level of pressure during the application motion. An admittance control scheme can make this possible; a predetermined force can be set to match a certain pressure level. Unfortunately, to maintain the stability of this admittance control, the application motion needs to be significantly slowed down. As a result, we also explore using a trajectory generated by the admittance control, which can then be executed at a higher speed. The following sections will detail the functioning of the admittance control, the methodology used for various tests, and the corresponding results. In the final section of this chapter, we will provide an interpretation of these results.

7.1 Admittance Control

The admittance control has been implemented using the Real-Time Data Exchange (RTDE) interface from Universal robots[1]. The RTDE makes it possible to receive data from a UR robot controller and send instructions to it at a frequency of up to 500 Hz. With this interface, the admittance control loop was programmed inside a Python script. The data received from the UR5e robot is the forces at the tool center in the base coordinate system (*actual_TCP_force*)[2]. Using these actual tool forces enables the abstraction of the robot's kinematics, which makes the admittance control easy to implement. The admittance control can be visualized as adding a virtual mass-spring-damper system between a target position and the actual robot position (see Figure 7.1). The spring pulls the robot toward the target position, at a force proportional to the distance between its desired position and the actual robot position (for the orientation, it would

[1] RTDE guide: https://www.universal-robots.com/articles/ur/interface-communication/real-time-data-exchange-rtde-guide/

[2] (*actual_TCP_force*) is a six-dimensional vector that contains the generalized forces in the TCP. It compensates the measurement for forces and torques generated by the payload. The forces are measured via force sensors at the flange and then corrected by the robot controller. (Information retrieved from the ROBOT CONTROLLER OUTPUTS section in the previous URL link)

be a torsion spring). The damper creates a force that opposes the speed of the end-effector. It can also be visualized as moving the robotic arm in a viscous liquid. Finally, the virtual mass, with its inertia, resists the change in speed of the tool tip; it stores and releases virtual energy through accelerations. Additionally, for every degree of freedom (3 translations and 3 rotations), it is possible to have different spring, damper, and mass coefficients. The dynamics of the system can be described by the following equation:

$$M\ddot{r} + B\dot{r} + K\,r = f_{TCP} \tag{7.1}$$

Where r is the tool position and orientation vector, M is the mass matrix coefficient, B is the damper matrix coefficient, and K is the spring matrix coefficient. The f_{TCP} term refers to the force vector as returned by the robot controller. It is possible to control the dynamics of the system by adding a target position and a target force, Equation 7.1 becomes:

$$M\ddot{r} + B\dot{r} + K\,(r - r_{target}) = f_{TCP} - f_{target} \tag{7.2}$$

Figure 7.1 illustrates how the admittance control can be visualized, as well as presenting the control law diagram. The mass, spring, and damper coefficients can take different values, but some combinations might lead to instabilities or oscillations. For example, setting the damper coefficients to 0 would result in a continuous oscillation of the robotic arm since no energy is expelled from the virtual system. Alternatively, setting the spring coefficients to 0, while keeping the damper coefficients, would make it possible to move around the robotic tool tip like in a viscous fluid (similar to collaborative robots teach mode or free mode). One can also selectively choose which degrees of freedom will be affected by the admittance control loop. In our case, only a force perpendicular to the surface of application is needed. In the admittance tests, the surface of application is in the XY plane, therefore the force control was only necessary for the Z axis. Furthermore, the spring coefficient is eliminated as a pulling force proportional to a distance isn't required. As such, the control law from Equation 7.2 simplifies to:

$$m_z\ddot{r}_z + b_z\dot{r}_z = f_{TCP\ z} - f_{target\ z} \tag{7.3}$$

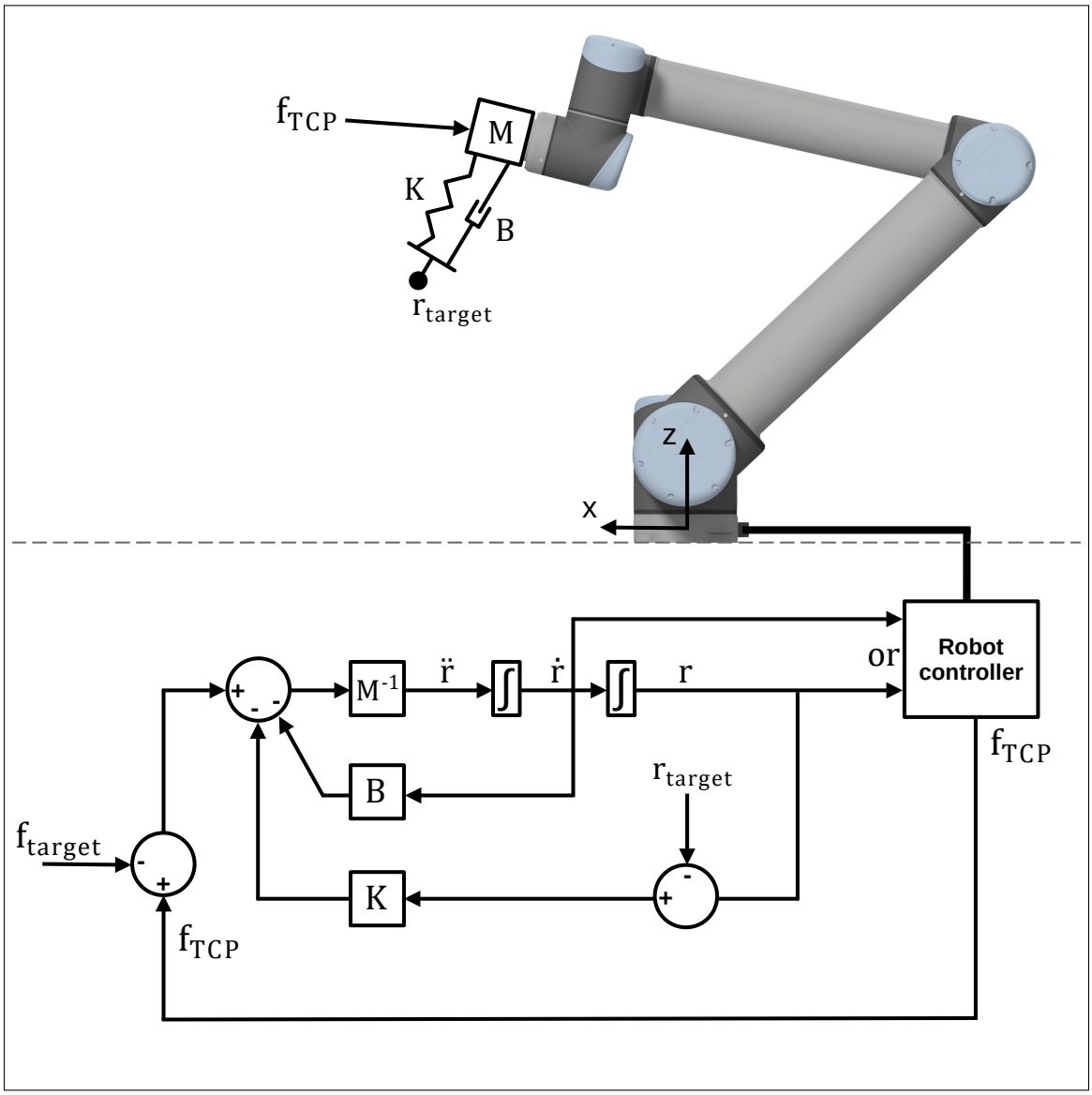

Figure 7.1 Admittance Control - (TOP) Illustration of the virtual mass-spring-damper system. - (BOTTOM) Admittance control block diagram from equation 7.2.

Finally, as shown in the control diagram in Figure 7.1, the robot can be controlled in either position or speed (r or $\dot{r}$). We found that controlling in speed mode was a little smoother. It was achieved via the *speedl()* UR script function.

7.2 Methodology

To assess the potential of employing admittance control with a UR robot for foam pad application, we conducted three distinct tests. The objective of the first test was to evaluate the efficacy of the admittance control in maintaining a constant force throughout the application motion. The second test explored the concept of utilizing a trajectory, generated by admittance control, at a higher speed. The final test aimed to compare the force readings from the UR5e wrist force sensor with those derived from the force plate sensor. To carry out these tests, we employed a dummy gripper prototype designed to apply pressure on a large foam pad. This end-effector, composed of two parts separated by a polyurethane foam block for added compliance (as depicted in Figure 7.2), features a curved design facilitating the investigation of force control during the execution of the application motion. The desired motion was achieved by rotating the tool at a constant speed and matching this rotation with translation. This prevents the tool's surface from slipping on the foam pad (the kinematic principle used here is analogous to a rolling wheel). In each of the three tests, the end-effector first touches the foam pad, applying pressure close to the desired level. Then the motion is initiated, and the force applied to the foam pad is measured at 0.05-second intervals. In the force validation test, the force was measured using both the UR force sensor and the force plate sensor.

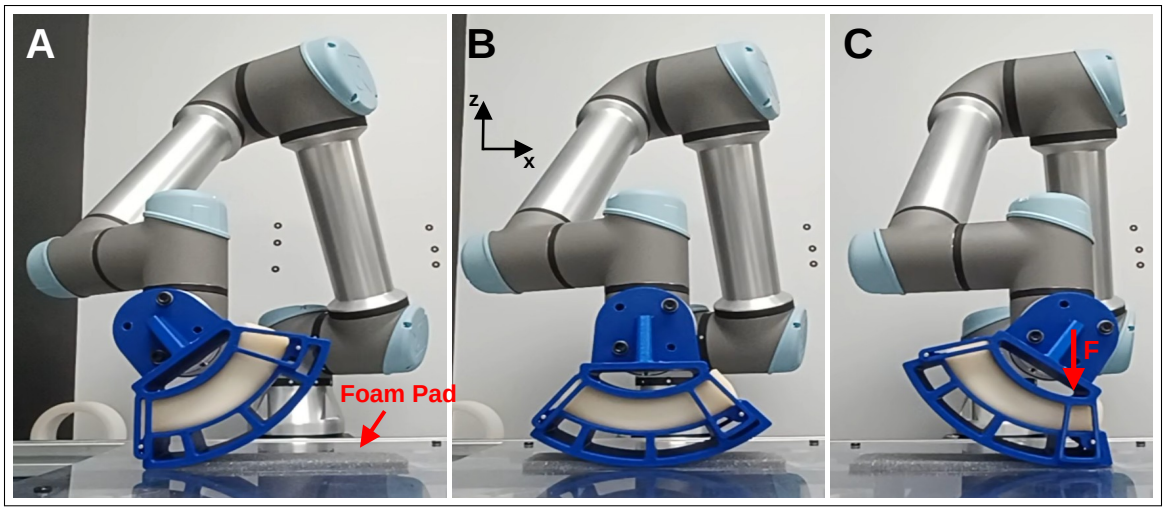

Figure 7.2 Admittance control test example. The large foam pad is positioned on the force plate sensor. The appliance motion test is executed from A to C

7.3 Results

7.3.1 Admittance control test

In this sub-section we present the admittance force control results. These tests simply consisted of maintaining a constant downward force throughout the appliance motion. Two different force settings have been tested: 10N and 20N. For each level of force, 10 tests have been conducted, each corresponding to one appliance motion. The force results are presented in Figure 7.3. The corresponding Z-axis positions are presented in Figure 7.4 (the only admittance-controlled axis). For the 10N tests, the minimum starting value was **7.68N**. After 1 second, the minimum and maximum values registered were **9.39N** and **10.44N**. For the 20N tests, the minimum starting value was **15.73N**. After 1 second, the minimum and maximum values registered were **19.07N** and **20.3N**.

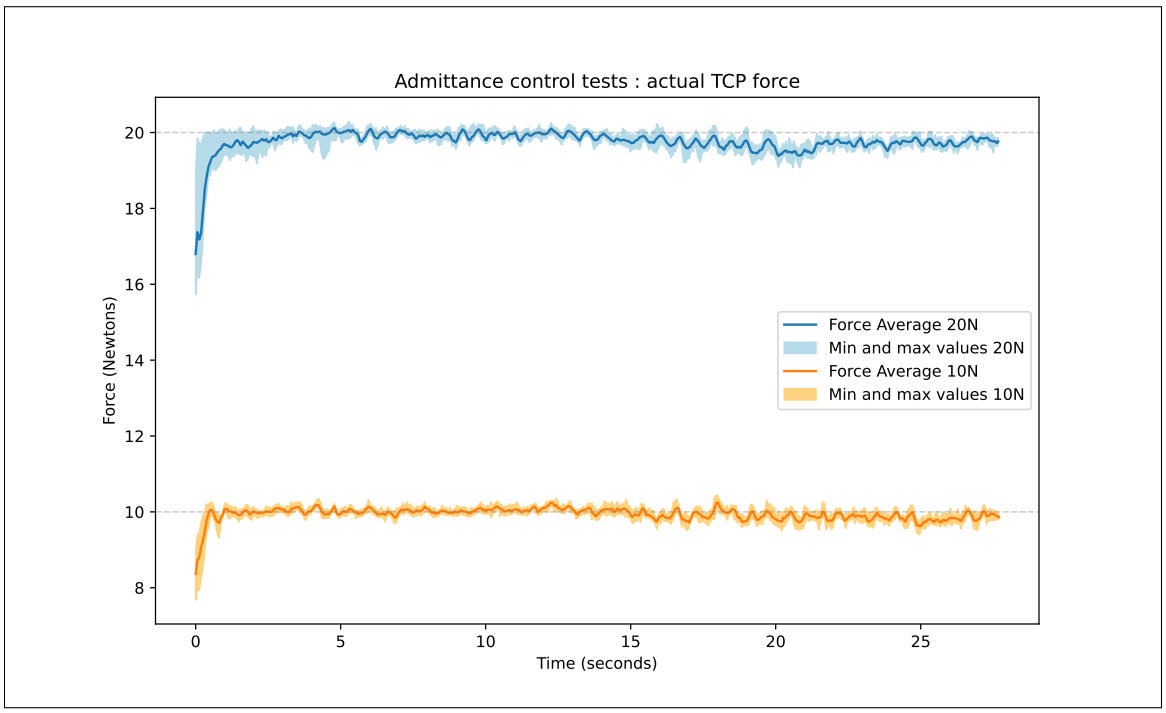

Figure 7.3 Admittance control tests; actual TCP registered force (Z axis). The two curves are an average of 10 different appliance motion tests each. The semitransparent band represents the maximum and minimum registered values at each time step

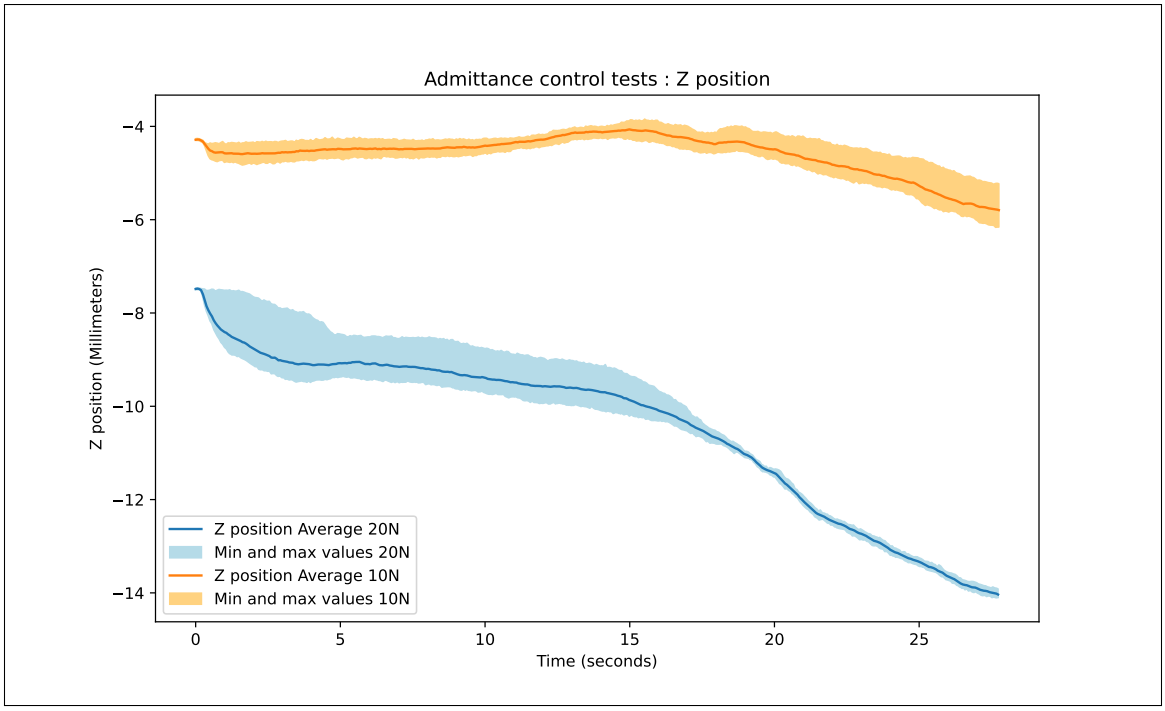

Figure 7.4 Admittance control tests; Z axis position. The two curves are an average of 10 different appliance motion tests each. The semitransparent band represents the maximum and minimum registered values at each time step

7.3.2 High-speed tests

This subsection presents the results of replaying an admittance-generated trajectory at higher speeds. The trajectory is first generated by doing an admittance-controlled motion, similar to the admittance control tests. The application motion was then repeated at 2, 4, 8, and 16 times the initial speed. Only the force graphics for the 4x and 16x tests are presented (Figures 7.5 and 7.6). The other two are in Appendix VI. All the maximal and minimal values for the tests are presented in Table 7.1, as well as the total motion time. Each curve shown in Figures 7.5 and 7.6 is an average over six high-speed tests. As usual, the band represents the maximal and minimal values at each time step.

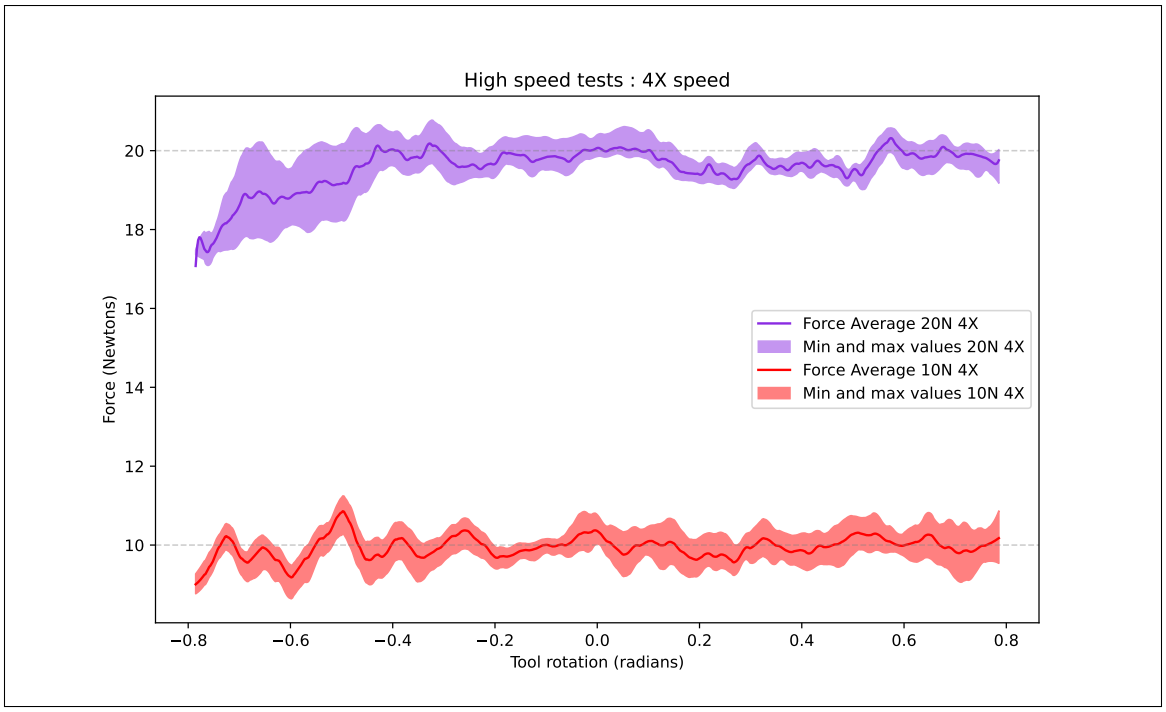

Figure 7.5 High-speed test : 4 times the speed

Table 7.1 High-speed tests results

Tests at 10 Newtons	Average force (N)	Minimal force (N)	Maximal force (N)	Time of completion (s)
Admittance controlled	9.95	7.68	10.44	27.7
2 time the speed	10.22	8.58	11.49	13.8
4 time the speed	9.95	8.57	11.19	6.9
8 time the speed	10.15	8.65	11.38	3.5
16 time the speed	10.18	8.49	11.36	1.7
Tests at 20 Newtons	Average force (N)	Minimal force (N)	Maximal force (N)	Time of completion
Admittance controlled	19.78	15.73	20.3	27.7
2 time the speed	19.61	16.79	20.97	13.8
4 time the speed	19.56	16.82	20.76	6.9
8 time the speed	20.02	16.93	21.45	3.5
16 time the speed	20.45	16.66	22.47	1.7

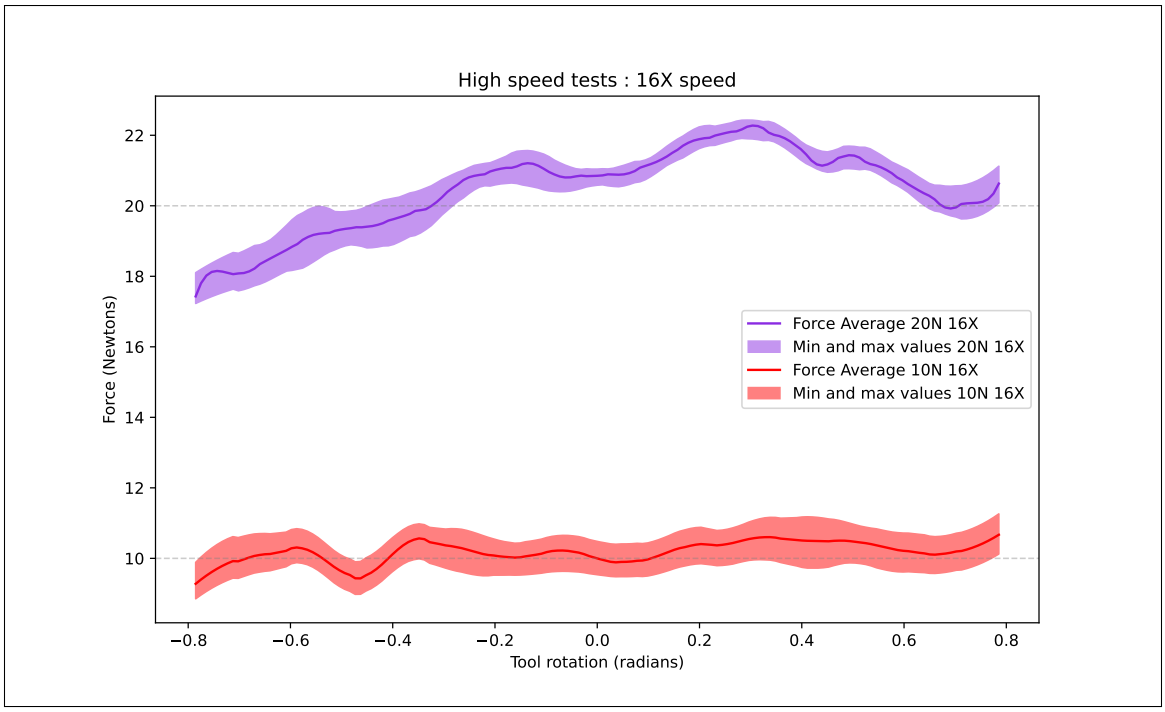

Figure 7.6 High-speed test : 16 times the speed

7.3.3 Validation test

We validated the admittance-controlled motion and present the results in this section. This validation was conducted using a force plate sensor for each of the admittance tests as described in Section 7.3.1. The force plate sensor was zeroed before each test. Figure 7.7 shows both the readings from the robot's force sensor and the force plate sensor during the appliance motion. We noted a discrepancy between the two force readings, which was unexpected. To delve deeper into this issue, we conducted another static experiment. This involved maintaining a force of 20N in admittance control at three different tool orientations (start, middle, and end position). In all three tests, we maintained a force for 5 seconds at the center of the force plate sensor (the tool made contact at the same point on the force plate in all three tests). The results indicated variance in force measurements across the different tool orientations, as illustrated in Figure 7.8.

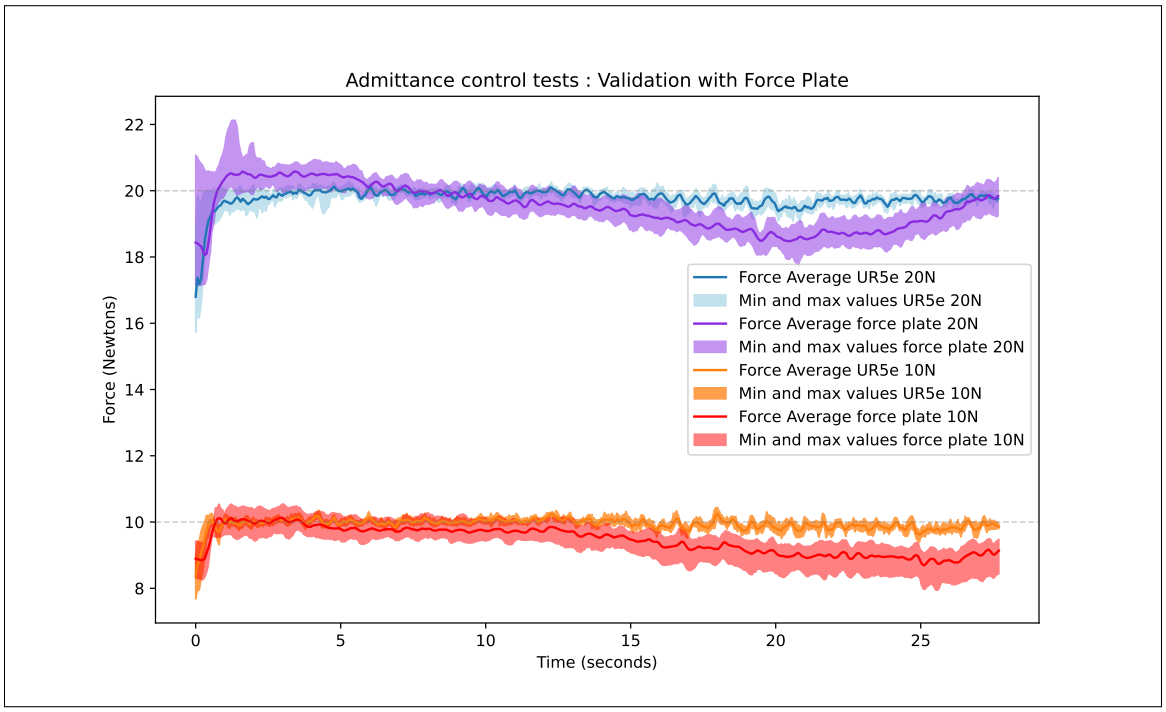

Figure 7.7 The purple and red curves represent the average of the force measured by the force plate, from the 10 appliance motion tests previously presented. The semitransparent band represents the maximum and minimum measured values at each time step

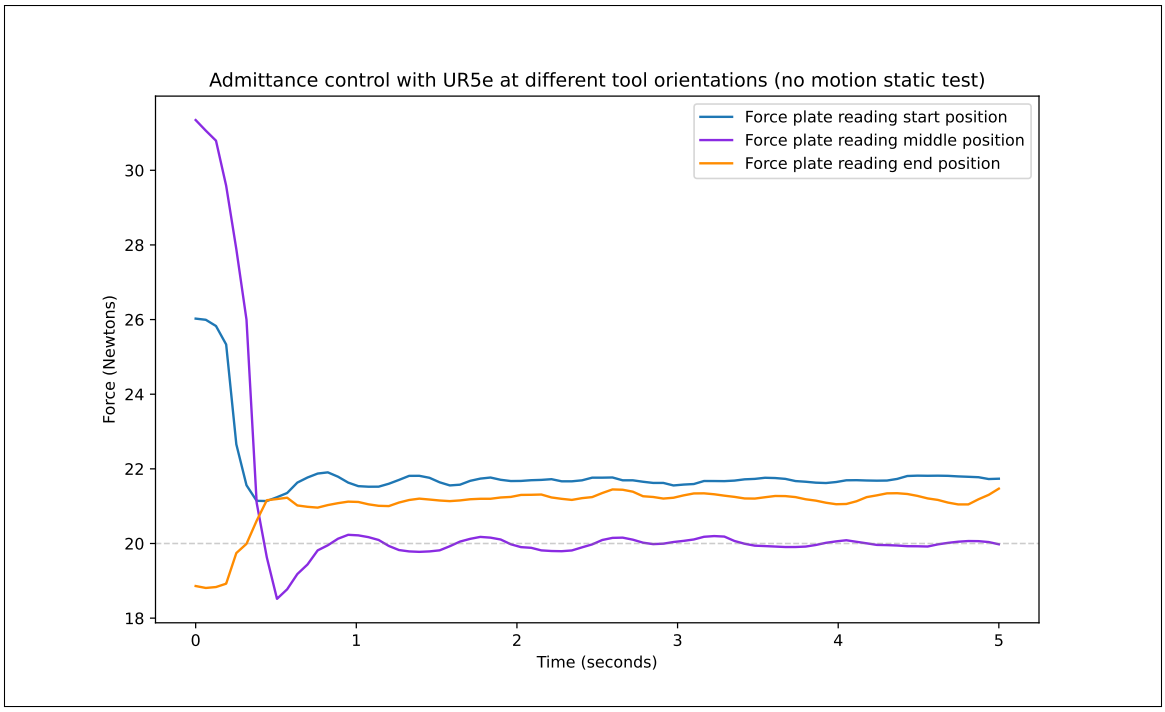

Figure 7.8 In each of these validation tests, the dummy gripper was centered on the force plate. Then, a downward force of 20N was applied using admittance control. All three force readings stabilized approximately 1 second after initiating the admittance control

7.4 Results interpretation

The force-controlled admittance tests demonstrated the capability to maintain a targeted force throughout the entire duration of the motion. However, the recorded force fluctuated and did not precisely match the predetermined value. In the first set of tests that were solely controlled through admittance for the entire motion duration, the variations did not exceed ±1N. We also discovered during these tests that there was a significant delay before the force reached the predetermined value. The initial loading force would ideally correspond to the predetermined application force, thus reducing the delay in reaching the set force when the admittance control initiates. For the stability of the admittance control, the speed of the motion was maintained at a relatively low level. The completion of the application motion for the chosen foam pad took 27.7 seconds. This duration is considerably too slow; for comparison, our collaborative station is required to grasp and place 5 foam pads in less than 45 seconds. Consequently, a second set

of tests explored the possibility of accelerating the speed of the replayed admittance trajectory. To accomplish this, a trajectory stably generated at a low speed was replayed at 2, 4, 8, and 16 times the speed. These accelerated tests increased variability in the application force. In the tests conducted at 16 times the original speed, these variations were up to 1.51N in the 10N tests, and up to 3.34N in the 20N tests. Representing respective differences of 15.1% and 16.7% from the predetermined forces. At 16 times the speed, the time of completion was reduced to 1.7 seconds, which is sufficiently rapid for consideration in our robotic application. Noticeably, for this same speed test, the recorded force seemed to overshoot the target value more dramatically. This discrepancy could be attributed to a damping effect caused by the polyurethane compliance. Switching to springs for compliance could potentially result in less overshooting of the target force at higher speeds. Finally, the validation tests indicated that there was a difference in the controlled force for different orientations of the end-effector. In other words: the target force was set to 20N, but the force as perceived by the UR5e changed depending on the arm configuration[3]. Thus, this suggests a possible software or hardware issue with the UR5e actual TCP Force functionality.

[3] The dummy gripper's center of mass was correctly configured inside the UR teach pendant.

CHAPTER 8

DISCUSSION

8.1 Summary of Experimental Findings

Our primary research objective was to develop and study a robotic tool that can pick and place foam pads. To the best of our knowledge, this is the first time that developing specialized grippers for foam pads has been attempted. Therefore, the challenges of the task and the industrial constraints were the main factors driving the development of the solution. To successfully implement a new robotic station in an industrial setting, the grippers needed to be highly robust. The results of the robustness tests showed that, when the motion was correctly programmed, the success rate of picking up foam pads was nearly perfect. Most of the faulty grasping resulted from the fact that the foam pads sometimes stick together, or from the fact that the vacuum plates weren't strong enough. Both of these problems could be partially or completely eliminated by methods other than modifying the developed grippers. Moreover, we conducted further specialized experimental tests with two different pneumatic effects: Venturi and Bernoulli. Six different trial prototypes using these two effects were investigated for grasping foam pads. The Bernoulli effect trial consumed considerably more compressed air for the same grasping force than did the Venturi-based trials. Nevertheless, when gripped freely, most of the vacuum openings created creases or folds in the foam pads. The best Venturi-based trial was the polyurethane vacuum cup, as it did not create pronounced folds across a great range of operating pressure. For completion, we tested the robustness of two different grippers using the promising vacuum cup and the Bernoulli effect. They both performed as well as the original ridge-opening prototype. These two gripper prototypes also possess the particularity of having a relatively flat surface in contact with the foam pads. This is useful for applying uniform pressure on the pads and ensuring their adhesion. Finally, we also investigated the application of pressure on foam pads in our last set of tests. To achieve this, we developed an admittance control to apply force through a UR robot. Applying a constant force on the foam pad throughout the movement proved to be highly accurate. While the force remained constant during the admittance control movement, the speed was too slow to be considered for a real-life assembly line. To address this

issue, replaying an admittance-generated trajectory was investigated. This solution proved to be a good compromise, with a speed-up of 16 times only doubling the force errors.

8.2 Relation to Other Research

In the literature review, we synthesized scientific research that could inform the design of a foam pad gripper. This review encompassed various gripper technologies, including pinch, needles, vacuum, Bernoulli, and electroadhesion. Additionally, we reviewed technologies for dispensing stickers and robotic applicators designed for such stickers. The resulting gripper was a combination of a pinch gripper and a pneumatic grasping mechanism. Using the pinch/clamp proved necessary, as it is the only solution robust enough to firmly grasp the foam pads during the peeling motion. While grasping deformable objects such as fabric can be tricky in this manner (Koustoumpardis and Aspragathos, 2004, p.231), the thickness of foam pads makes it straightforward. Moreover, the foam pads regain their original shape after being pinched, unlike fabric. When detached, the foam pads can easily be held in place by a pneumatic grasping gripper; however, like fabric, they can also be sucked into a vacuum opening. To address this, we used multiple smaller holes, as in the gripper studied by Fleischer et al. (2016). The grid trial prototypes served as an attempt to divide the vacuum openings into multiple smaller ones, which mitigated foam pad deformation compared to a single large opening. On the other hand, the vacuum still compressed the foam pads, resulting in creases and folds in the adhesive backing. Somewhat surprisingly, the polyurethane vacuum cup proved most effective at maintaining the shape of the foam pads. In existing literature, these are typically used to grasp smooth objects (Gabriel et al., 2020; Mykhailyshyn et al., 2022). Foam pads are indeed permeable to air (tested in Appendix VII), but it appears that they become less permeable when compressed. In fact, with all the vacuum trial prototypes tested, the vacuum levels were at good fractions of the optimal levels (Table 5.2). This behavior contrasts significantly with that of fabric and suggests a new avenue of research for the handling of foam. Regarding objects similar to stickers, which can be peeled and applied, our research corroborated the existing literature. As Björnsson et al. (2013) suggested, a combination of mechanical and pneumatic systems can be effective

for peeling objects similar to stickers. Using both a clamp and a pneumatic grasp provided a successful solution to our challenge. To apply foam pad stickers, we required gripper compliance to minimize the force spikes resulting from hard contact between a solid surface and a robot with a high reduction gear ratio. This added compliance has also been adopted by others for adhering objects to hard surfaces (Yuan et al., 2018 and 2020; CAB labeling applicator products[1].

8.3 Implications

We have demonstrated that up to five of these grippers can be used on a collaborative robot in an industrial setting, potentially reducing production costs and alleviating worker shortages. The gripper can also be adapted to accommodate various foam pad dimensions; this can be achieved by modifying the CAD file of the main component. The newly designed gripper can then be 3D printed and tested. This adaptation process is expedient because only the main component needs modification, and it is entirely 3D printable. Several other stations at the Exo-S plant, and potentially at other plants, could benefit from automated foam pad placement. Furthermore, the main component in all the grippers serves as a pneumatic manifold, substantially reducing the number of components in the end-effector assembly. We have also integrated 3D-printed Venturi vacuum generators into these components (see Appendix III for prototype images). It can thus further reduce the number of components, as well as the cost and complexity of assembly. This approach, which combines functional parts with pneumatic circuits and passive mechanisms, is promising for two reasons. Firstly, it has the potential to be applied in various other contexts for entirely different objectives. For example, a robotic finger could be 3D printed with an integrated Venturi ejector and vacuum openings on the fingertip. Alternatively, the main structural component of an end-effector could also function as a pneumatic manifold. Secondly, as 3D printers continue to become more affordable and versatile in the materials they can print, multifunctional components like ours are likely to become increasingly common. Our gripper serves as a compelling example of what can be achieved in this regard. Lastly, the trajectory generated by the admittance control can effectively apply pressure to the foam pads. This

[1] Products presented in the literature review, retrieved from https://www.cab.de/en/marking/marking-laser/lmplus/#anwendungenandhttps://www.cab.de/en/news/news/robotic

task, previously performed with a roller on another robotic station, can now be accomplished concurrently with foam pad placement.

8.4 Limitations

While the developed solution has been generally successful, it presents certain limitations. One significant limitation pertains to the shapes of parts on which the grippers can apply pressure. In its current form, the gripper cannot apply uniform pressure on geometries that possess a curvature perpendicular to that of the gripper (see Figure 8.1 A1 and A2). Additional complexities in geometry would also be incompatible with the existing design. Although the shape of the gripper could be adapted to match the shape of the part onto which the foam pad will be applied, challenges remain. For instance, since the foam pads must be peeled from cardboard on a flat surface, the clamp must be relatively straight. Furthermore, achieving a seal on the vacuum opening could prove challenging with more complex gripper geometries. Another significant limitation is related to the wear of the gripper over time. With a cycle time of 45 seconds and three 8-hour shifts per day, this amounts to up to 10,000 cycles per week. Various wear mechanisms could pose problems: friction between 3D-printed parts or metal, repeated pressure on the compliant parts, and repeated minor impacts on the gripper surface, among others. Wear was observed on the vacuum opening ridges of the grippers after a week of operation in the Exo-S plant. However, as some parts show signs of wear, these could be upgraded with more durable or low-friction materials. For example, foam compliance could be replaced with springs, and low-friction bushings could be added to the clamp. Lastly, it is worth mentioning a limitation concerning the shapes of foam pads that can be grasped and applied by the grippers. Our focus has been on rectangular foam pads, but Exo-S also commonly uses pads with other geometries. Longer and thinner foam pads are widely used for the same types of parts as rectangular foam pads (see Figure 8.1 B1 to B3). It remains uncertain whether the current gripper design could accommodate these alternative foam pad shapes.

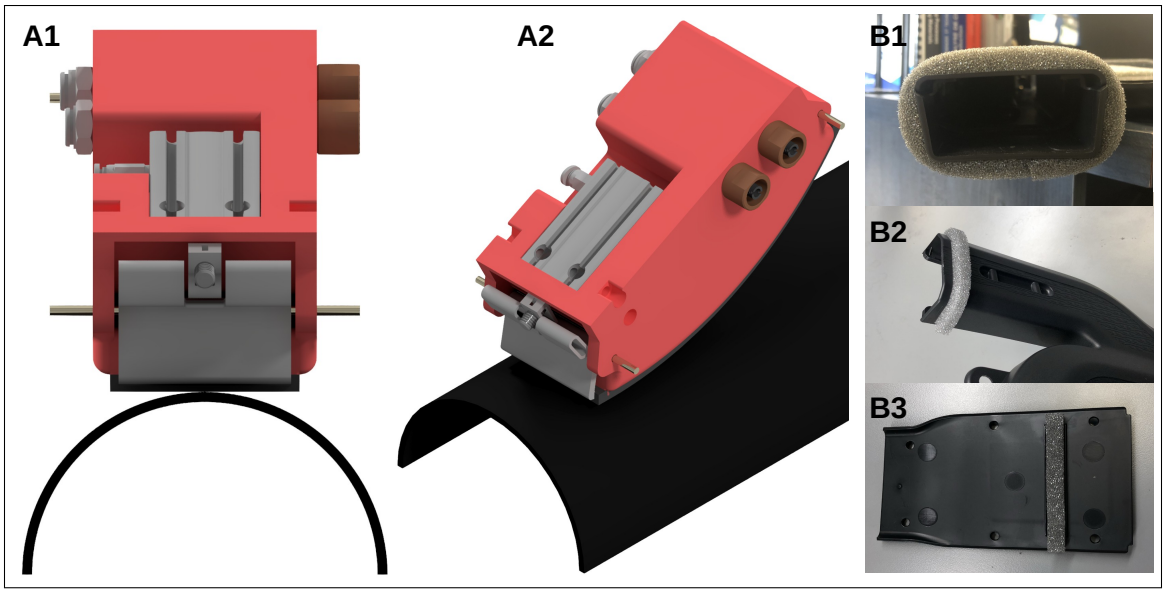

Figure 8.1 Limitations of the current gripper design. - A) A part with a curved geometry makes it impractical to apply uniform pressure to the foam pads due to the fixed geometry of the gripper. - B) Examples of longer foam pad types

8.5 Recommandations for Future Research

There are several different aspects of foam pad manipulation that could be investigated in the future, along with potential improvements for the grippers:

- **Manipulation of Long Foam Pads:** As noted in the limitations section, longer foam pads could pose unique challenges. First, their shape differs significantly and may require extensive modifications to our existing gripper design or even an entirely different approach. Secondly, unlike rectangular ones, they are often applied to curved geometries, and sometimes even go all around a part[2].
- **Deepening our understanding of Vacuum Openings for Foam Grasping:** In Section 5, we compared the performance of different vacuum openings for grasping foam pads. While this analysis informed us about the optimal geometry for maximizing force and which one is best for the free manipulation of foam pads, further research is required. For example, exploring how the porosity of open-cell foam changes when compressed.
- **Variations in Bernoulli Grippers:** Compared to vacuum openings, we did not explore a wide range of geometries for the 3D-printed Bernoulli grippers. Improvements in the design could potentially yield higher grasping forces or greater energy efficiency. Investigating different jet openings and varying distances/orientations between these jets could lead to performance improvements.
- **Combination of Clamps and Electroadhesion:** An interesting alternative to pneumatic grasping would be the use of an EA pad. Though it may offer lower grasping forces, it might be sufficient for holding foam pads against the gripper surface. Additionally, compared to a Venturi vacuum generator, it uses minimal energy, which may be advantageous over the long term. If the clamp is actuated electrically, the gripper would be fully electric, a beneficial feature if a plant lacks pneumatic lines.
- **Incorporating a Side-Pressing Mechanism:** To ensure that no other foam pads stick to the one being peeled by the gripper, a mechanical side-pressing mechanism could be added. This would press down on the adjacent foam pad(s), ensuring proper separation.

[2] They are used to create seals between parts, unlike rectangular foam pads, which are mainly used for noise reduction

- **Optimizing Vacuum Plates:** The existing vacuum plates could be redesigned to maximize their holding force. Additionally, a positioning mechanism could be introduced to guarantee accurate placement of the foam pad cardboards each time.
- **Exploring Admittance-Generated Trajectories with Varying Compliance Types:** To validate the approach of replaying high-speed admittance-generated trajectories, different types of compliance could be examined. Variations in amplitude, rigidity, and compliance type could offer insights into the method's applicability across a broader range of conditions.

Beyond the aforementioned points, other more generalized innovative ideas could be explored and integrated into the collaborative station. Currently, human intervention is still required to place and swap the parts where foam pads are applied. Automating this step would render the station fully independent from human workers. Such automation would necessitate a system capable of locating and grasping parts as they arrive from the conveyor, regardless of their position or orientation, and even when they are stacked on top of one another. This would most certainly mean new innovations in AI-controlled robotics.

8.6 Recommendations for Exo-s

In light of the current results and evidence presented in this thesis, we advise our industrial partner as follows:

- Utilize the vacuum cup variant for all grippers, ideally limiting to one vacuum cup per gripper to maintain adequate pressure.
- Retain the compliant part of the grippers, but consider replacing it with springs.
- Investigate the wear of the end effector and update parts of the solution accordingly.
- Investigate the application of pressure on foam pads on a production line, potentially with the assistance of a trajectory generated by admittance control.

CHAPTER 9

CONCLUSION

The work presented in this thesis details a solution for robotically handling foam pad stickers. As it was the first attempt at automating foam pad placement, the emphasis was placed on creating a solution that meets the challenges of the tasks and meets the necessary industrial constraints. Guided by these considerations and inspired by gripper literature, we then developed a type of gripper that incorporates multiple technologies. These include mechanical grasping, pneumatic grasping (using the Bernoulli and Venturi effects), added compliance, admittance control, and 3D-printed functional parts with integrated pneumatic circuits. All previously mentioned paradigms were eventually integrated into an end-effector with five foam pad grippers and tested in a collaborative cell at the industrial partner's plant. Additionally, some aspects of the solution were investigated more deeply: the performance of multiple vacuum openings on grasping foam pads was assessed, the grasping robustness was tested on five different gripper variations, and an admittance-based strategy for applying foam pads was tested. The results of these tests have interesting implications. Different end-effectors could be adapted to other production lines where rectangular foam pads are applied, or they could be integrated into future projects. Yet, there are limitations to the solution and certainly possible improvements. As enumerated in the Discussion section, different aspects of the solution could be researched more thoroughly. Nevertheless, the overall objective was met as all parts of the solution exceeded our expectations. The path taken to arrive at this solution involved generating ideas, making adequate design decisions, and validating concepts with rapid prototyping. Consequently, this thesis represents, in a sense, just the tip of the iceberg...

APPENDIX I

CLAMP FORCE TEST

This small test was conducted to quantify the force needed to unstick a foam pad. Specifically, we compared the force required to unstick the foam pad when grasping from the side versus the middle (see Figures I-1 and I-2). Four tests were conducted grasping the side, resulting in an average of 4.1 Newtons needed to unstick the foam pads. Two tests were conducted grasping the middle of the foam pads, both of which tore the foam pad before unsticking it. The average force to tear the foam pads was 23.1 N. Figure I-3 shows an image of a torn foam pad. These tests were conducted with a UR5 robotic arm and the force plate sensor.

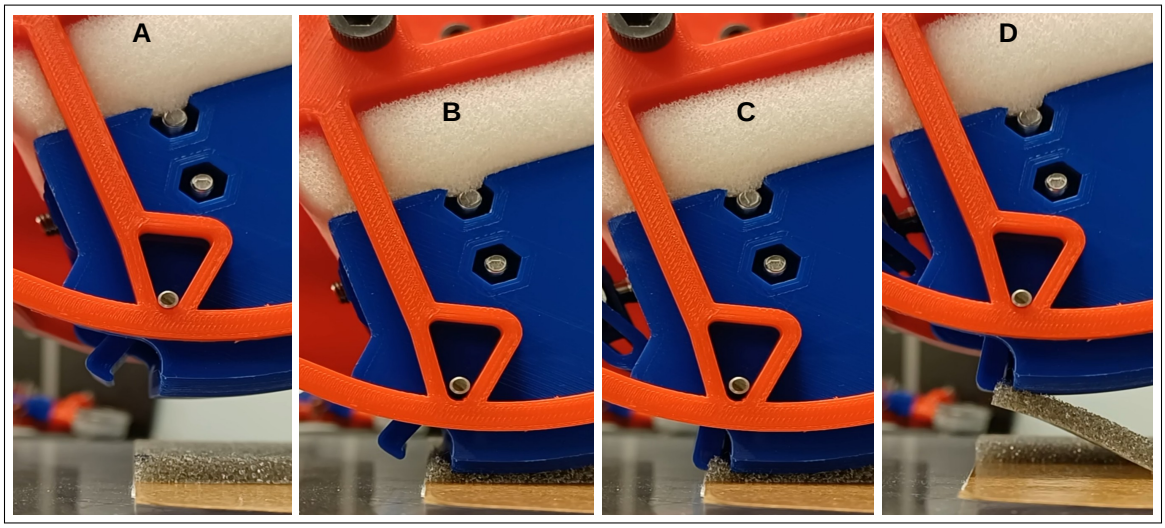

Figure-A I-1 Grasping a foam pad from the side

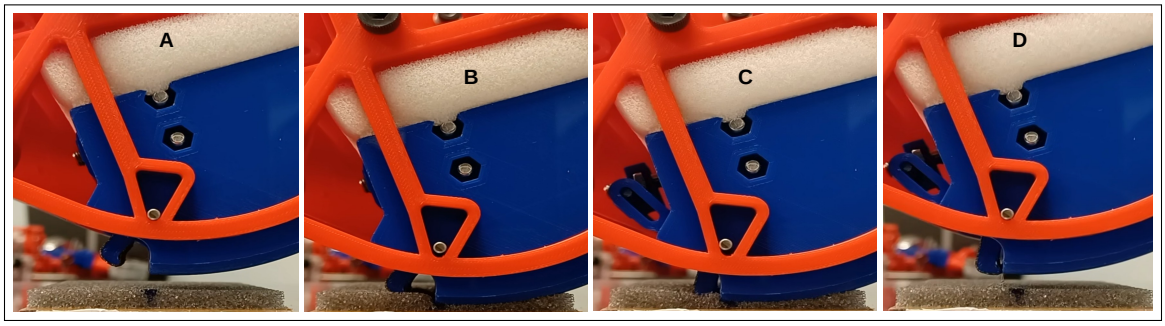

Figure-A I-2 Grasping a foam pad from the middle

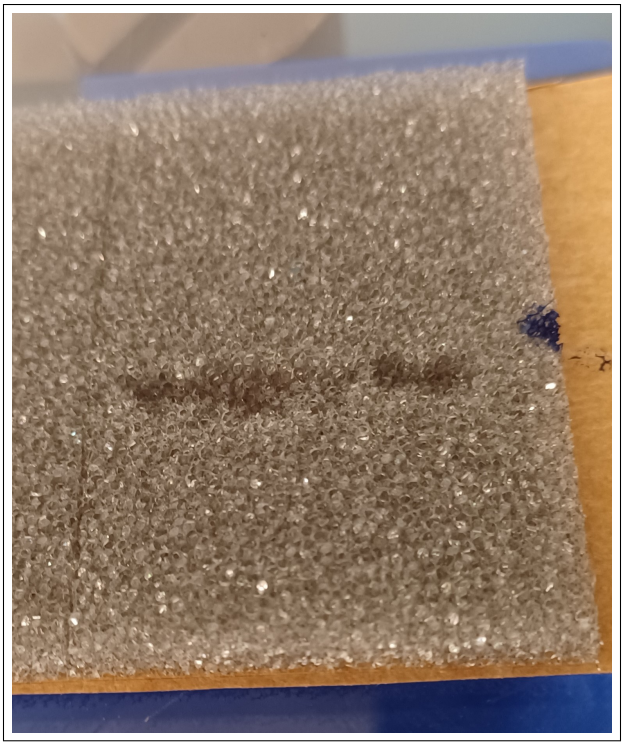

Figure-A I-3 Tore foam pad after attempting to grasp it from the middle

APPENDIX II

COLLABORATIVE ASSESSMENT

Here, we detail risk assessment and reduction for our end-effector relative to two different ISO standards: The ISO/TR 20218-1:2018 and ISO/TS 15066:2016. The first one provides guidance on safety measures for the design and integration of end-effectors, and the latter specifies safety requirements for collaborative industrial robot systems. We applied the methodologies from these standards in the following paragraphs.

1. Limits of the end-effector

1.1 a) Use limits

The end-effector, which has five foam pad grippers, will be used near a human worker. Nevertheless, there is no direct physical interaction between the worker and the end-effector. The foam pad's cardboards and parts should be separated in space. The workers should change the foam pad cardboards when the collaborative robot applies the foam pads to the parts or change the parts when the robot takes foam pads. There should be sufficient space between these two workstations to prevent any contact between the robot arm, end-effector, and the human worker. The end-effector and robotic station should be used exclusively with a collaborative robotic arm.

1.2 b) End-effector limits

The end-effector has five grippers. Each of these grippers has a clamp and Venturi vacuum generator. Both need to operate together at pressures between 30 psi and 100 psi.

2. Hazard identification

We identified the principal hazard as being an unintended interaction between the worker's hands and the end-effector. This could occur when the worker is changing parts/cardboard while the robot's appliance or pick-up sequence starts. It could result in the worker's hands being

compressed between one of the grippers and a solid surface (quasi-static contact). This can occur with the parts on the immobile jigs, or the vacuum plates. In the case where it happens during the picking motion, the gripper could also pinch the skin or fingers of the worker. Another hazard risk is the collision of the end-effector with a body part of the human worker when in motion (transient contact).

3. Risk estimation and evaluation

Using a certified collaborative robot, activation buttons, and sensors greatly reduce the severity and probability of the clamping hazard. The collaborative robot speed is maintained under 200 mm/s, which is a standard for collaborative robots. When working in proximity to a surface, it is slowed down to 100 mm/s. Sensors detect if the parts or cardboard haven't been changed, if not, the robot waits for the worker to change the parts or cardboard. Then a button is pressed by the worker to resume the program. This greatly reduces the potential for a clamping situation. Furthermore, the collaborative robot doesn't move in the worker's space, where the head or the body of the worker could be. The only intersecting space between the worker and robot occurs where the parts and cardboards are. These two spaces have the worker's hand and arm inside them when changing the parts or cardboard, but as explained earlier, not at the same time. The fact that the robot motion is predictable (the same motions run every 45 seconds) also reduces the likelihood of accidents.

4. Risk reduction measures

To further reduce the risks of injuries if any of the hazards occur, the collaborative end-effector shell has been developed to minimize sharp angles and cutting edges. The grippers have also been developed to minimize sharp angles and cutting edges. The gripper mass has also been kept to a minimal value, by using light 3D printed parts, and by not having the solenoid valves inside the end-effector (The total mass is 5 kg). This reduces the energy transferred during an impact, which in turn reduces the risk of injuries. The operating pressure should be kept to the minimal viable value for foam pick-up. This minimizes the clamp force and the potential

injuries from clamped skin or fingers. The collaborative robot also features impact detection, which stops the robot motion in case of contact or higher force than usual. The trigger for this maximal force should be set lower to minimize force during quasi-static contact (clamping of the hand(s) on the parts or vacuum plates).

5. Other possible risk reduction measures

Additional measures that do not compromise the performance could be taken to further reduce the risk of injuries. Paddings and cushioning material could be applied on the end-effector shell to further reduce the severity of potential impacts. A vision system could be installed to detect a possible intrusion of a worker's body part in the immediate working environment, the robot can either be stopped or greatly slowed down in response.

6. Collaborative clamp limit calculation

We decided to apply a limit of 100 N/cm2 of pressure. This is a more conservative value than the quasi-contact limit for the hand in table A2 from ISO/TS 15066:2016. We assume that the clamp finger's contact surface will be minimally 1cm2. The maximal force permissible is thus 100N. The pneumatic actuator cylinders transfer the force via a lever on the clamp. This lever reduces or maintains the same force for the grippers. Given that the cylinder has an interior diameter of 16mm, with an area of 201 mm2, this results in a maximal operating pressure of 72 psi to stay within collaborative limits. The fact that the cylinder is normally closed (by a spring) further reduces the force.

APPENDIX III

VENTURI TESTS

This section presents the characteristic curves from the three different Venturi vacuum generators used during this thesis project: a Coval vacuum cartridge, and two 3D printable designs. Both printable designs can be printed in functional parts or pneumatic manifolds (see Figure III-1). The characteristic curves were obtained by setting the operating pressure from 10 to 100 psi in 5 psi increments. At each operating pressure, the vacuum was measured by a vacuum gauge, and the air consumption measured by a ball flowmeter. The results are presented in figure III-2 and III-3. For all the Venturi, the air consumption is constant at a certain operating pressure and independent of the vacuum flow or level created at the vacuum end.

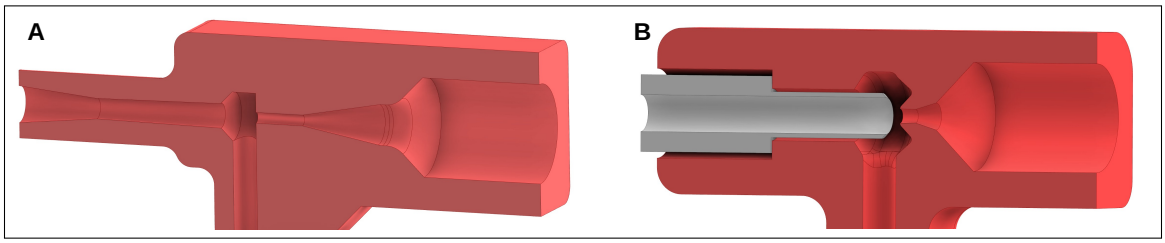

Figure-A III-1 The two 3D printed Venturi designs used in early prototypes. - A) Cutaway view of the single-part design. B) Cutaway view of the two-part design

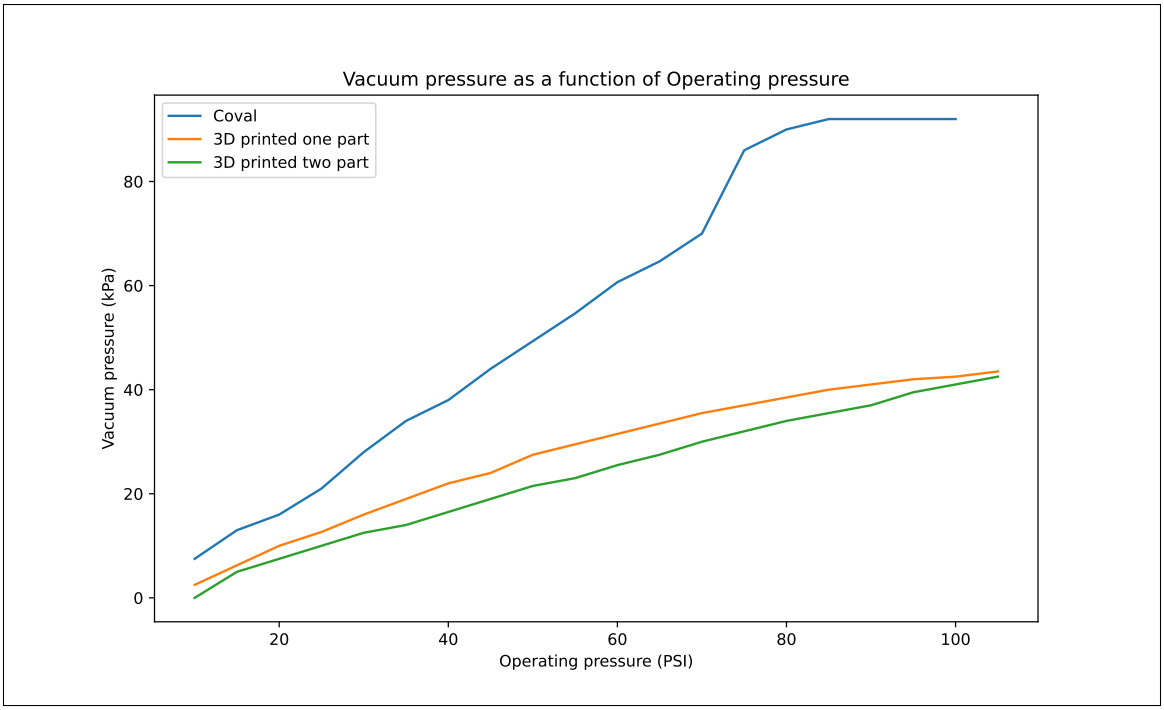

Figure-A III-2 Vacuum pressure as a function of the operating pressure for the three Venturi vacuum generators: the Coval Venturi cartridge (CVP90x12), the single-part 3D printed Venturi design, and the two-part Venturi design. The Coval curve match closely the one from the product documentation: https://doc.coval.com/g/CVP/doc/cvpc-cvp-cbp_doc_coval_2022_v02_us.pdf, p.8

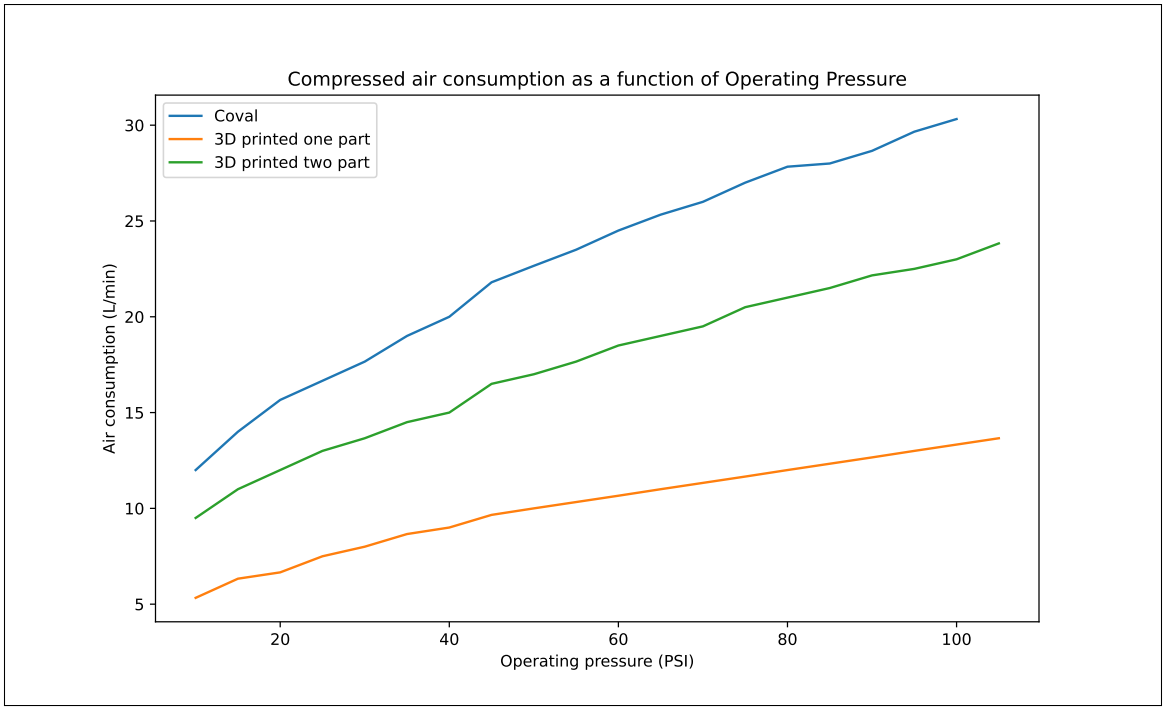

Figure-A III-3 Air consumption as a function of the operating pressure for the three Venturi vacuum generators: the Coval Venturi cartridge (CVP90x12), the single-part 3D printed Venturi design, and the two-part Venturi design

APPENDIX IV

FORCE PLATE SENSOR

The force plate sensor has four load cell sensors, one at each of its corners. These are connected to an HX711 amplifier that relays the signal to an Arduino Nano, which in turn sends the read values to a computer. It has been designed and fabricated as part of this thesis to assist in diverse tests (appliance tests, foam grasping force tests). Each load cell have each been individually calibrated using multiple standard weights, ranging from 20 grams to 1500 grams. Figure IV-1 shows the process of this calibration, which involves searching for the line that matches best the 26 different weight points. The maximum deviations from linearity for the four load cells were, respectively: **0.009 N**, **0.007 N**, **0.012 N**, and **0.008 N**.

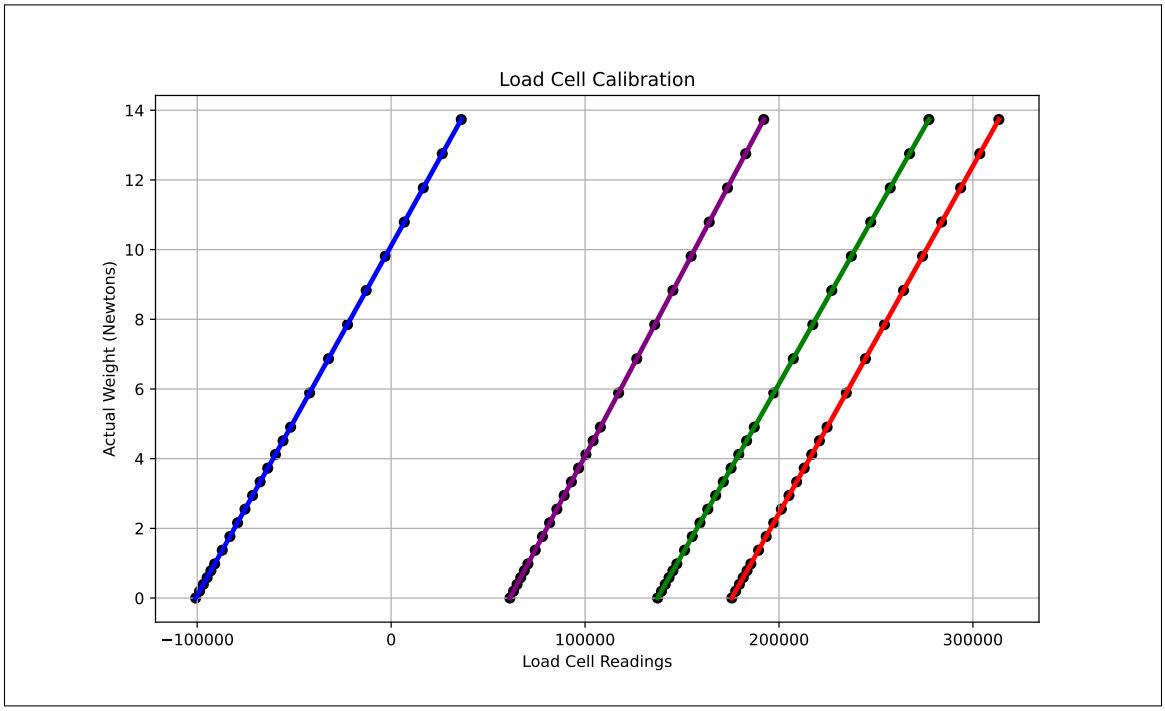

Figure-A IV-1 Load cells Calibration

APPENDIX V

PNEUMATIC GRASPING

1. Force tests

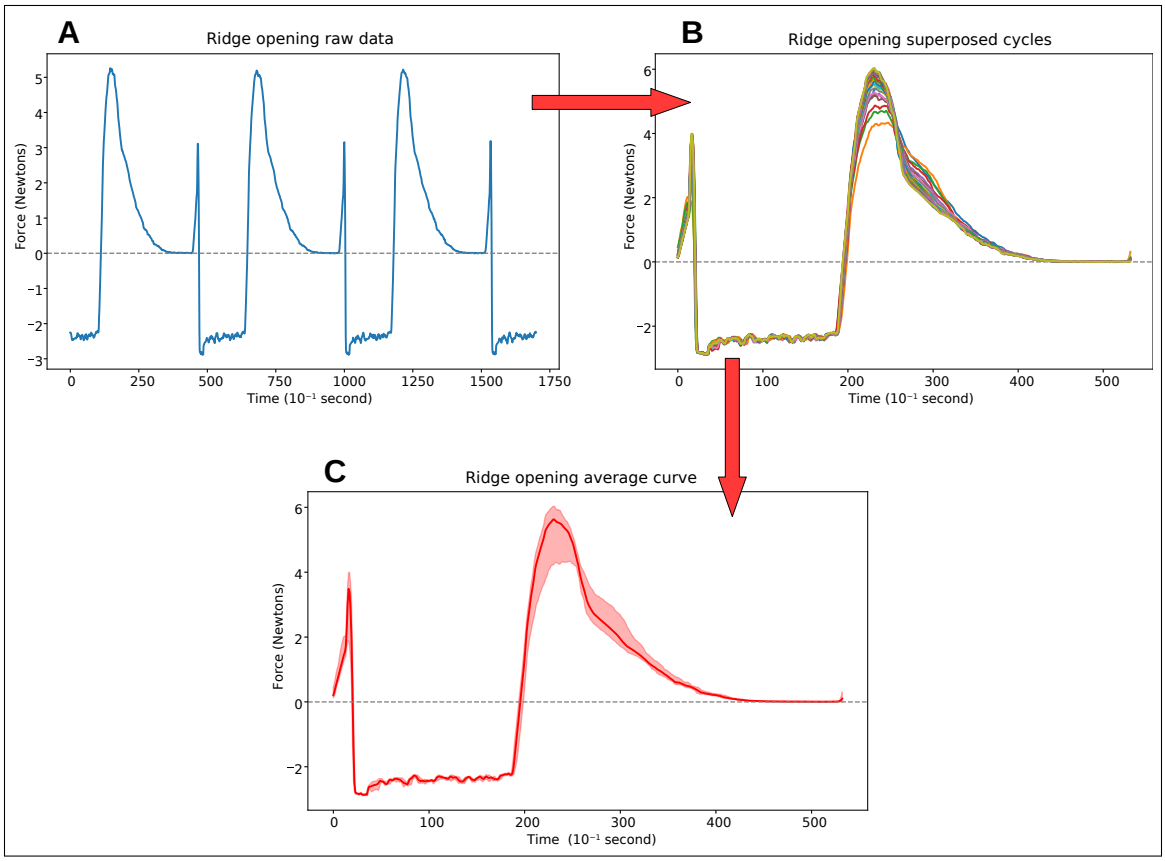

Figure-A V-1 Data processing example for the force tests. - A) Raw force data from one set of force tests (only 3 cycles out of 30 are shown). - B) All 30 cycle force curves are superposed. - C) The averaged curve from the 30 cycles and minimum and maximum values are calculated to obtain the final curve with a minimum/maximum band

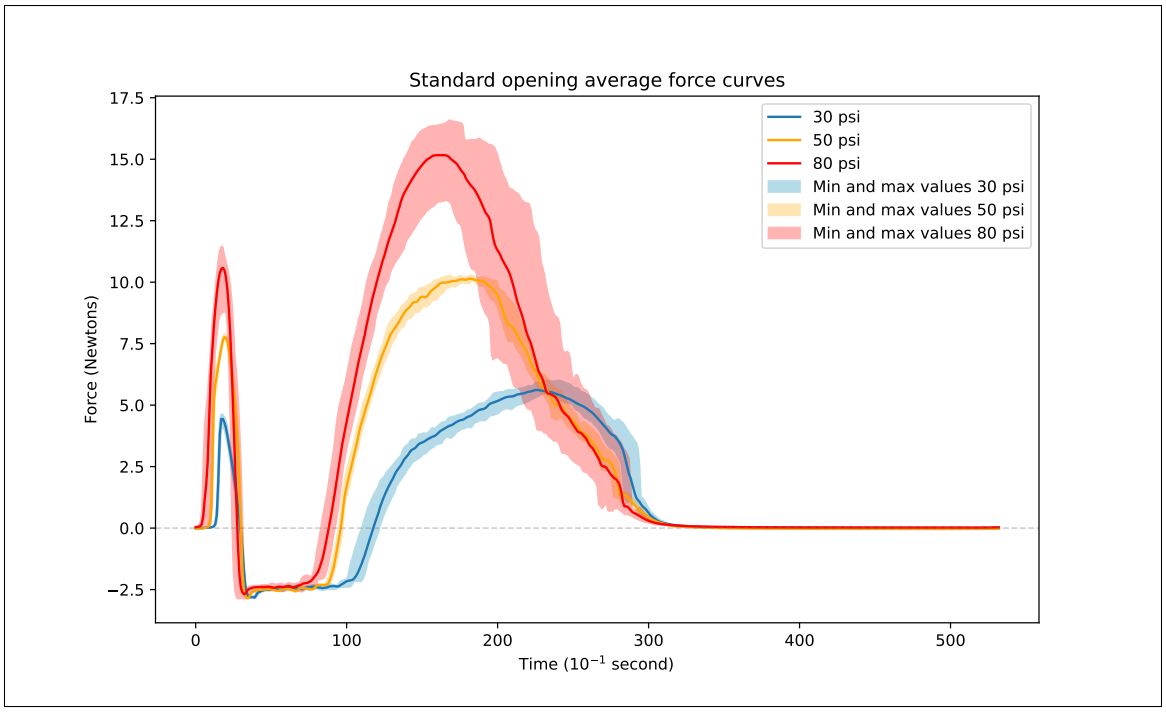

Figure-A V-2 Standard opening average force curves

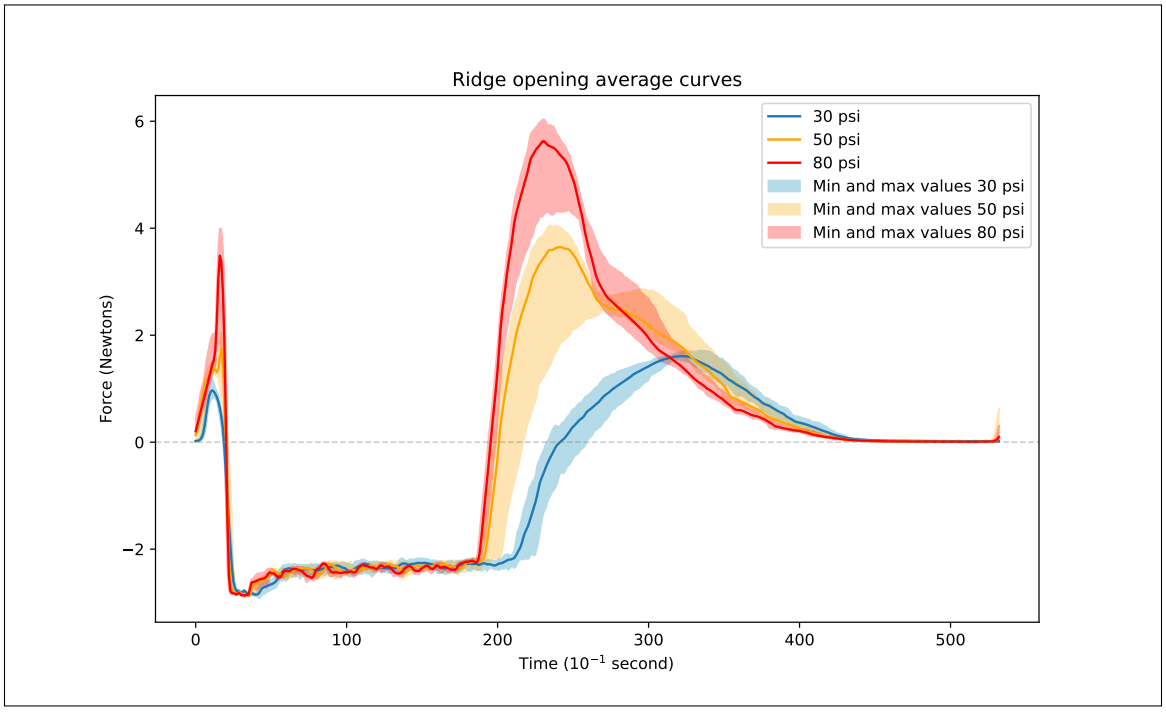

Figure-A V-3 Ridge opening average force curves

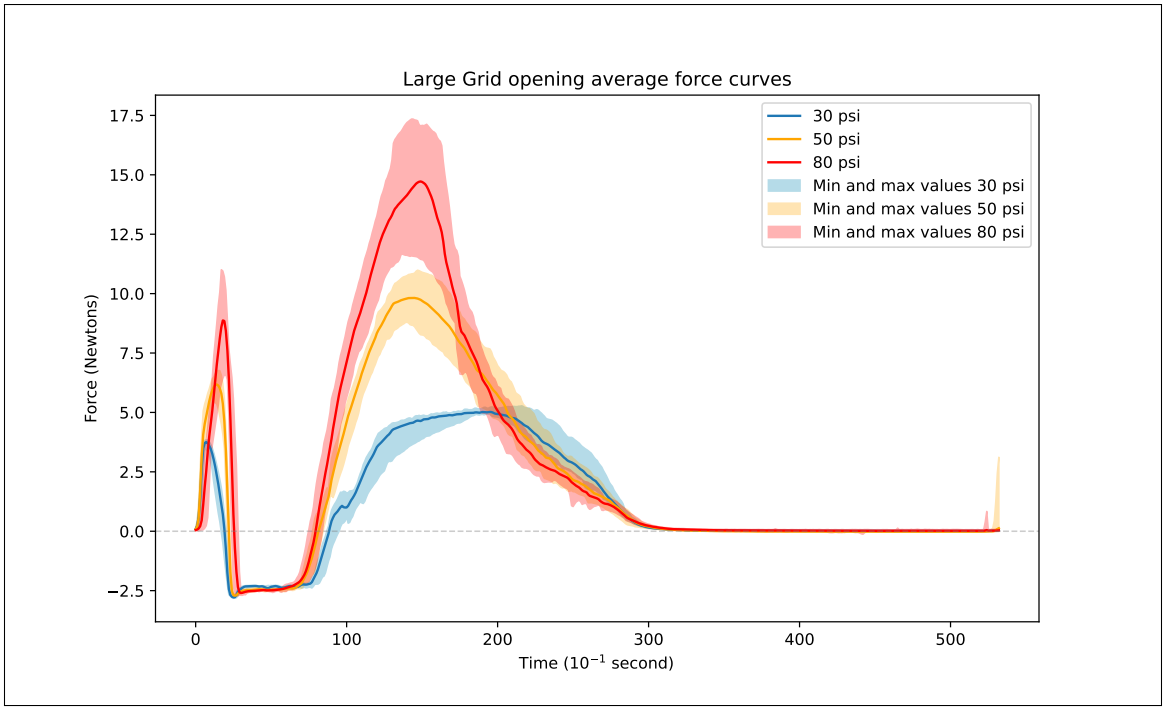

Figure-A V-4 Large Grid opening average force curves

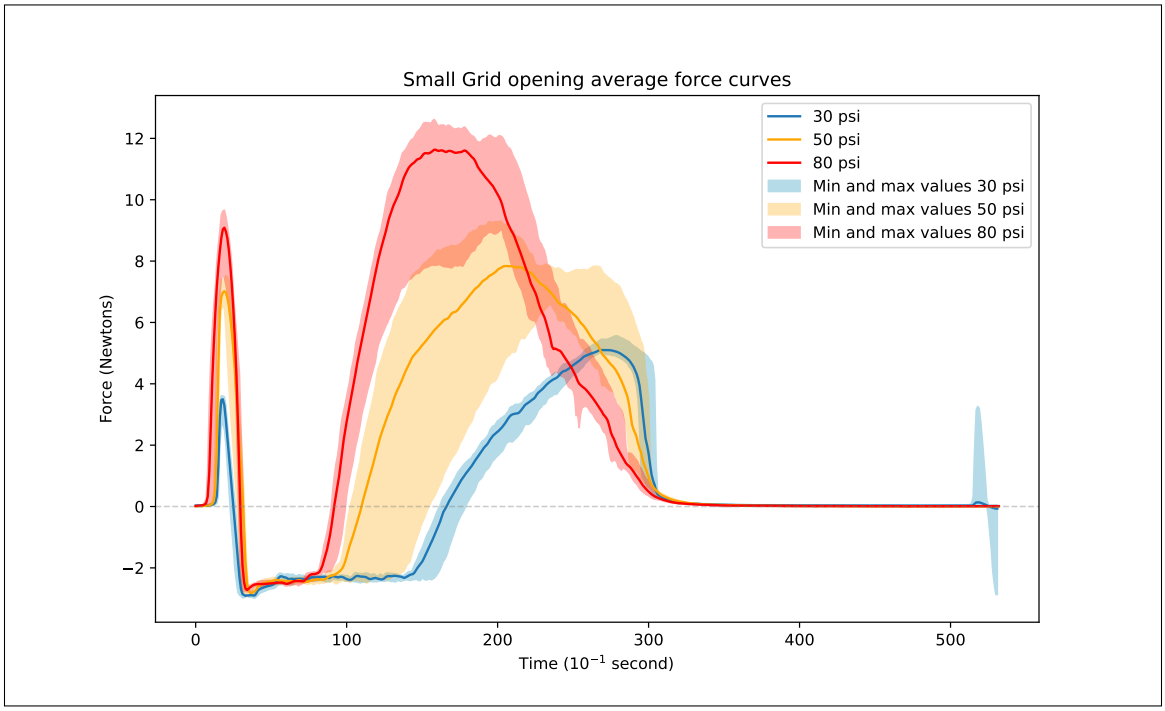

Figure-A V-5 Small Grid opening average force curves

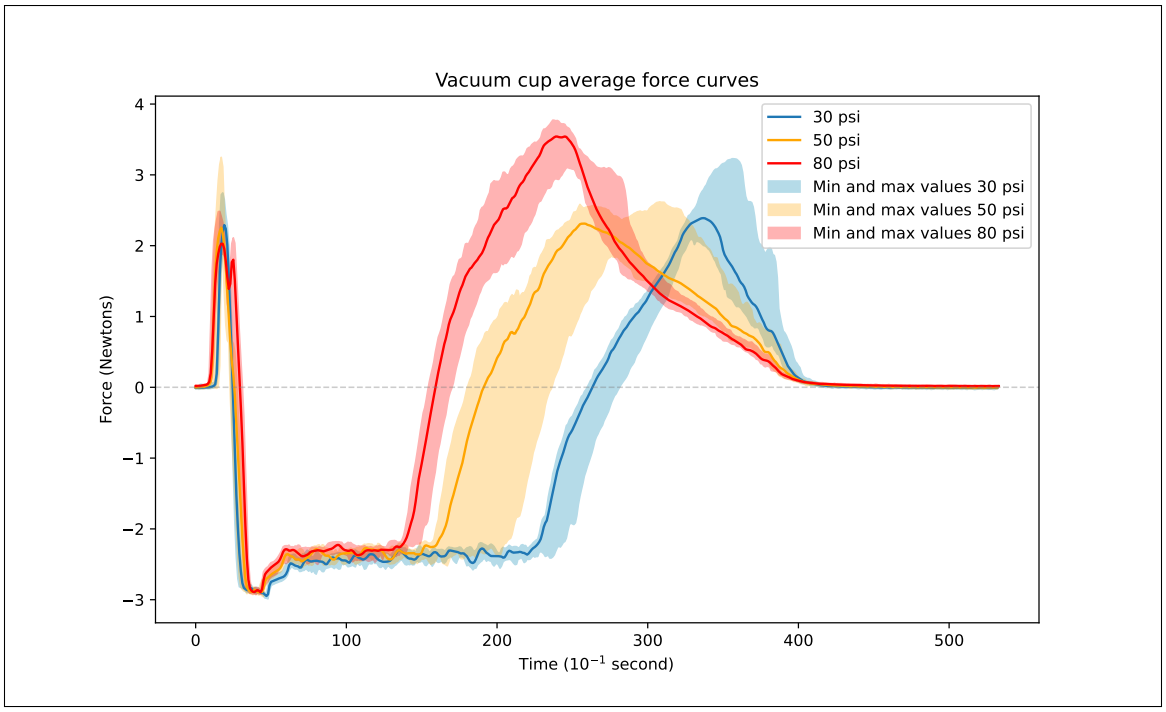

Figure-A V-6 Vacuum cup average force curves

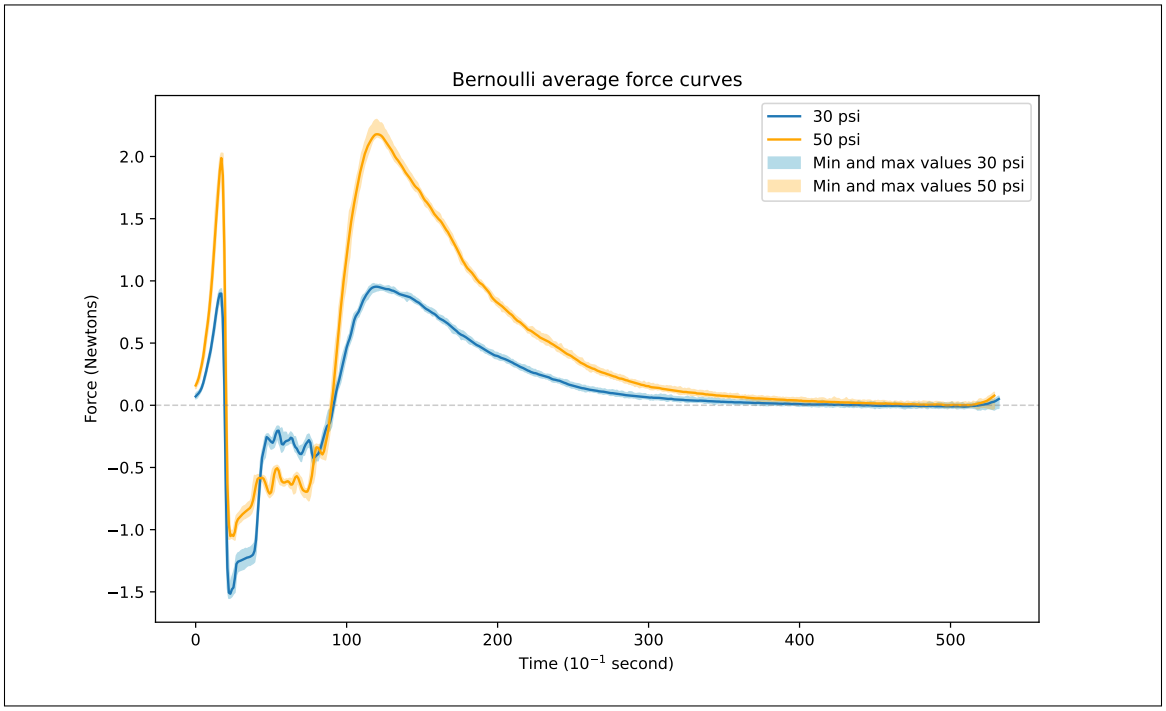

Figure-A V-7 Bernoulli trial average force curves

2. Vacuum Opening Qualitative tests

For all the following figure (V-8 to V-18) the associated letter for the picture correspond to : A) Side picture of the test trial supporting the foam pad. - B) Picture of the underneath of the trial prototype supporting the foam pad. - C) Top view picture of a Foam pad stuck to a flat transparent surface. - D) Underneath view picture of a foam pad stuck to a flat transparent surface.

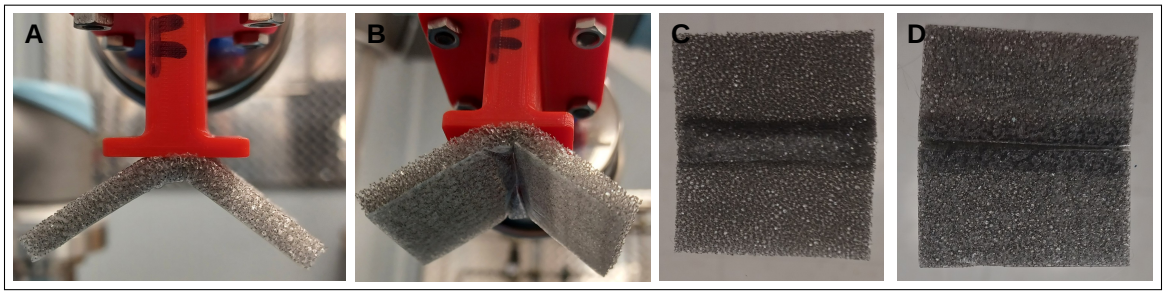

Figure-A V-8 Standard oblong opening at 30 psi

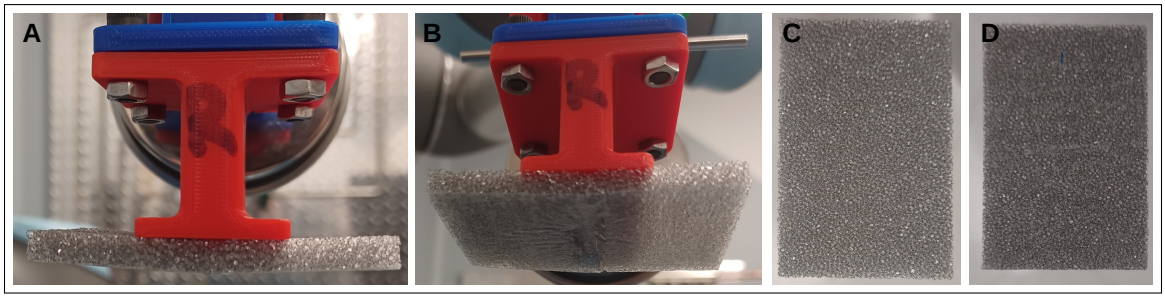

Figure-A V-9 Ridge oblong opening at 30 psi

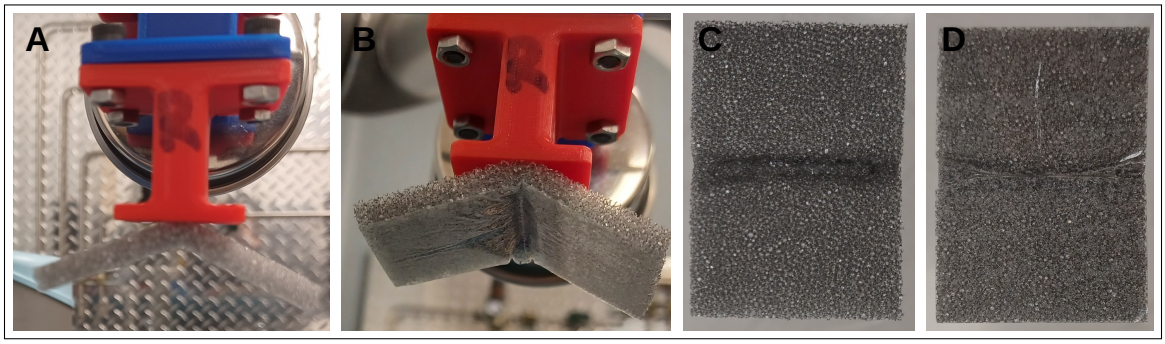

Figure-A V-10 Ridge oblong opening at 50 psi

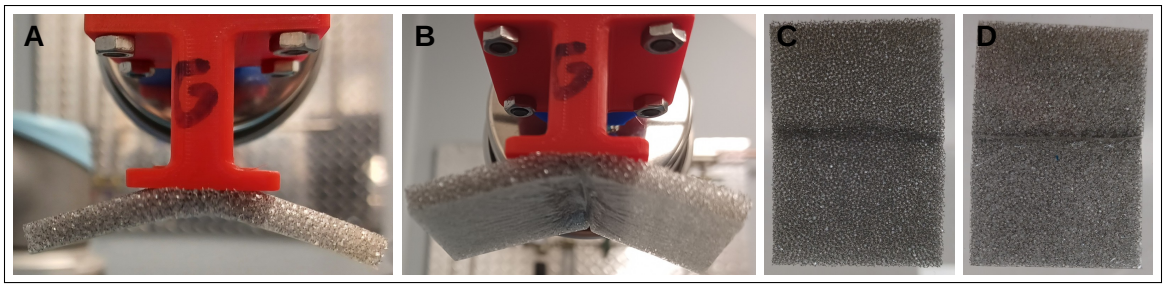

Figure-A V-11 Large Grid oblong opening at 30 psi

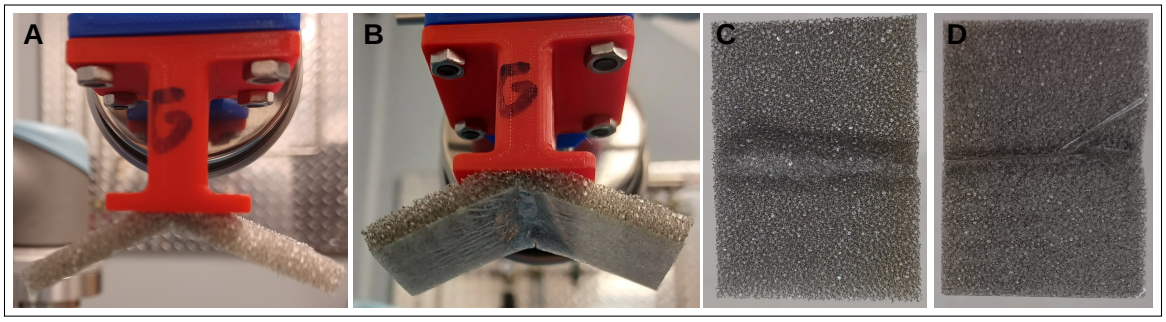

Figure-A V-12 Large Grid oblong opening at 50 psi

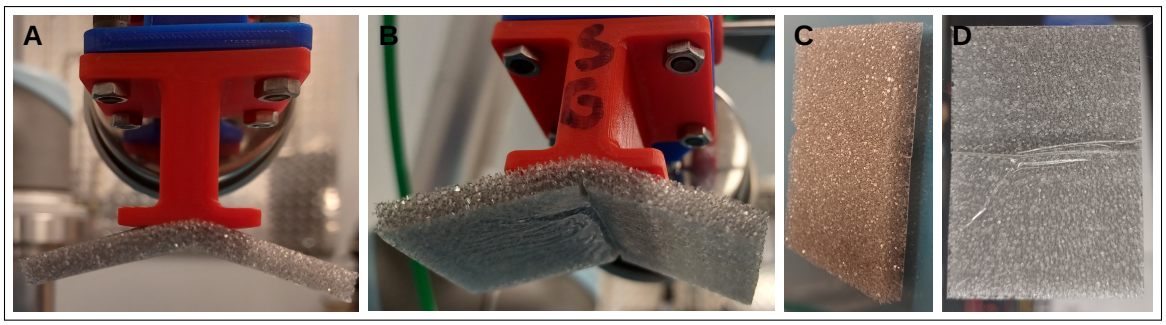

Figure-A V-13 Small Grid oblong opening at 30 psi

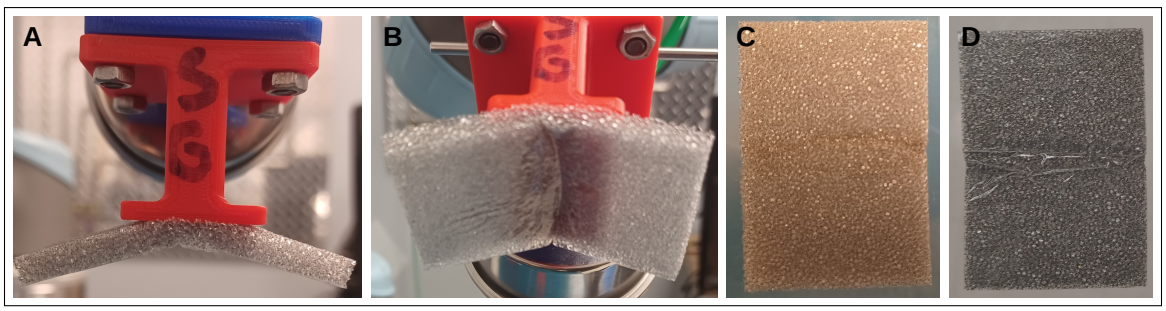

Figure-A V-14 Small Grid oblong opening at 50 psi

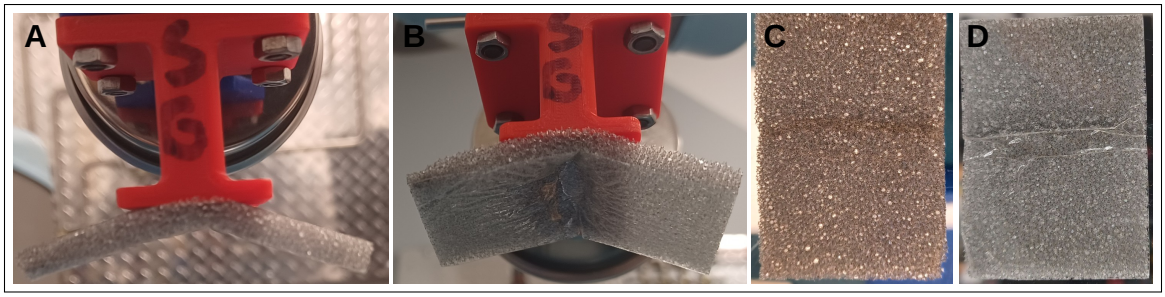

Figure-A V-15 Small Grid oblong opening at 80 psi

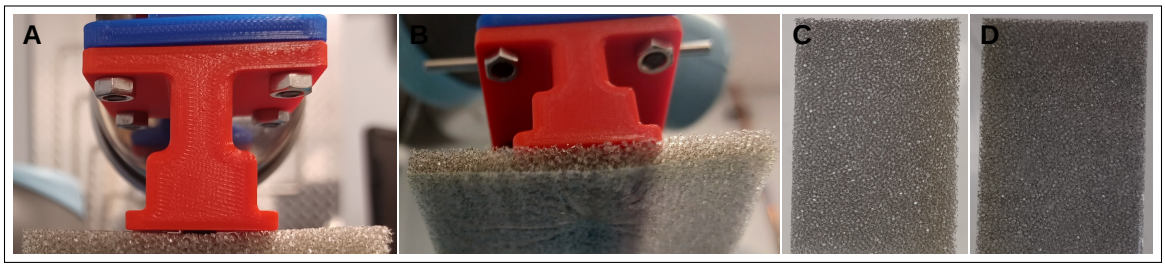

Figure-A V-16 Vacuum Cup at 30 psi

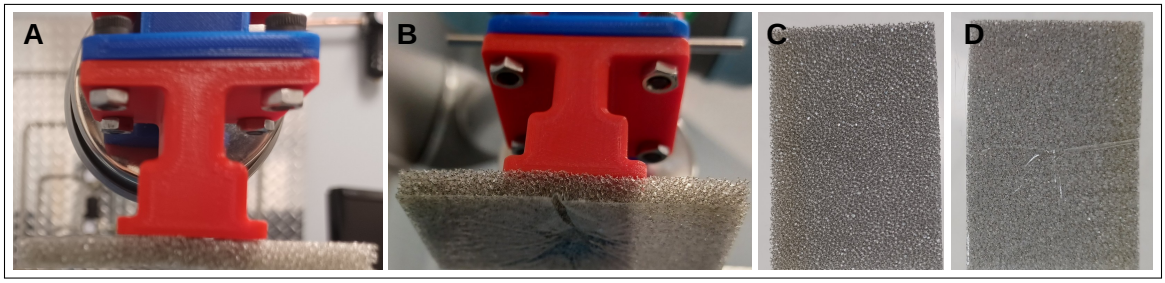

Figure-A V-17 Vacuum Cup at 50 psi

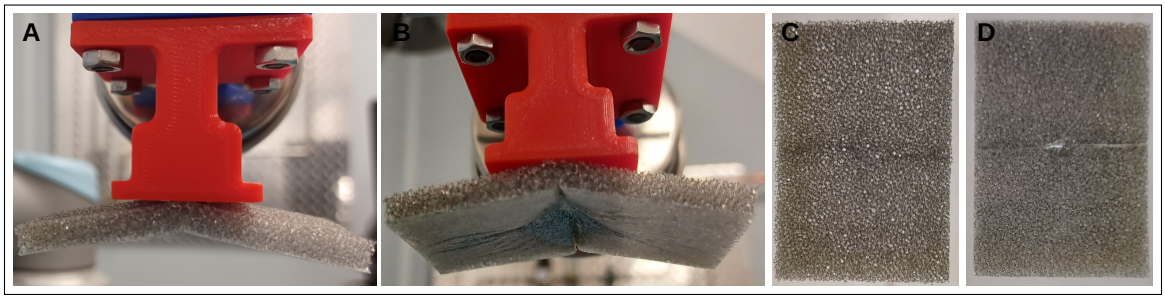

Figure-A V-18 Vacuum Cup at 80 psi

APPENDIX VI

APPLIANCE FORCE TESTS

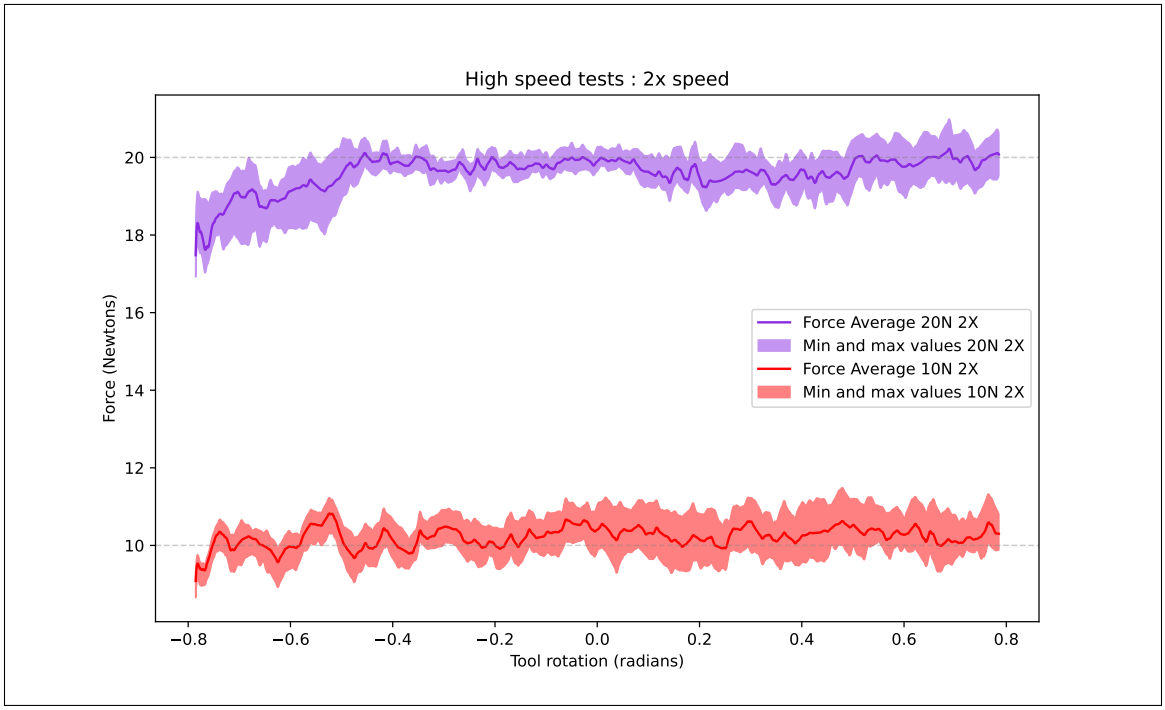

Figure-A VI-1 High speed test : 2 times the speed

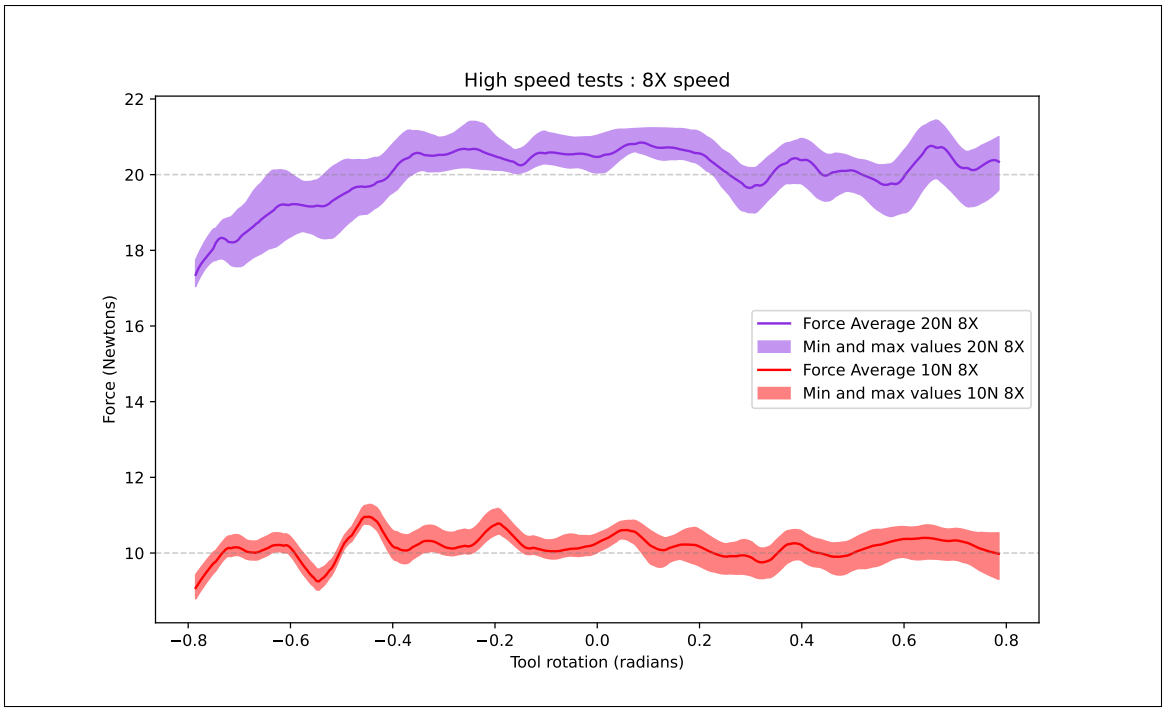

Figure-A VI-2 High speed test : 8 times the speed

APPENDIX VII

FOAM AIR PERMEABILITY TEST

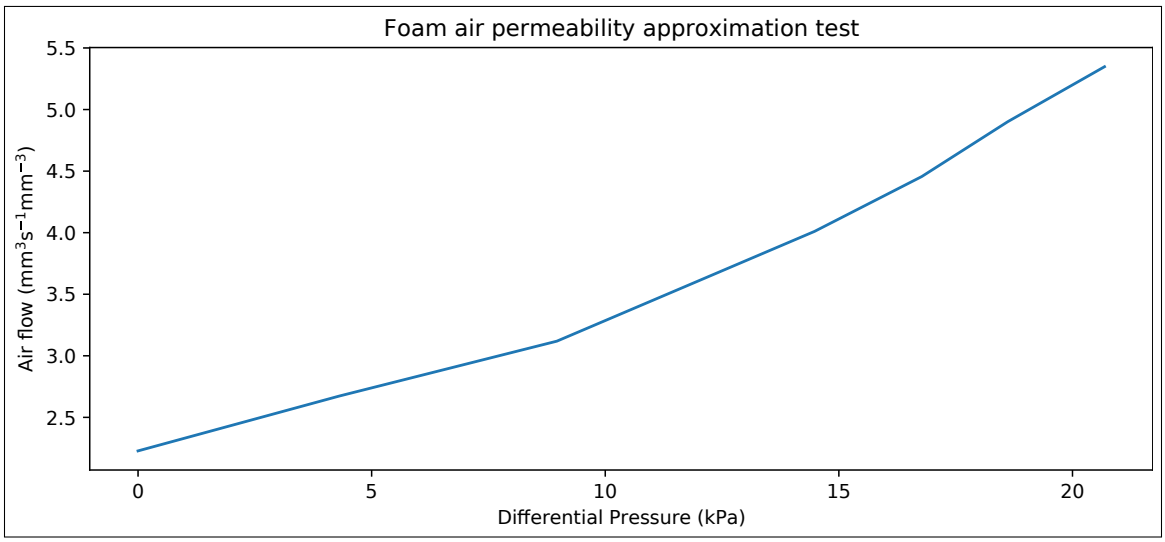

Figure-A VII-1 Experimental result of the foam air permeability, given in flow (mm^3s^{-1}) per volume of foam (mm^3). The differential pressure is the pressure difference between the two side of the foam tested

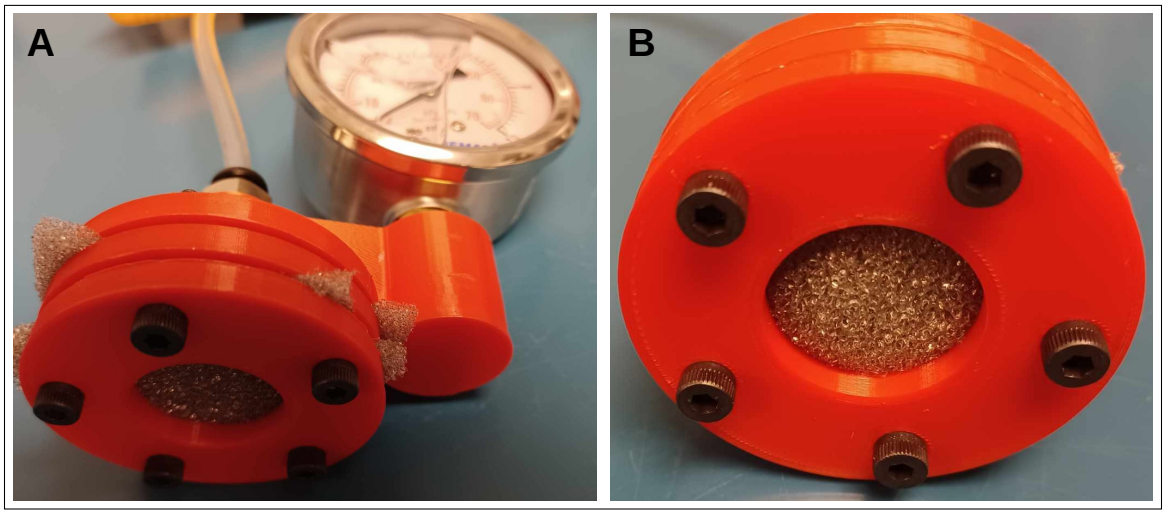

Figure-A VII-2 Experimental apparatus to estimate the foam permeability to air

BIBLIOGRAPHY

Asano, K., Hatakeyama, F. & Yatsuzuka, K. (2002). Fundamental Study of an Electrostatic Chuck for Silicon Wafer Handling. *IEEE TRANSACTIONS ON INDUSTRY APPLICATIONS*, 38(3).

Björnsson, A., Erik, J. & Johansen, K. (2013, September). *Automated Removal of Prepreg Backing Paper - A Sticky Problem*. Communication presented in SAE Aerotech Congress and Exhibition, Montreal, Canada.

Björnsson, A., Jonsson, M., Eklund, D., Lindbäck, J. E. & Björkman, M. (2017). Getting to grips with automated prepreg handling. (11), 445-453. doi: 10.1007/s11740-017-0763-2.

CAB. (2023). Label dispensers HS and VS [Format]. Retrieved from: https://www.cab.de/en/marking/label-dispenser/hsvs/.

Corporation., E. (2023). Needle Grippers [Format]. Retrieved from: https://www.emicorp.com/products/214/Needle-Grippers.

Fleischer, J., Förster, F. & Gebhardt, J. (2016). Sustainable manufacturing through energy efficient handling processes. *Procedia CIRP*, 40(136), 574-579. doi: 10.1016/j.procir.2016.01.136.

Gabriel, F., Fahning, M., Dietrich, F. & Dröder, K. (2020). Modeling of vacuum grippers for the design of energy efficient vacuum-based handling processes. *Production Engineering*, (14), 545-554. doi: https://doi.org/10.1007/s11740-020-00990-9.

Guo, J., Bamber, T., Chamberlain, M., Justham, L. & Jackson, M. (2016). Optimization and experimental verification of coplanar interdigital electroadhesives. *Journal of Physics D: Applied Physics*, 49. doi: 10.1088/0022-3727/49/41/415304.

Guo, J., Leng, J. & Rossiter, J. (2020). Electroadhesion Technologies for Robotics: A Comprehensive Review. *IEEE TRANSACTIONS ON ROBOTICS*, 36(2). doi: 10.1109/TRO.2019.2956869.

He, H., Saunders, G. & Wen, J. T. (2022, August). *Robotic Fabric Fusing using a Novel Electroadhesion Gripper*. Communication presented in IEEE 18th International Conference on Automation Science and Engineering (CASE), Mexico City, Mexico.

Inc., F. A. (2023a). Kenos KCS gripper – it's what Piab calls "your flexible cobot friend" [Format]. Retrieved from: https://www.fpeautomation.com/piabs-kenos-kcs-gripper-for-collaborative-robots.

Inc., I. A. (2023b). robotape [Format]. Retrieved from: https://robotape.com.

International Organization for Standardization. (2016). *Robots and robotic devices — Collaborative robots*. ISO/TS 15066.

International Organization for Standardization. (2018). *Robotics — Safety design for industrial robot systems — Part 1: End-effectors*. ISO/TS 20218.

Koustoumpardis, P. & Aspragathos, N. (2004, July). *A Review of Gripping Devices for Fabric Handling*. Review presented in International Conference on Intelligent Manipulation and Grasping IMG04, Genoa, Italy (pp. 229-234).

Koustoumpardis, P. N., Nastos, K. X. & Aspragathos, N. A. (2014, September). *Underactuated 3-finger robotic gripper for grasping fabrics*. Communication presented in 23rd International Conference on Robotics, Smolenice Castle, Slovakia.

Ku, S., Myeong, J., Kim, H.-Y. & Park, Y.-L. (2020). Delicate Fabric Handling Using a Soft Robotic Gripper With Embedded Microneedles. *IEEE ROBOTICS AND AUTOMATION LETTERS*, 5(3), 4852-4858.

Li, X., Li, N., Tao, G. & Kagawa, T. (2021). Experimental Comparison of Bernoulli Gripper and Vortex Gripper. *INTERNATIONAL JOURNAL OF PRECISION ENGINEERING AND MANUFACTURING*, 16(10), 2081-2090. doi: https://doi.org/10.1007/s12541-015-0270-3.

Lin, C.-Y., Wagshum, A. T. & Le, T.-S. (2016). *Robotic Label Applicator: Design, Development and Visual Servoing Based Control*. Review presented in International Conference on Computer and Automation Engineering, Melbourne, Australia. doi: DOI: 10.1051/matecconf/2016560.

Liu, D., Wang, M., Fang, N., Cong, M. & Du, Y. (2020). Design and tests of a non-contact Bernoulli gripper for rough-surfaced and fragile objects gripping. *Assembly Automation*, 40(5), 735-743. Retrieved from: https://doi.org/10.1108/AA-10-2019-0171.

Ltd., F. (2023). Parallel gripper DHPS [Format]. Retrieved from: https://www.festo.com/ie/en/p/parallel-gripper-id_DHPS.

LTD, S. I. P. (2023). SNG Needle Grippers [Format]. Retrieved from: https://schmalzindia.tradeindia.com/sng-needle-grippers-6979683.html.

Masahiro, F., Ikeda, S., Fujimoto, T., Shimizu, T., Ikemoto, S. & Miyamoto, T. (2018). Development of universal vacuum gripper for wallclimbing robot. *ADVANCED ROBOTICS*, 32(6), 283-296. doi: https://doi.org/10.1080/01691864.2018.1447238.

Mykhailyshyn, R., Savkiv, V., Maruschak, P. & Xiao, J. (2022). A systematic review on pneumatic gripping devices for industrial robots. *TRANSPORT*, 37(3), 201-231.

of America, S. C. (2022). ZHP, Vacuum Pad with Generator [Format]. Retrieved from: https://www.smcusa.com/products/zhp-vacuum-pad-with-generator~133355.

Prahlad, H., Pelrine, R., Stanford, S., Marlow, J. & Kornbluh, R. (2008, May). *Electroadhesive Robots—Wall Climbing Robots Enabled by a Novel, Robust, and Electrically Controllable Adhesion Technology*. Communication presented in IEEE International Conference on Robotics and Automation, Pasadena, CA, USA.

Rajagopalan, P., Muthu, M., Liu, Y., Luo, J., Wang, X. & Wan, C. (2022). Advancement of Electroadhesion Technology for Intelligent and Self-Reliant Robotic Applications. *Advanced Intelligent Systems*, (4). doi: 10.1002/aisy.202200064.

Robotiq. (2023). Products [Format]. Retrieved from: https://robotiq.com/products.

Schaffrath, R., Jäger, E., Winkler, G., Doant, J. & Todtermuschke, M. (2021). Vacuum gripper without central compressed air supply. *Procedia CIRP*, 97, 76-80. Retrieved from: https://doi.org/10.1016/j.procir.2020.05.207.

Schmalz. (2023a). Flow Grippers SCG [Format]. Retrieved from: https://www.schmalz.com/en/vacuum-technology-for-automation/vacuum-components/special-grippers/flow-grippers/flow-grippers-scg-306274.

Schmalz. (2023b). Vacuum Ejectors [Format]. Retrieved from: https://www.schmalz.com/en/vacuum-knowledge/the-vacuum-system-and-its-components/vacuum-generators/vacuum-ejectors.

Shintake, J., Rosset, S., Schubert, B., Floreano, D. & Shea, H. (2016). Versatile Soft Grippers with Intrinsic Electroadhesion Based on Multifunctional Polymer Actuators. (28), 231-238. doi: 10.1002/adma.201504264.

Taylor, P. M., Pollet, D. M. & GrieBer, M. T. (1996). Pinching grippers for the secure handling of fabric panels. *Assembly Automation*, 16(3), 16-21.

Teeple, C. B., Werfel, J. & Wood, R. (2022, May). Multi-Dimensional Compliance of Soft Grippers Enables Gentle Interaction with Thin, Flexible Objects. *International Conference on Robotics and Automation (ICRA)*, pp. 23-27.

VUOTOTECNICA. (2022). Solutions with Vuototecnica vacuum cups [Format]. Retrieved from: https://www.vuototecnica.biz/cup.php.

Wang, B. (2020). *Design and Development of a Soft Robotic Gripper for Fabric Material Handling*. (Master's thesis, University of Windsor, Windsor, Ontario, Canada). Retrieved from: https://scholar.uwindsor.ca/etd/8406.

Wang, Z., Makiyama, Y. & Hirai, S. (2021). A Soft Needle Gripper Capable of Grasping and Piercing for Handling Food Materials. *Journal of Robotics andMechatronics*, 33(4), 935-943. doi: 10.20965/jrm.2021.p0935.

West, J. D., Mici, J., Jaquith, J. F. & Lipson, H. (2020). Design and optimization of millimeter-scale electroadhesive grippers. *Journal of Physics D: Applied Physics*, 53. doi: 10.1088/1361-6463/aba1b0.

Yin, H., Varava, A. & Kragic, D. (2021). Modeling, learning, perception, and control methods for deformable object manipulation. *Science Robotics*, 54(6). doi: 10.1126/scirobotics.abd8803.

Yuan, Q., Chen, I.-M., Lembono, T. S., Landén, S. N. & Malmgren, V. (2018). Automatic robot taping system with compliant force control. *The International Journal of Advanced Manufacturing Technology*, (94), 4105-4113. doi: DOI 10.1007/s00170-017-1082-7.

Zoller, Z., Zentay, P., Meggyes, A. & Arz, G. (1999). Robotical handling of polyurethane foams with needle grippers. *PERIODICA POLYTECHNICA SER. MECH. ENG*, 43(2), 229-238.